7-7-2014 12:00 AM

Functional Co-substituted Poly[(amino acid ester)phosphazene] Biomaterials

Amanda L. Baillargeon
The University of Western Ontario

Supervisor
Dr. Kibret Mequanint
The University of Western Ontario

FUNCTIONAL CO-SUBSTITUTED POLY[(AMINO ACID ESTER)PHOSPHAZENE] BIOMATERIALS

(Thesis format: Monograph)

by

Amanda Lee <u>Baillargeon</u>

Graduate Program in Biomedical Engineering

**A thesis submitted in partial fulfillment
of the requirements for the degree of
Master of Engineering Science**

**The School of Graduate and Postdoctoral Studies
The University of Western Ontario
London, Ontario, Canada**

Abstract

The development of new and improved biomaterials is essential for tissue engineering and regenerative medicine applications. Amino acid-based polyphosphazenes are being explored as scaffold materials for tissue engineering applications due to their non-toxic degradation products and tunable material properties. This work focuses on the synthesis of non-functional and novel functional poly[(amino acid ester)phosphazene]s using a facile method of thermal ring opening polymerization followed by one-pot room temperature substitution. The family of polyphosphazenes developed in this work is based on L-alanine (PP-A's), L-phenylalanine (PP-F's), and L-methionine (PP-M's) with L-glutamic acid imparting the functionality. Characterization of these materials demonstrated that the one-pot substitution was successful in developing mono- and co-substituted poly[(amino acid ester)phosphazene]s. Cytotoxicity studies on two-dimensional films showed these materials to be compatible with NIH-3T3 fibroblasts over the five-day study. The PP-F's also showed significantly enhanced cell viability over tissue culture polystyrene at day 1 ($p<0.001$) and day 3 ($p<0.01$). As a proof of concept, electrospinning of PP-A$_{100}$ blended with poly(caprolactone) (PCL) (50% PP-A$_{100}$/50% PCL) was conducted to fabricate three-dimensional scaffolds. Overall, this study has shown that poly[(amino acid ester)phosphazene]s can be synthesized with good yields and better reaction conditions, leading to materials with promising cytocompatibility for use in biomedical applications.

Keywords

Polyphosphazenes, poly[(amino acid ester)phosphazene]s, biomaterials, biodegradable polymers, tissue engineering, scaffolds, electrospinning

Acknowledgments

I would like to acknowledge my supervisor, Dr. Kibret Mequanint, for his continued support and guidance throughout my Master's degree. I really appreciated the amount of time he designated weekly to meet with his students and ensure that they were progressing well with their research; it definitely pushed me to always have new findings to share with him. I would also like to thank the Natural Sciences and Engineering Research Council (NSERC) of Canada and the Strategic Training Program in Vascular Research supported by the Canadian Institutes for Health Research (CIHR) for the financial aid and skills training.

I would like to thank Dr. Darryl Knight and Dr. Kalin Panev for their help in synthetic chemistry problems, experimental setup, and elucidation of NMR spectra. I also would like to acknowledge Dr. Shigang Lin for his help with the design and implementation of the cell culture experiments. I would like to thank Ryan Guterman of the Ragogna research group for his help in running TGA, DSC, and FTIR analyses. Lastly, I would like to thank Somiraa Said for her guidance with the electrospinning and planning of cell culture studies. All of the helpful feedback and discussions from other lab members (especially Tierney Deluzio) were greatly appreciated.

Finally, I would like to thank my mother and grandparents for their continued love and support throughout my study. I would not have been able to push through these stressful two years without you by my side.

Table of Contents

List of Tables

List of Figures

List of Schemes

List of Appendices

List of Abbreviations

2-D	Two-dimensional
3-D	Three-dimensional
3T3	Fibroblast cell line
1P RT	One-pot room temperature
Å	Angstrom
Ala, A	L-alanine
ANOVA	Analysis of variance
ATR	Attenuated total reflectance
Boc	t-Butyloxycarbonyl
Boc-Glu(OBzl)-OH	N-α- t-butyloxycarbonyl -L-glutamic acid γ-benzyl ester
Boc-Glu(OBzl)-OEt	N-α- t-butyloxycarbonyl -L-glutamic acid ethyl ester γ-benzyl ester
Bzl	Benzyl
CDCl$_3$	Deuterated chloroform
Da	Daltons, g/mol
DAPI	4'-6'-diamidino-2-phenylindole dihydrochloride
DCM	Dichloromethane
DI	Deionized
DMAP	4-(Dimethylamino)pyridine
DMF	N,N-Dimethylformamide
DMSO	Dimethyl sulfoxide
DMSO-d$_6$	Deuterated DMSO
dn/dc	Differential index of refraction, Refractive index increment
DSC	Differential scanning calorimetry
ECM	Extracellular matrix

EDCI	N-(3-dimethylaminopropyl)-N'-ethylcarbodiimide hydrochloride
EtOAc	Ethyl acetate
EtOH	Ethanol
F-actin	Filamentous actin
Fmoc	Fluorenylmethyloxycarbonyl
Fmoc-Glu(OBzl)-OH	N-α-fluorenylmethyloxycarbonyl-L-glutamic acid γ-benzyl ester
FTIR	Fourier transform infrared
GAG	Glycosaminoglycans
Glu, E	L-glutamic acid
GPC	Gel permeation chromatography
H-Ala-OEt•HCl	L-alanine ethyl ester hydrochloride
HBSS	Hank's balanced salt solution
HepG2	Human liver carcinoma cell line
H-Met-OEt•HCl	L-methionine ethyl ester hydrochloride
H-Phe-OEt•HCl	L-phenylalanine ethyl ester hydrochloride
LT 2S	Low temperature two-step
MC3T3-E1	Mouse osteoblast precursor cell line
MeOH	Methanol
Met, M	L-methionine
M_n	Number average molecular weight
MPa	Megapascal
MTT	3-(4,5-dimethylthiazol-2-yl)-2,5-diphenyltetrazolium bromide
M_w	Weight average molecular weight
N	Newton
NIH-3T3	Mouse fibroblast cell line
NMR	Nuclear magnetic resonance

PBS	Phosphate-buffered saline
PCL	Poly(caprolactone)
Pd/C	Palladium on carbon
PDCP	Poly[(dichloro)phosphazene]
PDI	Polydispersity index
Phe, P	L-phenylalanine
PLA	Poly(lactic acid)
PLAGA	Poly(lactic acid –co– glycolic acid)
PMN	Polymorphonuclear leukocytes
PNEA	Poly[bis(ethyl alanato)phosphazene] (literature)
PNEF	Poly[bis(ethyl phenylalanato)phosphazene] (literature)
PNEM	Poly[bis(ethyl methionato)phosphazene] (literature)
PP-A$_{100}$	Poly[bis(ethyl alanato)phosphazene] (this work)
PP-A$_{90}$E$^{*}_{10}$	90% Ala-OEt / 10% Glu(OBzl)-OEt polyphosphazene
PP-F$_{100}$	Poly[bis(ethyl phenylalanato)phosphazene] (this work)
PP-F$_{90}$E$^{*}_{10}$	90% Phe-OEt / 10% Glu(OBzl)-OEt polyphosphazene
PP-M$_{100}$	Poly[bis(ethyl methionato)phosphazene] (this work)
PP-M$_{90}$E$^{*}_{10}$	90% Met-OEt / 10% Glu(OBzl)-OEt polyphosphazene
^{i}PrOH	iso-Propanol, 2-Propanol
psi	Pounds per square inch
RALS/LALS	Right angle light scattering/Low angle light scattering
RI	Refractive index
RT 2S	Room temperature two-step
SDH	Succinic dehydrogenase
SDS	Sodium dodecyl sulfate
SEM	Scanning electron microscopy

TCPS	Tissue culture polystyrene
T_d	Decomposition temperature
TEA, NEt_3	Triethylamine
TFA	Trifluoroacetic acid
T_g	Glass transition temperature
TGA	Thermogravimetric analysis
THF	Tetrahydrofuran
T_m	Melting temperature
TROP	Thermal ring opening polymerization
UV	Ultraviolet
wt %	Weight by weight percent
w/v %	Weight by volume percent

Chapter 1

1 Scope and Thesis Outline

1.1 Scope

As the fields of tissue engineering and regenerative medicine continue to emerge as promising alternatives to current treatment options for failed or otherwise diseased tissues, so too has the development of suitable biomaterials.[1] Materials-mediated tissue engineering is the most frequently employed strategy, where a porous scaffold, which is ideally degradable, acts as a support for the developing tissue either *in vitro* or *in vivo*. The scaffolds themselves must possess specific material and biological characteristics, such as desirable mechanical properties, degradation rates that parallel tissue formation, and biocompatibility, to ensure their success in tissue engineering applications.[1] As such, numerous natural and synthetic materials have been investigated for their use in biomedical applications.[2-4] Natural materials, like cellulose, chitosan, and collagen, have been extensively studied due to their inherent biocompatibility and favourable cell-material interactions; however, they fall short as ideal materials due to their uncontrolled degradation rates, poor mechanical properties, and batch-to-batch variability.[4] Synthetic polymers, on the other hand, have shown to be an improvement over natural materials with their tunable and well-controlled mechanical properties and degradation rates, ease of processing, and availability.[5, 6] That being said, degradable synthetic polymers, like poly(acids), have their own drawbacks such as the formation of acidic degradation products.[7-9] Another limitation of synthetic materials is their inability to instruct cells since they do not contain the biochemical cues that are present on the native extracellular matrix, which direct proper tissue formation.[10, 11] Therefore, degradable biomaterials that can be tailored with respect to mechanical and degradation properties to suit their intended applications and that degrade into non-toxic products are being actively pursued.[1, 5]

Polyphosphazenes, especially poly[(amino acid ester)phosphazene]s, have been shown to have tunable material properties and degrade into non-toxic degradation products that are easily dealt with by the body, making them great candidates for use as scaffold

biomaterials.[12, 13] Since these materials are based on amino acids, it is also possible to incorporate functionality into the polymers, which would allow for subsequent attachment of biomolecules shown to improve cell-material properties, potentially overcoming the main inadequacy of current synthetic materials. Current synthetic methods for the fabrication of poly[(amino acid ester)phosphazene]s are cumbersome[14] and development of a facile synthesis technique would make studying these materials more accessible. With increased accessibility of poly[(amino acid ester)phosphazene]s, these materials could be studied for their utility in a wider range of applications not just orthopaedics, which has been the main application to date.[15] Also, the facile synthesis would allow for the development of novel co-substituted poly[(amino acid ester)phosphazene]s with functional handles for biomolecule conjugation. In this work, a facile synthesis of poly[(amino acid ester)phosphazene]s was developed and the resulting materials were characterized extensively, investigated for cytotoxicity, and explored for their potential in fabricating three-dimensional constructs.

1.2   Thesis Outline

This thesis contains five chapters. Chapter 2 provides an in-depth literature review of tissue engineering, requirements of scaffold biomaterials, current natural and synthetic materials and their limitations, the synthesis of polyphosphazenes, and the suitability of polyphosphazenes as biomaterials in terms of biocompatibility, degradability, and mechanical properties. The rationale and objectives for this work are also included at the end of Chapter 2. Chapter 3 describes the materials and methods for the synthesis of the poly[(amino acid ester)phosphazene]s materials, as well as the setup parameters and experimental conditions for characterization, cell studies, and electrospinning experiments. Chapter 4 presents and discusses all research findings of this work. Lastly, Chapter 5 provides a general conclusion of the major findings in this study and future directives for this project.

Chapter 2

2 Literature Review, Objectives, and Rationale[*]

2.1 Tissue Engineering Methodology

There are four main strategies of tissue engineering that could be explored for tissue repair and remodeling, cell transplantation, scaffold transplantation, and two forms of cell-seeded scaffold transplantation. The cell transplantation strategy involves simply injecting cells, whether they are stem cells or primary cells, to the damaged area and allowing the cells to interact with the natural extracellular matrix (ECM) and mature into working tissue *in vivo*. In this case, the host body serves as the "bioreactor" that produces the necessary mechanical stimulation and other signals to guide the maturation and remodeling process. A limitation of this technique is that despite injection of the cells to the damaged tissue, functional tissue generation is not guaranteed.[16] The rejection of the cells by the host's immune system can also be problematic as cell sources are typically from donors or sources other than the patients themselves.[17, 18] The new cells are also required to secrete their own ECM support system to fully integrate with the existing tissue and if the necessary cues are not received by the cells this may not occur.[19]

The second strategy of tissue engineering tackles the development of new tissues from a scaffold-based approach. In this approach, an unseeded scaffold, which can be based on natural[4, 5, 10] or synthetic material[1, 5], is implanted directly into the patient and relies on the already present neighboring cells to migrate and infiltrate the scaffold. The types of scaffolds used in this technique can range from natural polymers to synthetic materials, both of which maybe either stable or degradable. If cell migration cues on the scaffold are missing or the cells do not interact favourably with the material, infiltration may be poor, leading to a tissue with limited functionality and poor success rates.[20]

The last two paradigms of tissue engineering both rely on the use of an external cell source and scaffold to create the new tissue. The first type, cell-seeded scaffold implantation, involves transplanting the scaffold into the patient following seeding the cells onto the scaffold and allowing them to begin to adhere. In this method, the new tissue relies on the patient's body to act as the "bioreactor" for *in vivo* tissue maturation and remodeling, while the cell-seeded scaffold receives signals from the surrounding tissues and experiences mechanical forces and other stimuli to properly guide the tissue maturation process. In the second type, *in vitro* tissue engineering (**Figure 2.1**), the cell-seeded scaffold is allowed to mature in an artificial bioreactor *in vitro* prior to implantation in the patient. In the bioreactor, the scaffold and cells are subjected to appropriate forces, such as pulsatile flow and shear forces simulating those experienced in native vessels for the development of tissue-engineered blood vessels, in order to improve the maturation process to form completely functional tissues prior to implantation.[16] These stimuli, along with other factors including chemical signals, have been shown to affect the development of functionally viable tissues, especially the phenotype of vascular smooth muscle cells in vascular tissue engineering, and therefore are important in generating useful tissue-engineered graft materials.[21] These two methods often include the incorporation of biomolecules alongside the cells and scaffold that can improve cell-material interactions and enhance signaling for proper development of a functional tissue. These biomolecules are typically growth factors and other small protein molecules that can direct the proliferation, migration, and adhesion of cells onto the scaffold material.[22] The scaffolds themselves serve as a temporary template for the cells to proliferate on until they are capable of secreting their own natural ECM as support, and therefore must have the appropriate cell-material interactions and material properties. If biostable materials are selected, it is important to consider not only the mechanical properties of the scaffold material, but also the characteristics of the scaffold and newly secreted ECM together, making sure that these match the material properties of the native tissue. If a degradable material is chosen, it is ideal for the degradation rate of the material to be comparable to the rate of secretion of the ECM by the cells. Overall, ideal materials for all forms of scaffold-guided tissue engineering are yet to be realized and are still under investigation, which is the basis for this research.
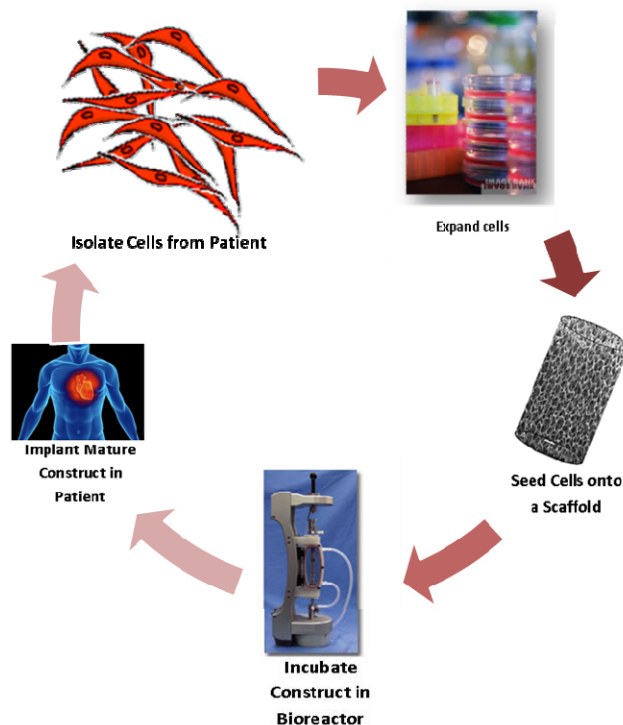
Figure 2.1: A diagrammatic representation of the *in vitro* tissue engineering process; where a cell-seeded scaffold is matured *in vitro* in a bioreactor prior to implantation into the patient.

2.2   Requirements of Tissue Engineering Scaffolds

In order for a scaffold to be successful in tissue engineering applications it should mimic the natural ECM of the tissue that is being repaired, regenerated, or replaced in both material and biological properties.[23, 24] By mirroring the ECM, the likelihood of developing functional tissues is improved by encouraging proper cell proliferation, migration, adhesion, and tissue assembly. The scaffolds themselves can be based on either natural polymers, such as collagen, elastin, chitosan, and hyaluronic acid, or synthetic polymers designed to mimic natural materials.[4, 5, 10] Another key factor to consider is the wide range of ECM morphology and structural arrangement across tissue types, which is important for directing proper cell growth, and should therefore be closely emulated in the natural and synthetic scaffolds using appropriate fabrication methods.[25] The biological and material properties of scaffolds, described in detail below, are one of the remaining critical issues in tissue engineering and serve as a guideline for the development of new scaffold biomaterials.[1]

The material properties that are important to consider are mechanical properties, porosity, processability, degradability, surface chemistry, and sterilizability. In terms of mechanical properties, the materials must be physically strong in order to withstand normal forces experienced within the specific type of tissue being engineered.[26] For example, in blood vessels the tissues experience shear forces and pulsatile blood flow, so the materials should have adequate tensile strength and elastic modulus to endure these forces.[27] The natural ECM is highly porous allowing for substantial cell infiltration and the development of complex tissues, likewise, the scaffold materials should be porous and give cells the necessary space to penetrate, explore, and adhere throughout the 3-D scaffold.[28-30] Along with high porosity, there should also be a high surface area-to-volume ratio and appropriate pore diameters to accommodate the type of cells seeded into the structure. This ensures that the cells are not only capable of infiltrating through the pores, but also have sufficient surface area on which they can adhere. It is also important that the pores of the scaffold are uniformly distributed across the 3-D construct and that the pores are interconnected, allowing the cells to explore freely throughout the entire matrix without encountering blockages. By selecting an appropriate fabrication technique, such as freeze drying, solvent casting/particulate leaching, or electrospinning, the desired characteristics of the scaffold can be achieved, such as a specific average pore size and structural arrangement,.[29-32] In solvent casting/particulate leaching methods, for example, the pore size of the resulting scaffold can be well controlled by selecting a porogen of appropriate diameter and selectively dissolving these out of the scaffold once the polymer matrix is fully set.[33, 34] Some limiting factors to consider when selecting a fabrication method is the processability of the material, including properties such a melting temperature (T_m), glass transition temperature (T_g), decomposition temperature (T_d), and solubility in appropriate solvents. For instance, solvent casting/particulate leaching cannot be employed if there are no two solvents available that selectively dissolve only the polymer in one and only the porogen in the other.[33] The degradability of scaffolds was described above in scaffold-based tissue engineering (Section 2.1), although if degradable materials are to be used, it should be noted that their degradation rate should coordinate well with the secretion rate of the new ECM by the cells. This will ensure adequate mechanical strength of the scaffold and that there is sufficient support

material for the proliferating cells.[32, 35] Cells not only migrate along the scaffold surface, but they also form focal adhesions and interact with the material itself. In order to improve cell-material interactions and encourage the proliferation and adhesion of the cells throughout the scaffold, it is important to include surface chemistry that is favourable for cells on the materials.[30, 36] In synthetic polymers this can be realized by incorporating functional handles on the material surface that allow for the attachment of biomolecules known to enhance cell-material interactions and cell proliferation. Lastly, as these materials will eventually be implanted in patients, they must be sterilizable to minimize the chance of bacterial and other small organismal infections in the patient from the tissue-engineered constructs.

The biological requirements of scaffolds have been touched upon in the material properties discussion, although the key traits they must possess include biocompatibility and promotion of cell proliferation and adhesion. Considering the fact that these materials will undoubtedly be used *in vivo*, they must not elicit immune response in the patients that would be harmful to their well-being, including any degradation products in the case of degradable materials. As such, materials are studied extensively *in vitro* and *in vivo* prior to clinical trials, exploring cytoxicity, cell morphology, and inflammatory response, to name a few.[37] The tissue-engineered product, including the scaffold, must also interact favourably and incorporate well with the existing tissues.

In conclusion, it is necessary to consider both the material and biological properties of both natural polymers and synthetic materials used for scaffold fabrication, like those described in the proceeding sections, to ensure they are well-suited for their intended tissue engineering application.

2.2.1 Natural Polymers

Natural materials for scaffolds are often based on ECM components such as collagen[3, 29, 38, 39], fibrinogen[40-42], hyaluronic acid[43-45] and glycosaminoglycans (GAGs)[46, 47] since these materials have the bioactivity and compatibility required of a scaffold biomaterial. Other natural materials such as chitosan, gelatin, and cellulose[4, 48] are also known to be highly biocompatible and therefore have been extensively studied for tissue engineering and

other biomedical applications. The main advantage of natural materials is that they intrinsically contain biological cues and signal molecules required for proper cell adhesion and migration, which are lacking with unmodified synthetic materials, thus limiting suitable cell-material interactions. Recently, Chen *et al.*[25] developed knit silk-collagen scaffolds for tendon tissue engineering applications, that when seeded with human embryonic stem cell-derived mesenchymal stem cells caused overexpression of scleraxis; a tendon differentiation marker protein by the cells ideal for tendon regeneration. Also, He *et al.* [49] fabricated aligned electrospun scaffolds of cellulose nanocrystal reinforced nanocomposites for tissue engineering applications. The scaffolds showed improved tensile and elastic properties and displayed non-toxic behavior in toxicity assays with primary human dental follicle cells. The main drawbacks of natural materials are their inadequate mechanical strength, uncontrolled degradation rates, poorly defined structure, batch-to-batch variability, and limitations with purification and sterilization processes leading to immunorejection.[1, 4] These limitations have directed researchers to investigate synthetic polymers as an alternative to natural materials.

2.2.2   Biodegradable Synthetic Polymers

Biodegradability is a desirable feature of a biomaterial used in tissue engineering since the goal for it is to act as a temporary scaffold, holding the growing tissue in place until the natural ECM has developed sufficiently. Beyond that point, the scaffold should break down into non-toxic degradation products capable of being disposed of by the body, leaving only the newly formed tissue. Synthetic polymers have the advantages of being relatively inexpensive and readily available over natural materials. They also have tunable material properties that can be matched to the intended application, whereas natural polymers have set material properties that limit their use in a range of applications. There are a wide variety of synthetic biodegradable polymers that have been, and continue to be, explored, including polyesters, polyanhydrides, polyacetals, and poly (α-amino acids).[50-55] Recently, Kim *et al.*[56] fabricated a poly(ethylene glycol) dimethacrylate and gelatin methacrylate-based hydrogel scaffold with controlled stiffness and degradation properties for use in vascular tissue engineering. The scaffold was shown to improve human umbilical vein endothelial cell attachment with elongated

morphology showing progress towards improved *in vivo* endothelialization of tissue-engineered small diameter vascular grafts, which has previously been a limitation in that field. Amino acid-based synthetic polymers have been of great interest for biomedical applications due to the fact that part of their degradation products are naturally occurring amino acids, which are handled well by the body. Poly(ester amide)s[53, 55] are one branch of these polymers and have been shown not only to be biocompatible with various cell types, but are also capable of being formed into 3-D constructs via various scaffold fabrication techniques. Despite their improvement over natural polymers with regards to degradation and mechanical properties, synthetic polymers have their own limitations. Control of mechanical and degradation properties of synthetic polymers are limited when the synthesis of materials is based on a single monomer, such as the case with polyesters. Another common problem with synthetic polymers, such as poly(lactic acid) (PLA), is the formation of acidic products during the degradation process which leads to diminished mechanical strength of the material and compromised cell function in the acidic environment.[7-9] Unfunctionalized synthetic materials have a tendency to interact poorly with cells due to the lack of biological signaling molecules present on the material surface, unlike the native ECM which is rich in biomolecules for proper cell-material interactions. The quest for biomaterials with tunable degradation rates and mechanical properties, but that also maintain cell function and lack the formation of toxic degradation products is an active area of research.[6, 57]

2.2.3   Biomimetic Materials

In order to improve the efficiency of interactions between synthetic polymers and cells, the materials are often modified, either chemically or physically, prior to seeding cells into the scaffold materials. Typical biological cues present on the natural ECM include hormones, growth factors, and other small protein molecules, which direct cell adhesion, proliferation, and migration. These molecules can be incorporated into synthetic materials via bulk or surface modifications, although bulk modifications can significantly alter the material properties of polymers.[11] Surface alterations, on the other hand, only slightly change the material properties of the polymers, thus maintaining the mechanical strength of the scaffolds after modification. Physical attachment of biomolecules is usually

achieved via adsorption, which relies on non-covalent bonding (hydrophobic interactions, hydrogen bonding, etc.). The main disadvantage of this method is that the biochemical signals can leach away from the scaffold when exposed to culture media, potentially resulting in a diminished effect of the biomolecule on cell-material interactions. When chemical modification is used instead, the molecules are retained at the scaffold surface by covalent linkages, which are not disrupted when the scaffold is submerged in culture media, leading to prolonged biomolecule-mediated cell-material interactions.[11] Chemical linking of the bioactive compound to the material is limited by the availability of functional groups on the surface of the materials which can be reacted with available reactive sites on the biomolecule. This can be overcome by developing biomaterials that contain reactive groups as functional handles for biomolecule conjugation, like the carboxylic acid group of glutamic acid that has been explored in this work.

2.2.4   Scaffold Fabrication

In order for a biomaterial to be useful in tissue engineering applications, it must be processable into a 3-D construct since natural tissues are inherently three-dimensional. Traditional fabrication methods that have been studied extensively include freeze-drying, fiber bonding, and solvent casting/particulate leaching.[33, 51, 58] More recently, researchers have been exploring electrospinning as a scaffold fabrication method due to its versatility in forming fibers with diameters from the micron range down to the nanometer range.[59, 60] The non-woven fibrous mats can also be collected and formed into specific construct shapes, such as tubular for application in vascular tissue engineering, based on the type of collector used and other spinning modifications.[11, 60] The electrospinning process involves the application of theories of electrostatic repulsion and surface tension, resulting in the formation of a very small jet of polymer solution, which is then collected as fibers on a collector. The general setup for electrospinning includes a high voltage DC power supply, a syringe pump and syringe containing the polymer solution, and a grounded collector upon which the fibers are deposited. A solution containing the desired concentration of polymer in a suitable solvent is prepared and loaded into a syringe secured on the syringe pump. A needle on the end of the syringe is attached to the high voltage source and a ground is attached to the collector, which can be stationary

or rotating. The syringe pump begins to push the polymer solution into the needle tip where the voltage induces a charge on the solution. Within the needle tip there is a fine balance between the surface tension forces keeping the solution together and the electrostatic repulsive forces driving the solution to spread. When the electrostatic forces exceed the surface tension, a polymer jet escapes the needle and begins to travel towards the grounded collector.[60, 61] During flight, the polymer jet experiences whipping instability, which increases travel time and path length to the collector. This increase in travel time allows sufficient time for the majority of the solvent to evaporate, leaving only the polymer behind as fibers on the collector and decreasing fiber diameter.[30, 62, 63] By optimizing the solution and processing variables (e.g. solvent, concentration, voltage, distance to the collector, flow rate, needle diameter, etc.), fibers with well-defined diameters and morphology are achievable, which in turn affects the construct's mechanical properties.[63-65] Overall, electrospinning is an ideal process for developing 3-D scaffolds for tissue engineering applications due to its relatively inexpensive setup and adaptability for numerous applications.

2.3   Synthesis of Polyphosphazenes

Sustained research towards new biomaterials for tissue engineering and regenerative medicine applications has led to the utilization of polyphosphazenes as a class of novel materials. Polyphosphazenes are comprised of an inorganic backbone of repeating phosphorus and nitrogen atoms with alternating single and double bonds (**Figure 2.2**, Structure 1c). Extending from each of the phosphorus atoms are two organic side chains, which can range from alkoxy and aryloxy substituents to amino acids, giving a large variety of potential polymers. Changing the organic side groups and their ratios, if multiple different side groups are attached to the same polymer backbone, allows substantial tunability of the physical, mechanical, and degradation properties of the material. Therefore, altering the organic substituents can be quite useful in tailoring the mechanical properties and degradation rates of the biomaterial to suit the desired tissue engineering application, such as bone tissue or blood vessels, which require drastically different properties.
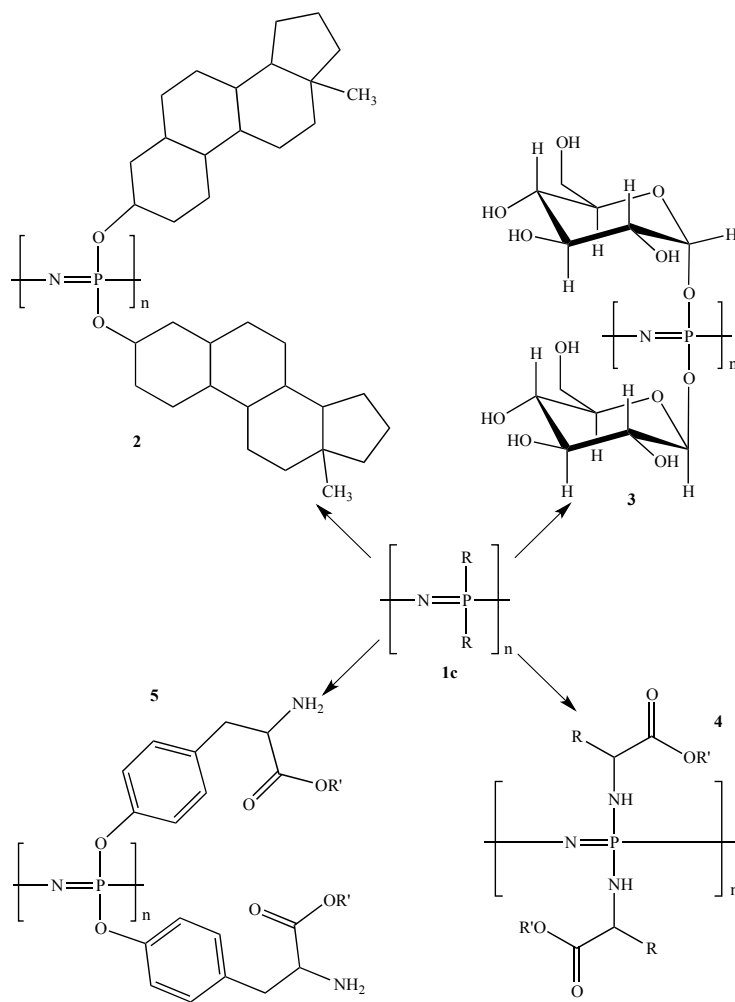
Figure 2.2: Structures of various polyphosphazenes including steroidal substituents (2), carbohydrates (3), amino acid esters (4), and side chain bound amino acid esters (5), to name a few.

The synthesis of polyphosphazenes, as shown in **Scheme 2.1,** are typically synthesized via a two-step reaction, beginning with the thermal ring opening polymerization of hexachlorocyclotriphosphazene (**1a**), the cyclic trimer, to the linear poly[(dichloro)phosphazene] (**1b**) precursor. Next, the organic side chains are attached to the polymer backbone through a nucleophilic macromolecular substitution of the organic substituents for the phosphorus-bound chlorine atoms.[66-68] The following two sections will succinctly describe the individual steps of poly(organophosphazene) synthesis, showing the different chemical routes previously reported and the vast range of materials that can be generated.

2.3.1　Polymerization to Poly[(dichloro)phosphazene]

2.3.1.1　Thermal Ring Opening Polymerization – Bulk Phase

Although the thermal ring polymerization of the trimer (**1a**) to linear poly[(dichloro)phosphazene] was attempted in the late 1800s by H. N. Stokes[69], a useful material that was soluble and capable of being functionalized was not realized until the 1960s. The initial thermal ring opening polymerization performed by Stokes led to a product that was insoluble, due to crosslinking, and that was readily susceptible to hydrolysis when exposed to moisture. In 1965, Allcock and Kugel[70] were able to synthesize linear poly[(dichloro)phosphazene] through a well-controlled thermal ring opening polymerization from the cyclic trimer hexachlorocyclotriphosphazene according to **Scheme 2.1**. The product obtained was soluble, allowing it to be modified further by macromolecular substitution of the reactive P-Cl bonds with organic and organometallic nucleophiles. The thermal ring opening polymerization technique developed by Allcock *et al.* is the most commonly used route to prepare the linear poly[(dichloro)phosphazene] precursor.[15, 67] A typical process involves reacting hexachlorocyclotriphosphazene trimer, which was purified via sublimation techniques prior to reaction, at 250°C over 5 days in an evacuated polymerization tube with continuous rocking of the reaction vessel. At this point, soluble poly[(dichloro)phosphazene] has been formed and can be purified and functionalized via the macromolecular substitution reaction (**Scheme 2.1**, **1a** → **1b**).[67] The yields obtained for these reactions reached a maximum of 75%.
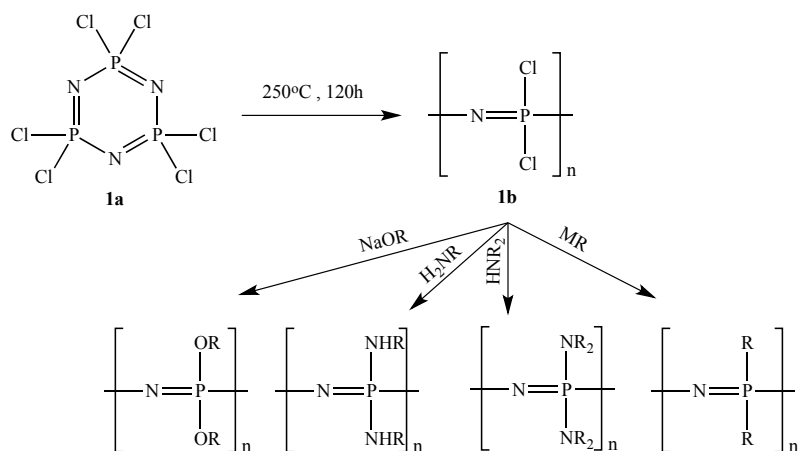
Scheme 2.1: Scheme showing the synthesis and functionalization of poly[(dichloro)phosphazene] (1b) in the overall synthesis of polyphosphazenes from hexachlorocyclotriphosphazene (1a) via the thermal ring opening polymerization method.[15]

Despite the success of this reaction, researchers have explored other ways of forming linear poly[(dichloro)phosphazene] in order to overcome some of the limitations of the thermal ring opening polymerization since it requires specialized equipment, the use of extreme temperatures, and high purity of the starting trimer.

2.3.1.2   Thermal Ring Opening Polymerization – Solution Phase

In 1990, Magill and co-workers[71] developed a new solution phase ring opening polymerization method for the synthesis of poly[(dichloro)phosphazene], which eliminated the need for a specialized oven that allowed for continuous rocking of the sample throughout the reaction. Also, the new Magill method substantially decreased the reaction time from 5 days down to roughly one hour. The Magill method used a three-neck round bottom flask as the reaction vessel, which allowed for the attachment of a reflux condenser and a gas inlet for N_2 bubbling (to protect the hydrolytically sensitive polymer from moisture). In their method, they dissolved the trimer in 1,2,4-trichlorobenzene and added small amounts of sulfamic acid ($HSO_3(NH_2)$) and calcium sulfate dihydrate (gypsum, $CaSO_4 \bullet 2\ H_2O$) as catalyst and promoter, respectively (**Scheme 2.2**). They allowed the mixture to react at reflux with dry N_2 bubbling and stirring until the solution was sufficiently viscous, which was approximately 45 to 60 minutes depending on the experiment. The experimenter needed to be attentive to the

reaction because if it was allowed to proceed beyond this point crosslinking occurred and the linear poly[(dichloro)phosphazene] was no longer useful as it was insoluble. They obtained yields of approximately 35% using this method. A major drawback of this method over the bulk polymerization is that it uses solvents, which are expensive and can be problematic for biocompatibility if they are not fully removed prior to cell seeding and implantation, and the necessity of the experimenter to be ever present, unlike the bulk phase TROP that can be controlled by a self-timed oven.
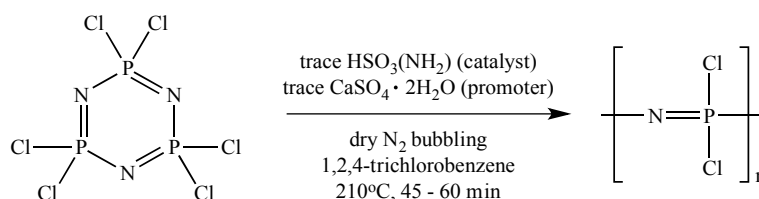
Scheme 2.2: Reaction scheme for the solution phase thermal ring opening polymerization of hexachlorocyclotriphosphazene (cyclic trimer) to linear poly[(dichloro)phosphazene] using a sulfamic acid catalyst and calcium sulfate dehydrate promoter – The Magill Method.

2.3.1.3   "Living" Cationic Polymerization

Polymerization methods that do not rely on the thermal ring opening of hexachlorocyclotriphosphazene have also been reported in the synthesis of poly[(dichloro)phosphazene].[72-80] In 1995, Allcock and co-workers [75] proposed a room temperature synthesis of linear poly[(dichloro)phosphazene] that overcame the obstacle of high temperature synthesis experienced with the previously described ring opening polymerization, both in the bulk and solution phase. In their research, they developed a synthesis of poly[(dichloro)phosphazene] from the phosphorus pentachloride (PCl$_5$) initiated polycondensation of trichlorotrimethylsilylphosphoranimine (Cl$_3$P=NSiMe$_3$). This reaction proceeded with trace amounts up to 2 equivalents of PCl$_5$ initiator for every 1 equivalent of Cl$_3$P=NSiMe$_3$, leading to the elimination of trimethylsilyl chloride (Me$_3$SiCl) as a by-product (**Scheme 2.3**). The use of trace amounts of PCl$_5$ allowed for quantitative conversion of the monomer to linear poly[(dichloro)phosphazene], although preparing reaction mixtures with specified equivalents of initiator to monomer increased the molecular weight of the resultant poly[(dichloro)phosphazene], with 2 equivalents of PCl$_5$ to every 1 equivalent of Cl$_3$P=NSiMe$_3$ producing the highest molecular weight

product. In bulk phase preparation, freshly distilled $Cl_3P=NSiMe_3$ and trace PCl_5 were reacted via a heterogeneous reaction in an evacuated, heat-sealed Pyrex tube, similar to those used for the bulk phase thermal ring opening polymerizations previously discussed, at room temperature over 24 hours.[70] Molecular weight control proved challenging in bulk phase polymerization, even as the ratio of initiator to monomer was varied, leading the researchers to look into solution phase polycondensation polymerization. In solution phase preparation, PCl_5 was added to a solution of $Cl_3P=NSiMe_3$ dissolved in dichloromethane (DCM) under nitrogen. The mixture was stirred and allowed to react for 24 hours at 25°C. The proposed reaction mechanism of the "living" cationic polymerization is presented in **Scheme 2.4**. The polycondensation reaction described above has also been studied in numerous other solvents to determine solvent effects and reaction kinetics.[72, 73] Although the reaction times of the polycondensation of $Cl_3P=NSiMe_3$ are much less than those used in bulk thermal ring-opening polymerizations, they require the use of PCl_5 which is a highly moisture sensitive compound that reacts violently with water and poses a potential safety concern. Also, the hydrolysis of PCl_5 leads to the formation of hydrogen chloride (HCl), which could cause problems with cell viability, as in the case of polymers that hydrolyze into acidic by-products, if the starting material is not reacted completely and remains in the product due to insufficient purification.[81]
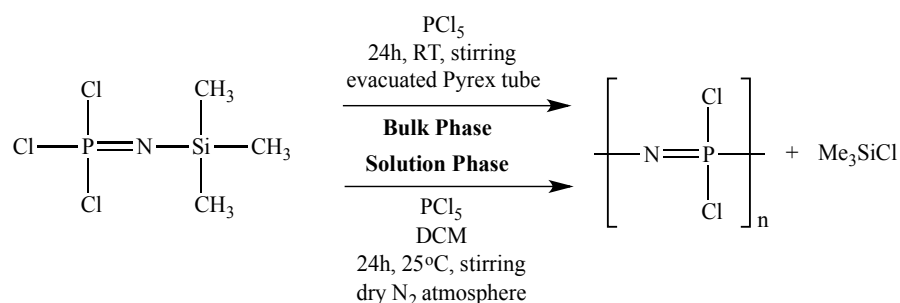
Scheme 2.3: Reaction scheme for the phosphorus pentachloride (PCl_5) initiated bulk and solution phase polycondensation of trichlorotrimethylsilylphosphoranimine ($Cl_3P=NSiMe_3$) to poly[(dichloro)phosphazene] ($[NPCl_2]_n$) – The "Living" Cationic Polymerization Method.
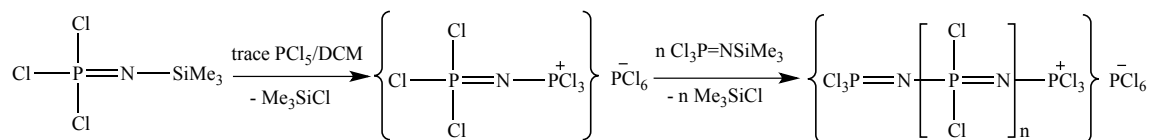
Scheme 2.4: Proposed cationic polymerization step-wise mechanism of the PCl$_5$ initiated polycondensation reaction of Cl$_3$P=NSiMe$_3$ to [N=PCl$_2$]$_n$.

2.3.1.4   One-Pot De Jaeger Polymerization

In the early 1980s, De Jaeger and co-workers[79, 80] developed an alternative route to poly[(dichloro)phosphazene] ([NPCl$_2$]$_n$) using trichloro-N-(dichlorophosphoryl)-monophosphazene (Cl$_3$P=NP(O)Cl), rather than the standard thermal ring opening polymerization. In their synthesis, Cl$_3$P=NP(O)Cl monomer is reacted in the bulk through a thermal polycondensation reaction that releases P(O)Cl$_3$ (**Scheme 2.5**). This reaction is performed in a three-neck reaction vessel with a dry nitrogen gas inlet, motorized stirring, and two condensers (one with oil cooling at 130°C and the other with traditional water cooling). The monomer was added to the vessel at 245°C and allowed to react for approximately 18 hours, at which point trichlorobiphenyl was added as a solvent to decrease the viscosity of the reaction mixture and improve the conversion of the monomer to poly[(dichloro)phosphazene]. The reaction mixture dissolved in trichlorobiphenyl was allowed to react for up to another 34 hours at 276°C. It is not well documented how the poly[(dichloro)phosphazene] polymer is collected from the reaction solution, although it is presumed that the solution was concentrated under reduced pressure and the polymer was reprecipitated with a miscible non-solvent. This method gives almost quantitative conversion of the monomer to linear poly[(dichloro)phosphazene] and an easily removable P(O)Cl$_3$ byproduct. Drawbacks of this reaction are the requirement to synthesize the monomer prior to its use in the polycondensation, which is time consuming and synthetically demanding. The monomer must also be extremely pure to ensure that the polymerization is successful. Furthermore, the addition of the trichlorobiphenyl solvent is not ideal for the development of biomaterials as it is highly toxic and may cause organ damage, and therefore if any remains in the material following purification it is likely to be cytotoxic. Another deterrent from using trichlorobiphenyl solvent is that it is extremely expensive, which is

not ideal if the ultimate intention is for these materials to be scaled-up for use in the development of clinically viable tissue-engineered grafts.
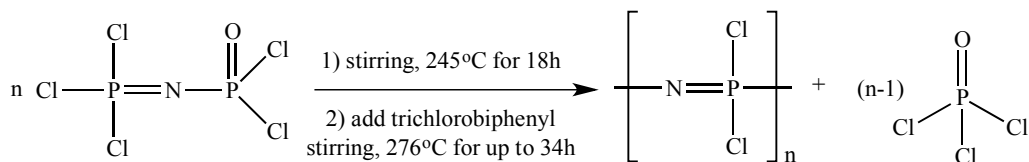
Scheme 2.5: Reaction scheme for the synthesis of poly[(dichloro)phosphazene] from the polycondensation reaction of Cl₃P=NP(O)Cl₂ – The De Jaeger Method.

Overall, the thermal ring opening polymerization involves the least synthetic chemistry and has the fewest by-products and potential solvent contaminants, which is ideal for materials intended for biomedical applications. Therefore, a facile thermal ring opening polymerization that does not require expensive equipment like rocking machinery within the oven or the use of a glovebox would be ideal in synthesizing polyphosphazenes for biomedical applications such as tissue engineering.

2.3.2   Macromolecular Substitution of Poly[(dichloro)phosphazene] with Organic Nucleophiles

Once high molecular weight linear poly[(dichloro)phosphazene] is synthesized, the polymer can be modified by substituting the phosphorus-bound chlorine atoms with organic side groups. The polymer undergoes a macromolecular substitution (**Scheme 2.1**, reaction of compound **1b** into four potential polyphosphazene structures) when subjected to organic and organometallic nucleophiles, forming a large class of polyphosphazenes as shown in **Figure 2.2**.[66, 67] All of the polyphosphazenes shown in **Figure 2.2** have one type of side chain throughout the entire polymer, although it has been shown that developing co-substituted materials with well-defined ratios of side chains are possible by controlling the amount and order of addition of the nucleophiles.[67, 68, 82] The modification of type and ratio of the side chains of the polymer affords the ability to fine-tune degradation rates and physical properties based on these substituents, which is key to the synthesis of a biomaterial suitable for tissue engineering and therapeutic delivery.[83]

The main substitution method for amino acid esters that has been described in the literature entails a two-step reaction in which the free base of the amino acid is generated prior to substitution by reacting the amino acid ester hydrochloride salt with a non-nucleophilic base, typically triethylamine (TEA, NEt$_3$).[12, 15, 55, 67, 83-94] Harry Allcock and co-workers, the largest players in the field of poly(organophosphazene)s, developed this method in the 1970s, and have been using it ever since.[95] In their synthetic scheme, the amino acid ester hydrochloride salt is suspended in anhydrous tetrahydrofuran (THF, b.p. 66°C) with an excess of TEA and allowed to reflux with stirring for 24 hours. The reaction mixture is then filtered and the filtrate is added to a flask containing poly[(dichloro)phosphazene] dissolved in anhydrous THF. This mixture is allowed to stir for an additional 48 hours at room temperature until complete substitution has been achieved. When preparing co-substituted poly[(amino acid ester)phosphazene]s, the same general procedure is followed to initially prepare the free bases of the amino acid esters although the substitution reaction is somewhat modified. In that case, the more bulky substituent is added first in stoichiometric amounts and allowed to react for a given time, based on the reactivity of the specific substituent, with the poly[(dichloro)phosphazene] precursor.[83] Next, the second substituent is added in excess to react at the remaining P-Cl bonds until the polymer is fully substituted. After substitution of either the mono-substituted polyphosphazene or co-substituted polyphosphazene is complete, the product is precipitated from the THF reaction solution using anhydrous hexanes. This process is repeated two additional times to remove the by-products and excess starting materials. The polymer is then occasionally purified further using cellulose membranes of specific molecular weight cutoffs. All of the aforementioned reactions and purification procedures are performed under moisture free conditions in either a glovebox or under dry nitrogen gas using standard Schlenk line techniques. Considering the requirement of advanced equipment, like a glovebox, making the polymers in this fashion is limited to researchers with access to these expensive pieces, which are not always available or are out of the budget, thus limiting research into novel polyphosphazene materials, which are suitable for biomedical applications, to research groups with access to this equipment and hindering the progress of the field as a whole.

Along with the reflux and room temperature mixing two-step substitution reaction described above, Allcock and co-workers also investigated the success of a two-step reaction at low temperatures as well.[95] In the low temperature synthetic scheme, the amino acid ester hydrochloride salt was reacted with excess triethylamine in refluxing dry benzene for 3.5 hours, at which point it was cooled and filtered. In a separate flask, poly[(dichloro)phosphazene] was dissolved in dry benzene and cooled to 0°C. The filtrate containing the free base of the amino acid ester was then added to this mixture drop-wise and the solution was allowed to stir for an additional 6 hours at 0°C, followed by 10 hours at room temperature. The final solution was filtered to remove insoluble salts and the solution was concentrated by rotary evaporation. The substituted polymer was collected as a solid by precipitation with *n*-heptane. This process of dissolution in benzene and repricipitation in *n*-heptane was performed twice more to satisfactorily purify the polymer. Another low temperature substitution method was studied by Parnigotto and co-workers,[77, 78] which used THF as the solvent rather than carcinogenic benzene and was successful in the synthesis of poly[(amino acid ester)phosphazene]s. An adapted two-step low temperature substitution was attempted in this work based on the low temperature variations reported in the literature.

2.4   Suitability of Polyphosphazene Biomaterials

In order for polyphosphazenes to be considered a suitable biomaterial they must be compatible with the biological environment they are intended to interact with.[2, 15, 96] They must also be either biostable or biodegradable into non-toxic degradation products. Bioerodible biomaterials are usually preferred since they leave only the natural tissue once the material has degraded, eliminating the long-term risk of immune response and potential negative outcomes.[2, 5, 13, 83-85, 88, 91, 93, 97-101] Lastly, the biomaterial must have mechanical properties that match or closely resemble those of the natural tissue so that issues such as compliance mismatch, a common problem, for example, in vascular tissue engineering, are reduced.[96, 102] In the next few sections, the current understanding regarding the biocompatibility, biodegradation, and mechanical properties of polyphosphazenes biomaterials is summarized. This section will focus on the suitability of polyphosphazenes, mainly poly[(amino acid ester)phosphazene]s, as biomaterials due

to their unique tunability of degradation and mechanical properties and non-toxic degradation products, making them useful in a wide range of biomedical applications including tissue engineering.[12, 15, 68]

2.4.1   *In Vitro* and *In Vivo* Biocompatibility

The cytocompatibility of amino acid ester functionalized polyphosphazene biomaterials was first studied by Laurencin *et al.*[88] who compared rat primary osteoblast adhesion to poly[(ethyl glycinato)phosphazene] (PNEG) with well-known poly(lactic acid-co-glycolic acid) (PLAGA) and poly(anhydrides).   Data from this study showed that the osteoblast cells adhered to the PNEG material to the same extent as the control materials for a period of 8 hours. The degradation of PNEG did not influence cell proliferation as it promoted cell growth to the same extent as the PLAGA control material. In a follow-up study[89], similar experiments on other ethyl glycinato/methyl phenoxy co-substituted polyphosphazenes using MC3T3-E1 cells (osteoblast precursor cell line from mice) were conducted. The results from this study also suggested that cells responded favourably to polyphosphazene materials, especially those with a high ratio of ethyl glycinato substituents, and that cell adhesion and proliferation characteristics were not diminished in comparison to tissue culture plate and PLAGA controls. The polymers with 50% and greater of ethyl glycinato substituents demonstrated improved cell growth in comparison to the tissue culture plate and the polymer with 25% ethyl glycinato substitution was only slightly less efficient than the tissue culture plate, although all of these were better than the PLAGA control, which has been widely accepted as a biocompatible material. Studies on co-substituted amino acid ester based polyphosphazenes containing an ethyl alanato substituent along with aryloxy substituents such as poly[(ethyl alanato)$_1$(ethyl oxybenzoate)$_1$ phosphazene] (PNEAEOB) and poly[(ethyl alanato)$_1$(propyl oxybenzoate)$_1$phosphazene] (PNEAPOB) demonstrated that neither PNEAEOB nor PNEAPOB posed a threat to cell growth, in comparison to the controls, as both materials were capable of promoting cell adhesion and proliferation.[93] Collectively, the results of the above studies from the Laurencin laboratory are promising since cell adhesion and proliferation are not affected in comparison to materials that have previously been extensively studied for their effect on cell viability.

Gumusderelioglu and Gur[103] performed a study that investigated the cytotoxicity of poly[bis(ethyl-4-aminobutyro)phosphazene] by analyzing the activity level of succinic dehydrogenase (SDH) through an MTT assay method. SDH plays a critical role in cellular metabolism and is therefore a good indicator of cytotoxicity.[104] For these experiments extracts collected from the incubation of the polymeric films with growth medium were added to 3T3 and HepG2 cells. For the negative control, extracts were collected from a polyethylene centrifuge tube that was incubated with the growth medium but lacked a sample of polymeric film.   It was shown that poly[bis(ethyl-4-aminobutyro)phosphazene] extracts did not significantly decrease cell viability in Swiss 3T3 and HepG2 cells in comparison to negative controls. The material maintained cell viability, as demonstrated by SDH activity level, greater than 80% of that of the control for all time points and for both cell types. This study was successful in showing the cytocompatibility of the material with respect to 3T3 and HepG2 cells, which are commonly used cell lines to study fibroblast and hepatocyte biology, respectively. The cytocompatibility of electrospun matrices of co-substituted poly[(amino acid ester)phosphazene]s towards rat endothelial cells was investigated by Carampin and co-workers.[105] They studied poly[(ethyl phenylalanato)$_{1.4}$(ethyl glycinato)$_{0.6}$phosphazene] for both cell adhesion and growth properties in comparison to a fibronectin-coated polystyrene tissue culture plate as the control. They found that the polymer only slightly improved cell adhesion (7% increase) in comparison to the culture plates, but that the polymer enhanced growth of the adhered cells by approximately 17%. These results reinforced the notion that polyphosphazenes could act as a biocompatible material for use in biomedical applications such as tissue engineering.

All of the aforementioned studies involved only *in vitro* analyses of the cytocompatibility of the polyphosphazenes despite the fact that their end goal is to be used as a biomaterial *in vivo*. Towards this end, *in vivo* studies of alanine-modified polyphosphazenes on rat and rabbit models for bone tissue engineering materials have been reported.[15, 93] In the rat model[93], subcutaneously implanted samples were monitored for biocompatibility through immune response. Inflammatory responses were categorized as minimal, mild, or moderate based on the accumulation of immune response cells (e.g. neutrophils/PMNs and lymphocytes) at the implantation site. It was observed that at two weeks post

implantation, [poly(ethyl alanato)phosphazene] (PNEA) induced a moderate inflammatory response that initially decreased to minimal at four weeks but then slightly increased to mild at 12 weeks. As for poly[(ethyl alanato)$_1$(p-methyl phenoxy)$_1$phosphazene] (PNEAmPh), the material caused a moderate inflammatory response at two weeks, which gradually decreased to a minimal response after 12 weeks. The poly[(ethyl alanato)$_1$(p-phenyl phenoxy)$_1$phosphazene] (PNEAPhPh) material elicited a mild initial response at two weeks, which slowly decreased to a minimal response at 12 weeks. Overall, the inflammatory responses for the PNEAmPh and PNEAPhPh were minimal suggesting that the materials are suitable for bone tissue engineering. The PNEA material triggered a greater inflammatory response than the two co-substituted polyphosphazenes although the response decreased over the time span of the study suggesting that, it too, is a good candidate. All three materials elicited immune responses that were acute and did not pose a long-term threat to the animals.

The potential utility of polyphosphazenes is not limited to bone tissue engineering. Langone *et al.*[106] conducted *in vivo* biocompatibility of polyphosphazenes as tubular nerve guides in rat models. Comparative studies of poly[(ethyl alanato)$_{1.4}$(imidazolyl)$_{0.6}$ phosphazene] (PNEAIL) nerve guides with traditional biostable silicone guides suggested the absence of inflammatory response to the polyphosphazene material after 30 and 60 days of implantation. Upon removal of the implanted nerve guide, it was noted that the stumps of the rat sciatic nerve, which had initially been transected, had reattached with components comprised primarily of nerve fiber bundles, akin the natural nerve tissue. This *in vivo* study suggested that PNEAIL was a biocompatible material, especially for use in nerve regeneration strategies, and highlights its potential utility in the future.

2.4.2   Biodegradability

Since it is desirable to use biodegradable biomaterials for tissue engineering and delivery of therapeutics many research groups have studied the degradation properties of polyphosphazenes.[13, 84, 85, 91, 93, 97, 98, 100, 101, 107] Polyphosphazenes are attractive because they have been shown to degrade into non-toxic by-products that are easily metabolized by the body. In the case of an amino acid ester phosphazene, these hydrolytic degradation products include the amino acid, the corresponding alcohol of the ester,

ammonia, and phosphates.[84] Unlike the acidic products produced from the hydrolysis of other polymers, the ammonia and phosphates act as a buffering system and prevent fluctuations in pH, which could otherwise be detrimental to the tissue.[108] Although the exact mechanism of degradation is not known, there are several pathways that have been proposed.[84] Overall, the first two steps of the degradation result in the hydrolysis of the ester of the amino acid, forming an alcohol, and detachment of the amino acid from the polyphosphazene backbone forming the amino acid itself. The backbone of the polyphosphazene is then hydrolyzed to phosphates and ammonia. The formation of phosphates during the degradation process was verified through the addition of silver nitrate or zirconyl chloride, which forms a yellow silver phosphate or white zirconyl phosphate precipitate, respectively.[84] The amino acids and ammonia degradation products can be demonstrated by ninhydrin test, which detects ammonia, primary, and secondary amines, whereas as ^{1}H nuclear magnetic resonance (NMR) spectroscopy can be utilized for detecting alcohols.

Another important factor with regards to biodegradability is the rate at which the material degrades since this can limit potential applications. It is important when designing a scaffold that the material degrades at a rate that is similar to the rate of tissue growth or therapeutic release rate depending on the application. For tissue engineering, if the scaffold material degrades too quickly there will be insufficient support for the underdeveloped tissue and mechanical weakness will ensue. If the material degrades too slowly or not at all, it may need to be surgically removed, which could in turn damage the neo-tissue and cause problems with mismatched mechanical properties relative to the natural tissue.[35] In order to determine the degradation rates of poly[(amino acid ester)phosphazene]s, the influence of changing the types and ratios of side chain substituents on the degradation properties of the polymers is an important factor. **Table 2.1** provides an overview of the degradation studies that have been performed on polyphosphazenes substituted with amino acid esters and other co-substituents.

Table 2.1: Summary of *in vitro* degradation studies of poly[(amino acid ester)phosphazene]s and their co-substituted polyphosphazenes. The ester refers to the chain attached to the carboxyl terminus of the amino acid. The detailed degradation profiles can be found in the cited references.

Amino Acid	Ester	Co-substituents	Study Length	Reference(s)
Glycine	Methyl		7 weeks	84
	Ethyl		35-120 days	84, 97, 107
		Alanine ethyl ester (50%)	7 weeks	83
		p-Methyl phenoxy (25-90%)	7 weeks	89
		Ethyl-2-(O-glycyl)lactate (0-25%) and Phenylalanine ethyl ester (70%)	120 days	107
	t-Butyl		5 weeks	84
	Benzyl		5 weeks	84
Alanine	Methyl		5 weeks	84
	Ethyl		7 weeks	83, 97
		p-Methyl phenoxy (50%)	7 weeks	83
		p-Phenyl phenoxy (50%)	7 weeks	83
	Benzyl		7 weeks	97
Valine	Methyl		5 weeks	84
Phenylalanine	Ethyl		5 weeks	84

In view of this, the degradation rates of poly[(amino acid ester)phosphazene]s with different amino acids and different esters of the amino acids were studied in solution- and solid-state, although solid-state degradation is more representative of how degradation would occur with *in vivo* scaffold materials and is the method that will be discussed.[84] The effect of changing the ester group was investigated using glycine based poly[(amino acid ester)phosphazene]s including poly[bis(methyl glycinat-N-yl)phosphazene] (PNMG), poly[bis(ethyl glycinat-N-yl)phosphazene] (PNEG), poly[bis(*tert*-butyl glycinat-N-yl)phosphazene] (PNtBG), and poly[bis(benzyl glycinat-N-yl)phosphazene] (PNBzG). In this systematic study, the molecular weight decline was in the order of PNBzG < PNtBG < PNEG < PNMG, with PNMG having the greatest decrease in molecular weight. This showed that as the hydrophobicity of the ester group increased (from methyl to benzyl), the molecular weight decline of the polymer decreased. The decreased molecular weight decline is due to the inability of water to approach the polymer due to its hydrophobicity, and therefore the hydrolysis of the material is hindered. The effect of changing the amino acid using poly[bis(methyl glycinat-N-yl)phosphazene] (PNMG), poly[bis(methyl alaninat-N-yl)phosphazene] (PNMA), poly[bis(methyl valinat-N-yl)phosphazene] (PNMV), and poly[bis(methyl phenylalaninat-N-yl)phosphazene] (PNMF) showed that the molecular weight decline

increased on the order of PNMF < PNMV < PNMA < PNMG. This trend was observed since the hydrophobicity of the polymer increased as larger non-polar side chain amino acids, like phenylalanine, were incorporated into the polyphosphazene. This study was a good initial demonstration of the biodegradability and hydrolysis properties of different poly[(amino acid ester)phosphazene]s, although a more suitable degradation medium would be phosphate buffer solution (PBS) at 37°C, which is more representative of the body fluid pH, temperature, and ion concentrations.

The effect that types of side groups had on the degradation rates of L-alanine co-substituted polyphosphazenes, specifically PNEA, poly[(ethyl alanato)$_1$(ethyl glycinato)$_1$phosphazene] (PNEAEG), PNEAmPh, and PNEAPhPh was also reported in a separate study.[83] As may be expected the ethyl glycinato substituted phosphazene (PNEAEG) had the fastest molecular weight decline, where as the biphenyl substituted phosphazene (PNEAPhPh) had the slowest molecular weight decline. The PNEAEG material hydrolyzed so quickly that molecular weight could not be evaluated beyond week two of the degradation study. It was noted that the pattern of molecular weight decline showed a quicker degradation rate for the smaller, more hydrophilic substituent polymers as compared to those substituted with large bulky hydrophobic substituents. Compared to imidazolyl side groups, increasing the amount of ethyl glycinato groups increased the degradation rate of the polymer, indicating that the incorporation of less sterically hindered, more hydrophilic groups causes the polymers to degrade more quickly.[89] The results of the study were successful in demonstrating the tunability of degradation properties of co-substituted polyphosphazenes, which is a key requirement in the development of a biomaterial for tissue engineering applications. Overall, this study effectively showed the ability to tune degradation rates of poly[(amino acid ester)phosphazene]s through careful selection of side group substituents. *In vivo* degradation studies showed substantial decline in molecular weight for the PNEA and PNEAmPh implants after 12 weeks, 80% and 98%, respectively.[93] PNEAPhPh, on the other hand, did not experience as great of a molecular weight decline as the other two implants and had a molecular weight decline of only 63% after 12 weeks. This is presumably due to the increased hydrophobicity of the biphenyl substituent, which limits the approach of water to the polymer backbone and therefore slows its hydrolysis. This

study proves the *in vivo* biodegradability of poly[(amino acid ester)phosphazene]s, as well as their biocompatibility. The results of this study should be taken with caution since the implant in this cited study was designed for bone tissue engineering applications and as such, it is implanted into a region of the rat where bone tissue is the predominant tissue type. Naturally occurring enzymes, which have the potential to significantly influence degradation rates if they recognize the materials, have different abundances across different types of tissues. Therefore, if the poly[(amino acid ester)phosphazene]s investigated in this study are to be applied to other tissue engineering applications, such as vascular tissue engineering, their degradation rates in those tissues may vary dramatically from those presented here due to differences in enzymatic degradation. The relative abundance of water in a tissue also determines rates of hydrolysis and the materials could therefore show significantly different hydrolytic degradation rates in different tissues.

Other studies were conducted on the effects of changing ratios of substituents on the degradation rates of the polymers.[99] Mass loss measurements following PBS incubation focused on co-substituted polyphosphazenes of ethyl 2-(O-glycyl)lactate and ethyl glycinate. Decreasing the ratio of ethyl glycinate: ethyl 2-(O-glycyl)lactate, for materials with varying side chain ratios between 100% ethyl glycinate: 0% ethyl 2-(O-glycyl)lactate to 75% ethyl glycinate: 25% ethyl 2-(O-glycyl)lactate, increased the mass loss rate of the polymer. This is due to the increased hydrolytic sensitivity of ethyl 2-(O-glycyl)lactate, in comparison to ethyl glycinate, which encourages polymer degradation and therefore mass loss as well. Even though mass loss is not a direct indication of molecular weight decline[83], it is still a good indicator of the *relative* degradation rates of the polymers and as such, it can be approximated that polymers with a higher ratio of ethyl glycinato substitution degrade less quickly than those with increased levels of ethyl 2-(O-glycyl)lactate. This study was useful in demonstrating the effect that varying ratios of substituents with different hydrolysis-sensitivities and solvation properties has on the degradation rates of the polymers, which can be useful for tailoring degradation properties of co-substituted polyphosphazenes according to their specific biomedical applications.

Taken together, these studies have been able to demonstrate not only that poly[(amino acid ester)phosphazene]s are biodegradable, but also that their degradation rates can be tuned by changing a variety of factors, such as type and ratio of side groups. The fact that bioerodability studies have been performed *in vitro* in body fluid simulating solutions and *in vivo* in rat models suggests that these polyphosphazene materials are suitable for use in tissue engineering applications such as scaffold biomaterials as well as for other biomedical applications that require the use of degradable materials.

2.4.3 Mechanical Properties

In order to produce clinically viable tissue engineered products, the mechanical properties of the constructs must match the properties of the natural tissues. If the mechanical properties, such as compressive strength and tensile strength, are not comparable to those of native tissues, problems with mismatch arise which often lead to failure of the tissue-engineered construct.[109-112] There have been only a limited number of studies carried out to investigate the mechanical properties of poly[(amino acid ester)phosphazene] materials. One such study was conducted by Sethuraman *et al.*[94] who investigated the mechanical properties of alanine-based polyphosphazenes for their application as bone tissue engineering biomaterials. For these studies polyphosphazenes were compared with the current standard for bone tissue engineering applications, PLAGA (85% lactic acid:15% glycolic acid). Cylindrical discs of each polymer were initially subjected to a compressive force of 1500 pounds per square inch (psi) for 15 min and analyzed using a uniaxial compressive testing instrument set with the following parameters, 500N load cell and 10 mm/min compression rate, until material failure. The compressive strengths of PNEA and PNEAmPh were comparable to that of PLAGA (34.9 ± 5.7 MPa), with compressive strengths of 46.61 ± 17.56 MPa and 24.98 ± 11.26 MPa, respectively. PNEAPhPh on the other hand had a compressive strength that was significantly higher than that of PLAGA due to the large aromatic groups increasing steric bulk and decreasing torsion of the polymer backbone. Together these increase the rigidity of the material and modulate its compressive properties. Therefore, it can be noted that the mechanical properties, like the degradation properties, of polyphosphazene materials can be tailored based on their proposed applications by changing the side group substituents.

The tensile strength and elasticity of several L-alanine based polyphosphazene materials (namely, PNEAEG, PNEA, PNEAmPh, and PNEAPhPh) were determined using micro-tensile testing techniques.[94] It was shown that increasing the steric bulk of the co-substituent increased both the tensile strength and elasticity of the material with more of an impact being observed as the side chain is changed from a small amino acid such as glycine or alanine ethyl ester, such as in PNEAEG and PNEA, to large aromatic substituents, such as in PNEAmPh and PNEAPhPh. This is because introducing large aryloxy substituents affects the glass transition temperature and molecular weight of the polymer, which in turn affects the mechanical properties of the material. Overall, this study shows how the mechanical properties of a polyphosphazene material can be tailored simply through co-substitution of large aromatic groups alongside amino acid esters.

Both of the above studies showed that changing the types and ratios of side group chemistries of polyphosphazene materials can modulate mechanical properties, such as compressive strength, tensile strength, and elasticity. Therefore, the mechanical properties of these materials can be tuned to suit the intended application, making polyphosphazenes useful as biomaterials in a wide range of different biomedical applications. One concern here is that changing the side groups not only affects mechanical properties but also degradation rates and therefore adapting the side chains to obtain suitable mechanical properties may cause the degradation rate of the material to be either too fast or too slow for the application, which is undesirable. As such, it is suggested that research into other methods to control mechanical properties that do not influence erosion properties should be developed. For example, it may be useful to investigate the effects of different processing methods or scaffold preparation techniques (e.g. electrospinning versus solvent casting and particulate leaching) on mechanical properties.

2.5   Objectives and Rationale

As was shown in the preceding literature review, poly(organophosphazene)s have been studied extensively for their use in many biomedical applications, including tissue engineering.   To date, the majority of research surrounding poly[(amino acid

ester)phosphazene]s focuses on orthopedic tissue engineering and drug delivery applications with limited use in vascular tissue engineering.[87-89, 93, 94, 113] A potential reason as to why these materials have been limited to mainly bone applications is that the synthesis of the precursor material (poly[(dichloro)phosphazene]) requires either extensive chemical synthesis and/or expensive specialized equipment before the actual poly[(amino acid ester)phosphazene] materials can be realized. By optimizing a thermal ring opening synthesis process that requires less harsh reaction conditions and fewer costly pieces of machinery, thus making it more accessible to researchers like ourselves, poly[(amino acid ester)phosphazene]s may be investigated for other biomedical applications, including vascular tissue engineering. It is also hoped that the substitution of poly[(dichloro)phosphazene] with organic nucleophiles can be simplified into a one-pot reaction and eliminate the necessity of liberating the free base of the amino acid ester at elevated temperatures prior to reaction. Once these two techniques are developed, it is proposed that they will be used to synthesize novel co-substituted poly[(amino acid ester)phosphazene]s that incorporate amino acids that have functional side chains (e.g. glutamic acid, aspartic acid, and lysine) and can be used for further surface modification of the materials. The functional handles that will be made available through the deprotection of the side chains will allow for the conjugation of biomolecules that are known to enhance cell-material interactions, which is ideal in developing biomaterials for scaffolds. Lastly, considering that scaffolds are required to have a 3-D configuration for vascular graft formation, electrospinning of the poly[(amino acid ester)phosphazene]s should be investigated.

In view of the above rationale, the objectives of this work were to:

- Develop a facile polymerization technique and compare substitution methods for the synthesis of poly(amino acid ester)phosphazenes

- Prepare the benzyl side chain protected glutamic acid ethyl ester via esterification and deprotection

- Synthesize and characterize (FTIR, NMR, TGA, DSC, and GPC) a family of non-functional and functional poly[(amino acid ester)phosphazene]s

- o Non-functional amino acid ethyl esters: alanine, phenylalanine, methionine

- o Functional amino acid ester: benzyl side chain protected glutamic acid ethyl ester

- Evaluate cytotoxicity of functional and non-functional poly[(amino acid ester)phosphazene]s on 2-D films

- Fabricate a polyphosphazene-based 3-D non-woven fibrous mat via electrospinning

Chapter 3

3   Materials and Methods

3.1   Thermal Ring Opening Polymerization (TROP)

3.1.1   Materials

The hexachlorocyclotriphosphazene cyclic trimer was purchased from Sigma Aldrich (Milwaukee, WI) and Alfa Aesar (Ward Hill, MA). Anhydrous tetrahydrofuran (THF), glass distilled hexanes-190, 2-propanol (^{i}PrOH), reagent grade hydrochloric acid (HCl), and potassium hydroxide (KOH) were obtained from Caledon Labs (Georgetown, ON). Krytox Performance Lubricant GPL207 high temperature grease was acquired from DuPont (Wilmington, DE). All chemicals and solvents were used as received without further purification.

3.1.2   Equipment

The polymerizations were performed in a VWR Symphony Horizontal Air Flow Oven (50L, 1.75cuft, 120V, 60Hz) purchased from VWR International (Radnor, PA). The glass reaction vessels and stainless steel vial rack shown in **Figure 3.1** were manufactured by the glass blowing and engineering machine shops at The University of Western Ontario (London, ON), respectively.
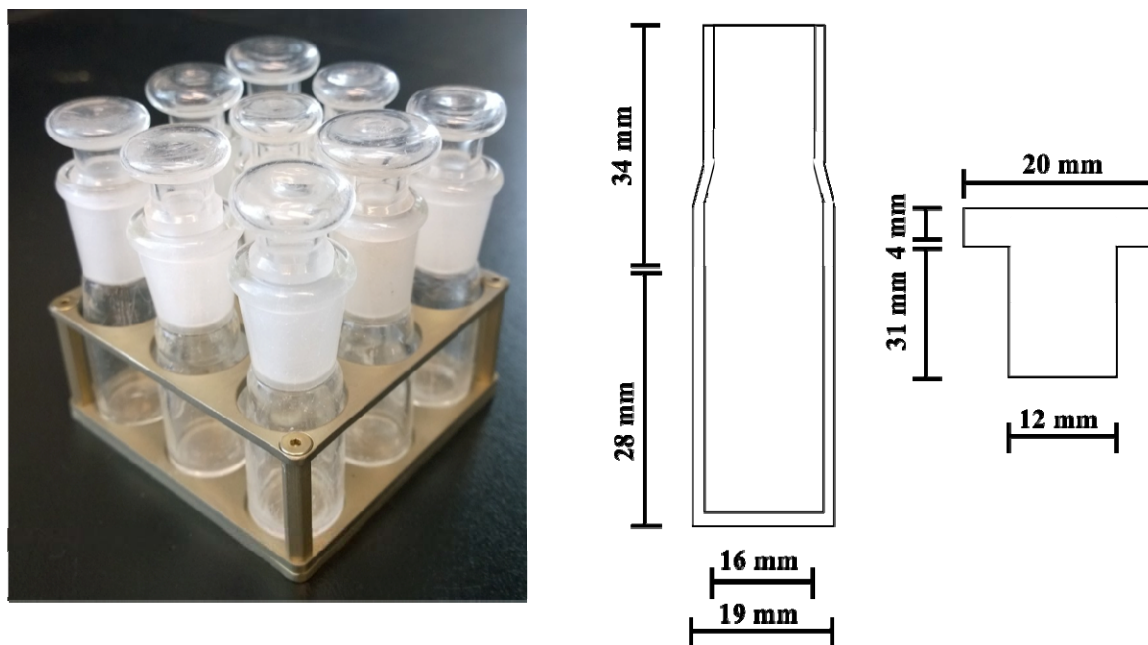
Figure 3.1: The glass vials and stainless steel vial rack that were manufactured in-house for the facile thermal ring opening polymerizations. The schematic on the right side shows approximately dimensions of the glass vials and stoppers used as the reaction vessels.

3.1.3   Method

The polymerizations were performed in batches of three reaction vessels, with each reaction vessel containing approximately 1.06g (3.05mmol, 1.0 equiv) of hexachlorocyclotriphosphazene. The vessels were prepared by weighing the trimer into the glass vial, lubricating the glass stopper with sufficient Krytox grease, and sealing the vial with the glass stopper. The vessels were then placed in a line in the vial rack and the rack was inserted into the preheated high temperature oven set at 230 °C with the vessels spanning from left to right in the oven and the rack being positioned approximately in the center of the oven. The optimized reaction scheme for the ring opening polymerization is presented in **Scheme 3.1**. A programmable timer on the oven was used to control the length of the reaction, where the oven would stop heating and would cool to room temperature after the specified time. It took approximately 6 minutes for the oven to cool to temperatures below 200 °C, which was likely too cool for polymerization to occur. Once the oven had cooled, the samples were removed from the oven and scrapped from the inside of the vials into a 50mL centrifuge tube, where they were then purified by

dissolving the product in minimal anhydrous THF and reprecipitating the polymer in hexanes. The crude product dissolved in anhydrous THF was filtered to remove insoluble impurities prior to repricipitation with hexanes. This dissolution/reprecipitation process was repeated three times. The poly[(dichloro)phosphazene] (PDCP) material is highly reactive and cannot be dried completely due to its quick decomposition when overnight drying under vacuum was attempted. This was also presumably due to rapid hydrolysis of the material upon exposure to even atmospheric moisture and therefore the material must be used in a substitution reaction immediately after its purification.

hexachlorocyclotriphosphazene
(cyclic trimer)

polydichlorophosphazene
(linear precursor, PDCP)
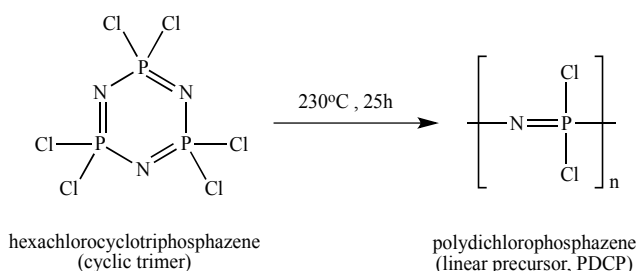
Scheme 3.1: Reaction scheme for the facile thermal ring opening polymerization (TROP) of hexachlorocyclotriphosphazene to linear poly[(dichloro)phosphazene] (PDCP).

After recovery of the PDCP product and in between polymerizations, the glass reaction vessels were cleaned using a base bath, water rinse, acid bath, water rinse, and drying method to remove any residual polymer or grease. The base bath used was a concentrated solution of KOH in 50/50 mixture of ^{i}PrOH and deionized (DI) H_2O. The acid bath was a concentrated solution of HCl in DI water. Typically, the reaction vessels were allowed to soak in the base bath overnight, were rinsed with DI water, and were scrubbed clean using a small wire scrub brush. The vessels were then rinsed with more DI H_2O and allowed to soak in the acid bath for a minimum of 2 hours. Upon removal from the acid bath, the vials were rinsed with DI H_2O one final time and were dried in a drying oven prior to their re-use.

3.2 Macromolecular Substitution of Non-Functional Amino Acid Esters

3.2.1 Materials

Anhydrous THF and glass-distilled hexanes were again acquired from Caledon Labs. All non-functional amino acid esters, L-alanine ethyl ester hydrochloride (H-Ala-OEt•HCl), L-phenylalanine ethyl ester hydrochloride (H-Phe-OEt•HCl), and L-methionine ethyl ester hydrochloride (H-Met-OEt•HCl), were from Alfa Aesar (Ward Hill, MA). Triethylamine (NEt$_3$) was purchased from Sigma Aldrich. The poly[(dichloro)phosphazene] (PDCP) material was obtained from the thermal ring opening polymerization described above. All chemicals and solvents were used as received.

3.2.2 Sample Nomenclature

The amino acid ester polyphosphazenes were named systematically as follows PP-A$_{100}$, where the PP indicates that the backbone is a polyphosphazene and the A$_{100}$ represents 100 mole percent (mol %) substitution with L-alanine ethyl ester substituents. In all cases the amino acid is connected to the phosphorus atoms of the polyphosphazene backbone through the N terminus amino group. Note that the one-letter abbreviations for alanine, phenylalanine, methionine, and glutamic acid are A, F, M, and E, respectively, although through out this work A, F, and M, represent the ethyl esters of the L-amino acids and E* represents the ethyl ester of L-glutamic acid which has its side chain carboxylic acid protected with a benzyl group.

3.2.3 Methods

Described in the next three sections are three different substitution methods performed at different temperatures and with or without the initial reaction to liberate the free base of the amino acid prior to substitution. These were variations performed to determine their influence, if any, on the poly[(amino acid ester)phosphazene] products.

3.2.3.1 Low Temperature Two-Step Reaction (LT 2S)

H-Ala-OEt•HCl (1.70g, 11.1mmol, 2.6 equiv) was added to 10mL of THF and mixed with an excess (x.s.) of NEt$_3$ (2.0mL, 1.5g, 14mmol, 3.3 equiv) for 1 hour at room temperature in a rubber septum sealed round bottom flask (**Scheme 3.2, Mixture A**). In a separate flask, PDCP (0.50g, 4.3mmol of NPCl$_2$ units, 1.0 equiv) recovered from the thermal ring opening polymerization step was dissolved in 5mL of THF. **Mixture A** was cooled in an ice bath to 0°C and the PDCP solution was added drop-wise through the rubber septum over a time span of 1 hour (**Mixture B**). **Mixture B** was then allowed to stir at room temperature for 48 hours after which the solution was filtered and the product was collected by repricipitation in hexanes. The product was purified by dissolving the polymer in anhydrous THF and reprecipitating in hexanes 3 times. The collected product was dried under vacuum at room temperature overnight. Percent yield was determined based on the approximate weight of PDCP. This technique slightly underestimates the yield collected as the PDCP is incapable of being dried completely and therefore the initial mass of PDCP added also includes the mass of residual solvents (THF and hexanes) from its purification after the thermal ring opening polymerization. **Scheme 3.2** below shows the overall synthetic scheme and the chemical structures of the starting materials and polyphosphazene product.
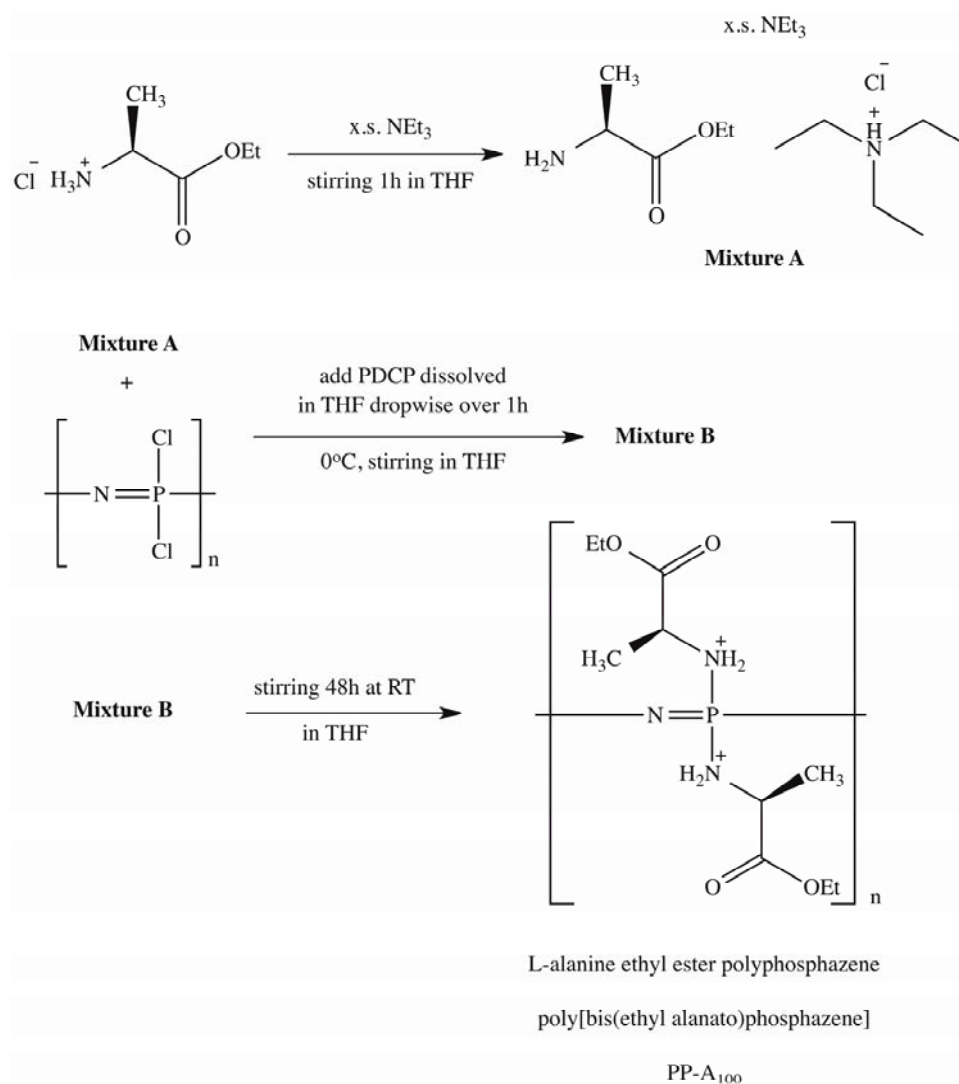
Scheme 3.2: Reaction scheme for the low-temperature macromolecular substitution of L-alanine ethyl ester with poly[(dichloro)phosphazene] (PDCP) forming poly[bis(ethyl alanato)phosphazene] (PP-A$_{100}$).

This method was also utilized in the synthesis of L-phenylalanine ethyl ester (PP-F$_{100}$) and L-methionine ethyl ester (PP-M$_{100}$) polyphosphazene materials (**Figure 3.2**), substituting H-Phe-OEt•HCl and H-Met-OEt•HCl for H-Ala-OEt•HCl, respectively.
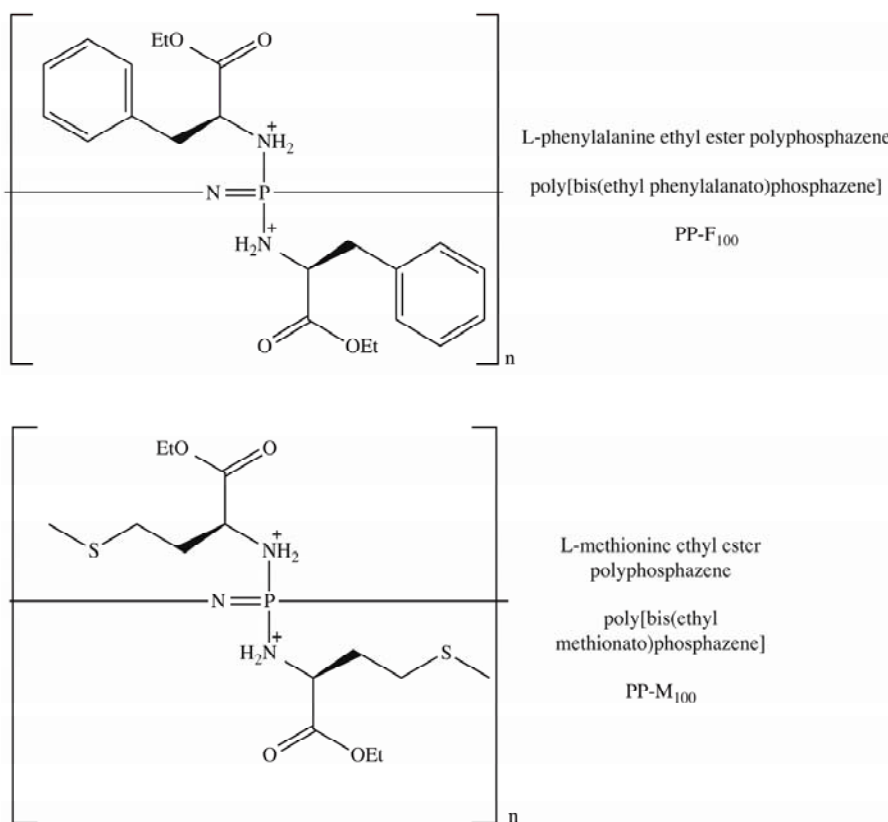
Figure 3.2: Chemical structures of the L-phenylalanine ethyl ester (PP-F$_{100}$) and L-methionine ethyl ester (PP-M$_{100}$) based polyphosphazene materials.

3.2.3.2   One-Pot Room Temperature Reaction (1P RT)

In an effort to simplify the substitution process the amino acid ester hydrochloride salt, triethylamine and poly[(dichloro)phosphazene] were all added to the reaction flask at the same time and allowed to stir for 72 hours at room temperature. H-Ala-OEt•HCl (1.70g, 10.4mmol, 2.6 equiv) was initially added to 10mL of anhydrous THF and sealed with a rubber septum. In a separate flask, poly[(dichloro)phosphazene] (0.50g, 4.3mmol of NPCl$_2$ units, 1.0 equiv) collected from the thermal ring opening polymerization was dissolved in 10mL of THF. Next, triethylamine (2.0mL, 1.5g, 14mmol, 3.3 equiv) and the PDCP solution were both added through the septum into the reaction flask containing the amino acid ester and THF solution. This mixture was stirred at room temperature for 72 hours (**Scheme 3.3**). The polyphosphazene product was purified in the same manner as the LT 2S method discussed above.
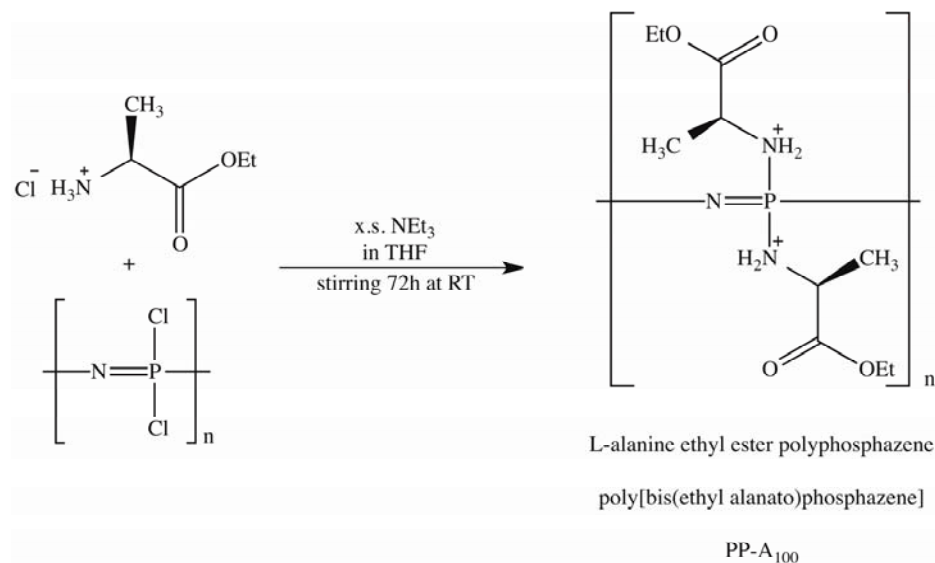
Scheme 3.3: Reaction scheme for the one-pot room temperature synthesis of poly[bis(ethyl alanato)phosphazene] (PP-A$_{100}$) from L-alanine ethyl ester hydrochloride (H-Ala-OEt•HCl) and poly[(dichloro)phosphazene] (PDCP).

As with the LT 2S method, L-phenylalanine ethyl ester and L-methionine ethyl ester based polyphosphazenes were also synthesized by replacing H-Ala-OEt•HCl with H-Phe-OEt•HCl and H-Met-OEt•HCl, respectively (**Figure 3.2**).

3.2.3.3   Room Temperature Two-Step Reaction (RT 2S)

The last reaction method similar to the widely used macromolecular substitution technique found in the literature, which involves refluxing the amino acid ester hydrochloride salt with triethylamine to liberate the free base of the amino acid ester prior to its addition to poly[(dichloro)phosphazene]. H-Ala-OEt•HCl (1.70g, 10.4mmol, 2.6 equiv) was added to a round bottom flask with 2mL of NEt$_3$ (1.5g, 14mmol, 3.3 equiv) and 10mL of anhydrous THF (BP 66°C). The mixture was refluxed for 24 hours and the product was filtered. The filtrate containing the free base of the amino acid ester was collected and added to another round bottom flask containing 0.50g of PDCP (4.3mmol of NPCl$_2$ units, 1.0 equiv) dissolved in 10mL of THF. This mixture was allowed to stir for 48 hours at room temperature (**Scheme 3.4**). The resulting polyphosphazene material was collected and purified using the same techniques used in the LT 2S and 1P RT methods.
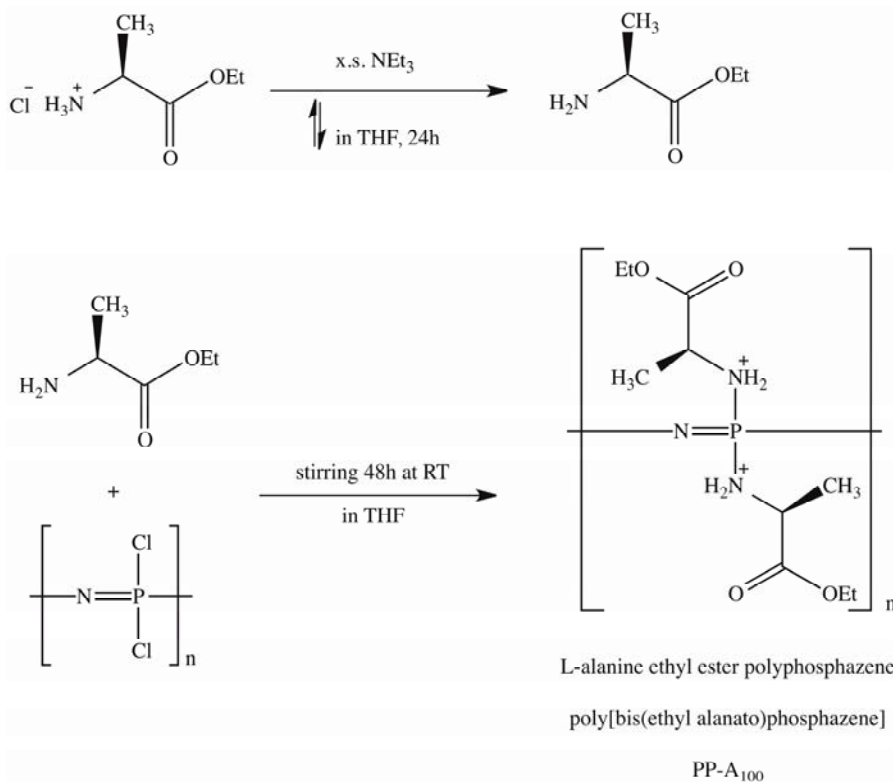
Scheme 3.4: Reaction scheme for the room temperature two-step substitution of poly[(dichloro)phosphazene] (PDCP) with L-alanine ethyl ester (H-Ala-OEt•HCl).

The L-phenylalanine ethyl ester (PP-F$_{100}$) and L-methionine ethyl ester (PP-M$_{100}$) polyphosphazene equivalents were made using the same reaction scheme and substituting H-Ala-OEt•HCl for H-Phe-OEt•HCl and H-Met-OEt•HCl, respectively (**Figure 3.2**).

3.3   Preparation of Glutamic Acid Ethyl Ester (E*)

3.3.1   Materials

Glass distilled dichloromethane (DCM), ethyl acetate (EtOAc), trifluoroacetic acid (TFA), sodium bicarbonate (NaHCO$_3$), and anhydrous magnesium sulphate (MgSO$_4$) were all obtained from Caledon Labs. Anhydrous ethanol (EtOH) was acquired from Commercial Alcohols Inc. (Brampton, ON). The DCM and EtOH were dried overnight over molecular sieves, 4Å and 3Å (Caledon Labs), respectively, prior to their use. 4-Dimethylaminopyridine (DMAP) and 1-(3-Dimethylaminopropyl)-3-ethylcarbodiimide hydrochloride (EDCI) were purchased from Alfa Aesar. Protected functional amino acids, N-α-fluorenylmethyloxycarbonyl-L-glutamic acid γ-benzyl ester (Fmoc-

Glu(OBzl)-OH) and N-α-*tert*-butyloxycarbonyl-L-glutamic acid γ-benzyl ester (Boc-Glu(OBzl)-OH), were procured from EMD Millipore Corporation (Chicago, IL). All chemicals and solvents were used as received unless stated otherwise.

3.3.2   Methods

Before reacting the functional glutamic acid ethyl ester with poly[(dichloro)phosphazene], the glutamic acid must first be converted to an ester at the carboxyl terminus (COOH) and the amino terminus (NH$_2$) must be deprotected to obtain the free base. See **Figure 3.3** for the chemical structures of the Fmoc and Boc protected glutamic acid starting materials noting that the esterification reaction will modify the COOH group to an ethyl ester.
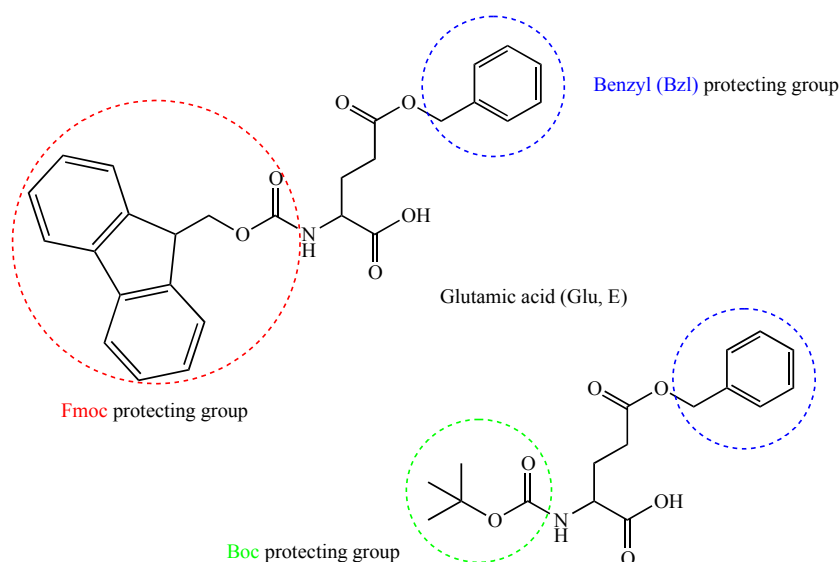
Figure 3.3: Chemical structures of Fmoc- and Boc-protected glutamic acid that will be esterified to their ethyl ester amino acid derivatives.

3.3.2.1   Ethyl Esterification of Fmoc-Glu(OBzl)-OH and Boc-Glu(OBzl)-OH

The Fmoc-Glu(OBzl)-OH (1.0g, 2.2mmol, 1.0 equiv) amino acid, EDCI coupling agent (0.46g, 2.4mmol, 1.1 equiv), and DMAP (0.024g, 0.2mmol, 0.1 equiv) catalyst were added to a 25mL round bottom flask, evacuated, and placed under inert N$_2$ atmosphere using a standard Schlenk line. Next, 8mL of dry DCM and 0.15mL of anhydrous EtOH (0.12g, 2.5mmol, 1.1 equiv) were added to the reaction flask and the mixture was allowed to stir at 0°C in an ice bath for 3 hours, followed by stirring for another 3 hours at room

temperature (**Scheme 3.5**). The mixture was concentrated *in vacuo* using a rotary evaporator followed by drying overnight on the in-house vacuum line. The crude product was weighed and taken up in 20mL of a 50/50 mixture of EtOAc and DI H_2O for purification. The solvent mixture containing the product was washed three times with 15mL of a saturated solution of $NaHCO_3$ in DI H_2O and three times with 15mL of pure DI H_2O at 60°C to remove water-soluble impurities. The EtOAc layer was collected and dried over $MgSO_4$ and concentrated *in vacuo*. The same procedure was used to prepare Boc-Glu(OBzl)-OEt by replacing Fmoc-Glu(OBzl)-OH with Boc-Glu(OBzl)-OH.
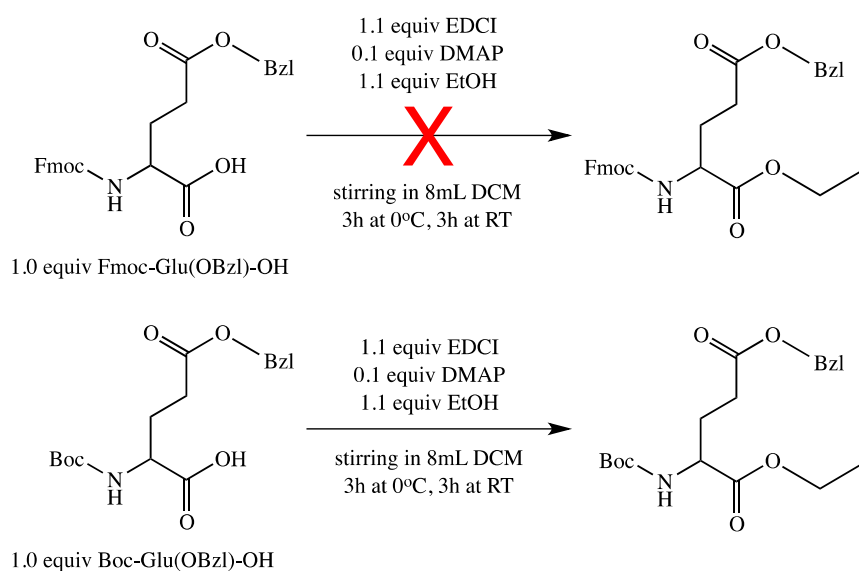
Scheme 3.5: Expected reaction schemes for the ethyl esterification of Fmoc-Glu(OBzl)-OH and Boc-Glu(OBzl)-OH to Fmoc-Glu(OBzl)-OEt and Boc-Glu(OBzl)-OEt, respectively, using carbodiimide coupling chemistry.

3.3.2.2   TFA Deprotection of Boc-Glu(OBzl)-OEt

The Boc protecting group was deprotected by dissolving the Boc-Glu(OBzl)-OEt in 1:3 TFA in DCM (**Scheme 3.6**). The amount of TFA/DCM solution used was based on the mass of Boc-Glu(OBzl)-OEt to be deprotected with 2mL of 25% TFA in DCM for every 75mg of protected amino acid. The TFA/DCM mixture and the amino acid were allowed to stir for 2 hours at room temperature and excess TFA was removed by bubbling N_2 gas through the solution for a minimum of 3 hours. Any remaining DCM solvent was removed *in vacuo* and the corresponding TFA salt of the deprotected glutamic acid ethyl ester was collected as a viscous oil.
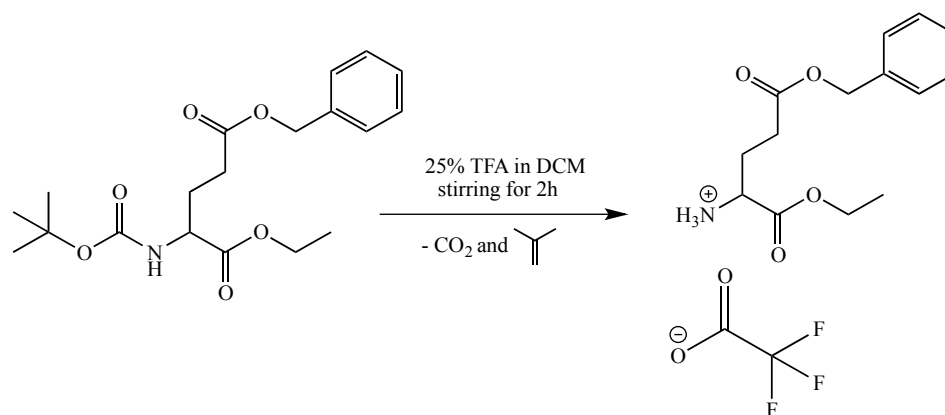
Scheme 3.6: Boc deprotection of glutamic acid ethyl ester (Boc-Glu(OBzl)-OEt) using a 1:3 mixture of trifluoroacetic acid (TFA) in dichloromethane (DCM).

3.4 Macromolecular Co-substitution of Non-Functional Amino Acids with Functional Glutamic Acid

3.4.1 Materials

Anhydrous tetrahydrofuran (THF) and glass-distilled hexanes-190 were obtained from Caledon Labs. Triethylamine (NEt$_3$) was purchased from Sigma Aldrich. All non-functional amino acid esters, L-alanine ethyl ester hydrochloride (H-Ala-OEt•HCl), L-phenylalanine ethyl ester hydrochloride (H-Phe-OEt•HCl), and L-methionine ethyl ester hydrochloride (H-Met-OEt•HCl), were from Alfa Aesar. The amine-deprotected glutamic acid ethyl ester (TFA$^-$ NH$_3^+$-Glu(OBzl)-OEt) was acquired from the preceding ethyl esterification and deprotection of Boc-Glu(OBzl)-OH procedures.

3.4.2 Methods

The general procedure for the synthesis of the co-substituted polyphosphazenes with both non-functional and functional amino acid esters was adapted from the one-pot room temperature substitution method used for the non-functional amino acids. Rather than adding the amino acids sequentially, which has been shown to cause very specific substitution patterns depending on the type of nucleophile, half of the total amount of the non-functional amino acid ester to be reacted was mixed initially with PDCP. After sufficient reaction time all of the functional amino acid ester was added to the mixture and allowed to react for 24 hours. Finally, the remaining amount of non-functional amino acid ester was added and the complete mixture was allowed to react for an

additional 48 hours, at which point the reaction solution was filtered and the co-substituted poly[(amino acid ester)phosphazene] was precipitated from the filtrate with hexanes. Described here in detail is the synthetic scheme for a co-substituted polyphosphazene with 90% Ala-OEt and 10% Glu(OBzl)-OEt (PP-$A_{90}E^*_{10}$) substituents although similar materials containing 90% Phe-OEt/10% Glu(OBzl)-OEt (PP-$F_{90}E^*_{10}$) and 90%Met-OEt/10%Glu(OBzl)-OEt (PP-$M_{90}E^*_{10}$) were also synthesized (**Figure 3.4**).
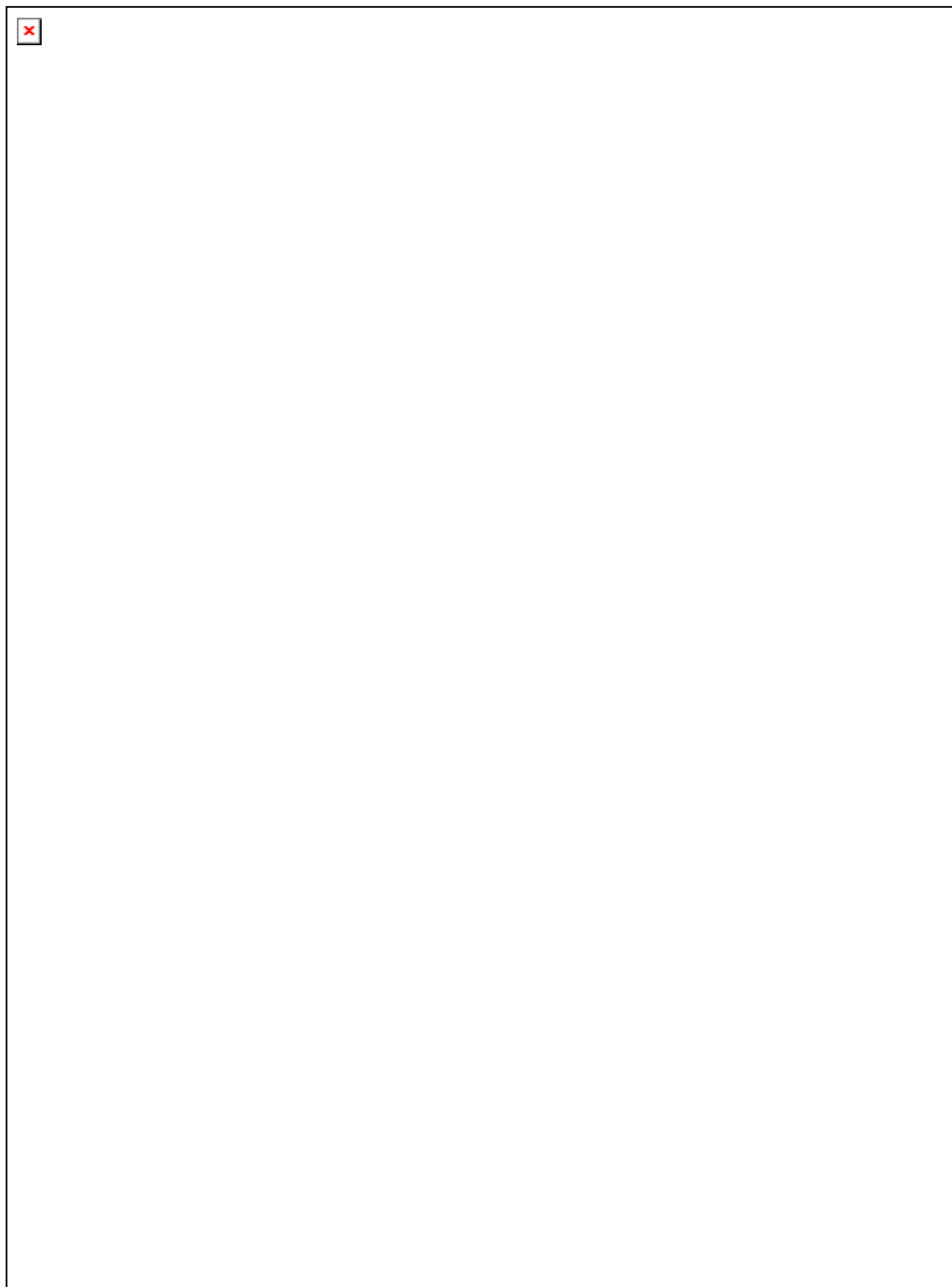
Figure 3.4: Chemical structures of the co-substituted poly[(amino acid ester)phosphazene]s based on the non-functional amino acid esters, Ala-OEt, Phe-OEt, Met-OEt, and side chain protected functional amino acid ester, Glu(OBzl)-OEt.

H-Ala-OEt•HCl (0.79g, 5.1mmol, 1.2 equiv) and 5mL of anhydrous THF were added to a 50mL round bottom flask and mixed at room temperature. Next, 0.9mL of NEt_3 (0.65g, 6.4mmol, 1.5 equiv) and a 5mL solution of poly[(dichloro)phosphazene] (0.50g, 4.3mmol of $NPCl_2$ units, 1.0 equiv) were added to the flask, the flask was sealed and the entire mixture was allowed to stir for 24 hours at room temperature. After 24 hours, TFA^- NH_3^+-Glu(OBzl)-OEt (0.32g, 0.86mmol, 0.2 equiv) dissolved in 5mL of THF and 0.2mL of NEt_3 (0.15g, 1.5mmol, 0.3 equiv) and the flask was resealed and allowed to stir for yet another 24 hours at room temperature. Finally, H-Ala-OEt•HCl (0.79g, 5.1mmol, 1.2 equiv), 5mL of anhydrous THF, and 0.9mL of NEt_3 (0.65g, 6.4mmol, 1.5 equiv) were added to the reaction flask and the complete mixture was stirred at room temperature for an additional 48 hours (**Scheme 3.7).** Upon completion of the reaction, the mixture was filtered to remove insoluble impurities and the product was precipitated from the THF solution using hexanes. Following this, the product was dissolved and precipitated from THF to hexanes a total of three times to help purify the polymer. Lastly, the polymer was dried *in vacuo* overnight on the in-house vacuum line.
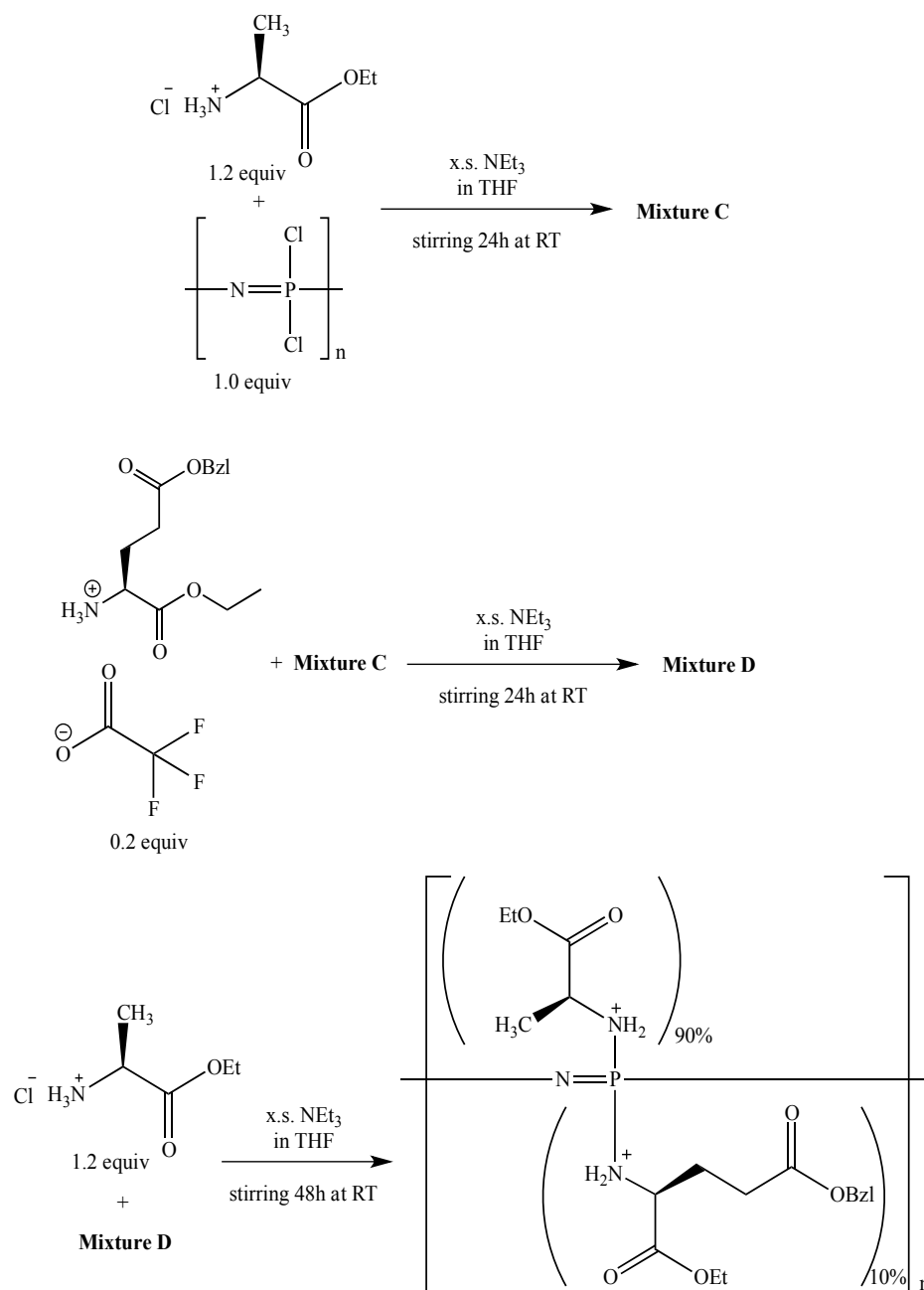
Scheme 3.7: One-pot three-stage room temperature reaction of a co-substituted poly[(amino acid ester)phosphazene] (PP-A$_{90}$E$^*_{10}$ shown here) from the functional amino acid ester (TFA$^-$ NH$_3^+$-Glu(OBzl)-OEt), non-functional amino acid ester (H-Ala-OEt•HCl) and poly[(dichloro)phosphazene] precursor (PDCP).

3.5 Conjugation of a Model Compound to the Functional Polyphosphazenes

In order to impart biological properties, materials are often coated or conjugated with biomolecules. These biomolecules, such as growth factors and signaling components, are typically small proteins and including a functional moiety in the biomaterial that can allow for the attachment of these types of molecules. Here, the pendant side chain carboxylic acid group of glutamic acid can be used as a site for biomolecule attachment and therefore its deprotection and reaction with a model compound have been explored as a proof of concept for attachment of biomolecules in the future.

3.5.1 Materials

The co-substituted functional polyphosphazenes containing glutamic acid side chains paired with non-functional amino acid side chains (PP-$A_{90}E^*_{10}$, PP-$F_{90}E^*_{10}$, and PP-$M_{90}E^*_{10}$) were obtained from the one-pot room temperature substitution method described above. Anhydrous EtOH was purchased from Commercial Alcohols Inc. The palladium on carbon (Pd/C) catalyst was purchased from Sigma Aldrich and had a loading of 10 wt. % on a matrix activated carbon support.

3.5.2 Methods

3.5.2.1 Hydrogenation of Benzyl Protecting Group

Hydrogenation of the benzyl ester protecting groups on the glutamic acid side chains was performed under a hydrogen atmosphere using a Pd/C catalyst. The PP-$A_{90}E^*_{10}$ (84mg, 0.27mmol of Ala/Glu(OBzl) substituted P=N units, 1.0 equiv) was dissolved in 4.5 mL of EtOH and the flask was evacuated under reduced pressure. The Pd/C catalyst (6 mg, 7 wt. % of polymer, 5.6μmol of Pd) was added to the reaction flask and the vessel was purged with H_2. The reaction mixture was allowed to stir for 3.5 hours at room temperature, at which point the hydrogenation was complete as determined by ^{1}H NMR spectroscopy (**Scheme 3.8**), although the reaction also lead to disruption of the polyphosphazene backbone (see Chapter 4 – Results and Discussion for further information). The Pd/C catalyst was removed by filtration through celite and the solvent was removed *in vacuo*.
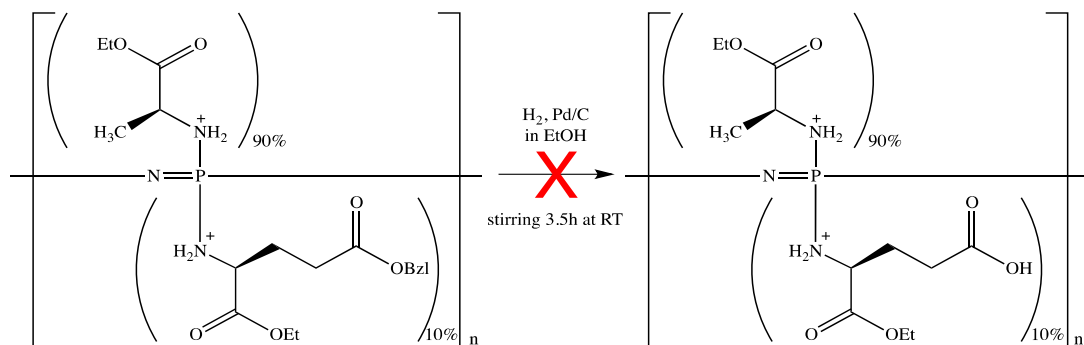
Scheme 3.8: Reaction scheme for the hydrogenation of benzyl ester protecting groups on glutamic acid in the co-substituted polyphosphazene of L-alanine ethyl ester (H-Ala-OEt) and benzyl protected L-glutamic acid ethyl ester (H-Glu(OBzl)-OEt).

3.6   Material Characterization

3.6.1   Nuclear Magnetic Resonance Spectroscopy (NMR)

Nuclear Magnetic Resonance (NMR) spectroscopy was performed on a Varian INOVA 400 MHz spectrometer (^{1}H 400.1 MHz, and ^{31}P{^{1}H} 161.8 MHz, Varian Canada Inc., Mississauga, ON). Chemical shifts are reported in parts per million (ppm) and were referenced relative to residual solvent signals of chloroform (CDCl$_3$, δ 7.27 ppm) for all non-functional amino acid ester hydrochloride salts (H-Ala-OEt•HCl and H-Met-OEt•HCl), Fmoc- and Boc-Glu(OBzl)-OH including products relating to the their esterification and deprotection, and all poly[(amino acid ester)phosphazene]s, except phenylalanine-based materials which were referenced to dimethyl sulfoxide (DMSO-d$_6$, δ 2.50 ppm). The hexachlorocyclotriphosphazene trimer and poly[(dichloro)phosphazene] TROP product were insoluble in CDCl$_3$ and were therefore run in non-deuterated anhydrous THF with referencing to an external phosphoric acid standard (85% H$_3$PO$_4$, δ 0.0 ppm).

3.6.2   Fourier-Transform Infrared Spectroscopy (FTIR)

Infrared spectroscopy was performed on a Bruker Vector 22 Spectrometer from Bruker Optics (Bruker Corporation, Billerica, MA) equipped with a MIRacle Attenuated Total Reflectance (ATR) diamond crystal plate sample cell (PIKE Technologies, Madison, WI). The samples were run as solid films in air for 32 scans with a resolution of 4 cm^{-1}

over the scan range of 600 cm^{-1} to 3200 cm^{-1}. Spectra were collected and processed in Opus 6.5 FTIR software (Bruker Optics) and reported in wavenumbers (cm^{-1}).

3.6.3   Thermogravimetric Analysis (TGA)

Thermal decomposition of the polymers was determined using TGA on a SDT Q600 TA Instrument (TA Instruments – Waters LLC, New Castle, DE). A sample of 5 – 15 mg was placed in an aluminum cup and heated at a rate of 20°C/min from room temperature to 500°C under dry nitrogen atmosphere.

3.6.4   Differential Scanning Calorimetry (DSC)

Glass transition temperatures (T_gs) and melting temperatures (T_ms), if applicable, were determined using a DSC Q20 TA Instrument. A sample of approximately 5 –15 mg was placed in an aluminum pan and subjected to a heat/cool/heat temperature profile ranging from -100 to 100°C. The experiments were performed under dry nitrogen atmosphere at a heating rate of 10°C/min and all T_gs were collected from the second heating cycle.

3.6.5   Gel Permeation Chromatography (GPC)

Molecular weights and polydispersities were obtained from Gel Permeation Chromatography (GPC) experiments generously performed by PolyAnalytik Inc. (London, ON). The experiments were conducted on a Viscotek TDA 302 GPC/SEC Instrument (Malvern Instruments, Malvern, UK) equipped with a triple detection system (Refractive Index (RI), Right Angle and Low Angle Light Scattering (RALS/LALS), and Four Capillary Differential Viscometer). There were four styrene-divinylbenzene SupeRes™ size exclusion columns (PolyAnalytik Inc., London, ON) connected in series, PAS-105, PAS-104, PAS-103, and PAS-102.5, with exclusion limits of 4×10^6, 4×10^5, 7×10^4, and 2×10^4 Daltons (Da), respectively. Samples (10mg/mL) dissolved in the eluent, consisting of 10 mM tetra-n-butylammonium nitrate in THF at 30°C, were passed through a 0.22 μm Teflon filter prior to injection (100 μL) into the instrument at a flow rate of 0.7 mL/min. The absolute molecular weights (number average (M_n) and weight average (M_w)) and polydispersities (PDI, M_w/M_n) were obtained using the triple detection method and are presented in Daltons (Da, g/mol). Molecular weights of the

polyphosphazenes were also calculated relative to polystyrene standards with known molecular weights using refractive index detection.

3.7   Cytotoxicity Studies of Polymeric Films Using MTT Assays

3.7.1   Thin Film Preparation

Thin films were prepared by adding 30.5 μL of a 1% weight by volume (w/v) solution of the polymer in absolute ethanol to the bottom of the well of a 96-well tissue culture plate (BD Falcon™, Franklin Lakes, NJ). The films were allowed to dry at room temperature for 24 hours. Uncoated tissue culture polystyrene (TCPS) were used as positive controls in these experiments. The tissue culture plate, including the dried films, was disinfected with ultraviolet (UV) light overnight. For pre-conditioning, the films were treated with Hank's Balanced Salt Solution (HBSS, 200 μL, Invitrogen Canada Inc., Burlington, ON) at room temperature overnight.

3.7.2   Fibroblast (NIH-3T3) Cell Study

Cell toxicity and proliferation assays were assessed using mouse embryonic fibroblasts (NIH-3T3 cell-line), which were seeded in the 96-well plate at a seeding density of 8,000 cells/well with 200 μL/well of advanced DMEM (GIBCO® Invitrogen, Burlington, ON, Canada) containing 5% FBS, 1% antibiotics, and 0.2 mM L-glutamine. The cells were maintained in a humidified incubator at 37°C and 5% CO_2. At time points of 1, 3, and 5 days cells were analyzed for viability using the MTT assay protocol described below.

3.7.3   MTT Assay Protocol

Cell toxicity and proliferation were quantified by colorimetric assays of the metabolic activity of viable cells using 3-(4,5-dimethylthiazol-2-yl)-2,5-diphenyltetrazolium bromide (MTT) (Vybrant® MTT Cell Proliferation Assay Kit, Invitrogen Canada Inc.) The MTT tetrazolium dye is reduced to insoluble formazan salts in correspondence to the activity level of NADPH-dependent oxidoreductase enzymes of metabolically active cells producing a purple colour. The concentration of the formazan salts, and therefore metabolic activity level of the cells present, is determined using optical density at $\lambda = 570$ nm. At time points of 1, 3, and 5 days, the spent culture media was aspirated and replaced

with fresh media (100 µL) followed by MTT (10 µL, Component A) and allowed to incubate for 4 hours. Sodium dodecyl sulphate (SDS) in dilute acid (100 µL, Component B) was added to the wells to solubilize the water insoluble formazan salts upon thorough mixing and incubation for another 4 hours.   The resultant coloured solution was quantified using a BioTek EL307C multiplate reader (BioTek Instruments, Inc., Winooski, VT) at the maximum absorbance wavelength of the formazan solution (570 nm).   The results of the MTT assays presented as the mean ± standard deviation for experiments conducted with 5 replicates (n=5). Statistical analysis was determined from two-way ANOVA with Bonferroni post-tests using GraphPad Prism 4 (GraphPad Software, Inc., La Jolla, CA), where a $p<0.05$ was deemed statistically significant.

3.8   Cell Morphology and Adhesion Studies on Polymer Films Using Confocal Microscopy

3.8.1   Thin Film Preparation

Polymer film-coated coverslips were prepared by twice dip-coating glass coverslips (12 mm diameter) in 1% w/v solutions of the polymers in absolute EtOH. After each coat the films were allowed to dry overnight at room temperature *in vacuo*. Once both coats had been thoroughly dried in *vacuo*, one glass coverslip was placed in each well of a 24-well tissue culture plate. Uncoated glass coverslips were used as a positive control in these experiments.   The cells were seeded at a density of 30,000 cells/well and cultured for 3 days prior to fixation and staining.

3.8.2   Cell Fixation, Staining, and Imaging

For immunostaining studies, cells were washed with PBS pre-warmed to 37°C immediately prior to fixing at ambient temperature for 10 min in 4% paraformaldehyde solution (1 mL; EMD Chemicals, Gibbstown, NJ) in divalent cation-free PBS. Following 3 washes in PBS, permeabilized with 0.1% Triton X-100 (0.5 mL; VWR International, Mississauga, ON) in PBS for 5 min and again washed 3 times with PBS. Following 3 washes in PBS, the cells were incubated in the dark at ambient temperature with Alexa Fluor® 568-conjugated phalloidin (1:50 dilution; Invitrogen Canada Inc., Burlington, ON) for 20 min in a 1% BSA/PBS solution to label the F-actin of the cytoskeleton

followed by another 3 washes with PBS. The fibroblasts were then counterstained with 4'-6-diamidino-2-phenylindole dihydrochloride (DAPI, 300 nM in PBS, 0.5 mL; Invitrogen Canada Inc., Burlington, ON) for 5 min to label the nuclei and again washed 3 times with PBS. Coverslips were mounted on microscope slides with SHURMount^{TM} – Toluene Based Liquid Mounting Media (Triangle Biomedical Sciences, Inc., Durham, NC). Samples were analyzed with a Zeiss LSM 5 Duo confocal microscope with 9 laser lines and appropriate filters (Carl Zeiss Canada Ltd., Toronto, ON).

3.9 Electrospinning of Polyphosphazenes and Polyphosphazene/ Polycaprolactone Blends

3.9.1 Electrospinning Parameters

Two approaches were investigated to develop 3-D fibers of the polyphosphazene materials. Solutions of poly[bis(ethyl alanato)phosphazene] (PNEA) alone and a mixture of PNEA and polycaprolactone (PCL, M_n = 80kDa, Sigma-Aldrich, Oakville, ON, Canada) in various solvents and co-solvent mixtures using chloroform ($CHCl_3$), N,N-dimethylformamide (DMF), ethanol (EtOH), tetrahydrofuran (THF), and dichloromethane (DCM) were attempted to be electrospun. The polymer solutions ranged in concentration from 3 to 37 % w/v and all solvents were from Caledon Labs except ethanol, which was from Commercial Alcohols Inc. The viscous polymer solutions were loaded into 0.5 mL glass syringes (Becton, Dickinson and Co., 0.5 cc, New Jersey, USA) equipped with blunt-tip stainless steel needles between 18- and 22-gauge (inner diameter 0.838 – 0.413 mm). An alligator clip was attached to the middle of the needle connecting it to the high voltage DC power supply (ES30P, Gamma High Voltage, USA) with an applied voltage between 7 and 20 kV and a syringe pump (KD101, KD Scientific, USA) was used to push the solution through the horizontal syringe and needle at a constant flow rate of 0.1 mL/h. An aluminium foil-covered static collector placed at a distance of 7 to 9 cm from the needle tip was used to catch the polymer fibers during the electrospinning process.

3.9.2   Scanning Electron Microscopy (SEM) Imaging of Electrospun Fibers

The electrospun fibers were visualized using scanning electron microscopy (S- 3400N, Hitachi, Ltd., Tokyo, Japan). The mat was mounted on carbon-taped aluminum stubs and coated with 5 nm of osmium using a sputter coating technique (Filgen OPC80T Osmium Plasma Coater, Filgen Nanosciences & Biosciences Inc., Japan). Secondary electron detection was achieved at a working distance of 10 mm and accelerating voltages between 3 and 5 kV at various magnifications. Images were acquired and processed using ImageJ software (NIH, Bethesda, MD).

Chapter 4

4   Results and Discussion

4.1   Optimization of Thermal Ring Opening Polymerization

Considering the limitations of the traditional thermal ring opening polymerization discussed in Chapter 1 and that it requires large amounts of starting material, a facile polymerization technique was developed in this work. The new method overcame the restrictions of large-scale synthesis making the procedure more ideal for the development of novel polyphosphazene biomaterials. The new method also bypassed the requirement of trimer purification prior to polymerization and handling of all materials in inert atmosphere using expensive glovebox techniques. The success of the new synthesis process was achieved by monitoring the reaction progress of 1g polymerizations using ^{31}P NMR and comparing the relative peak heights and integrations of the starting material and product. The polymerizations were performed at 230°C for time periods of 20 to 26 hours. From the literature, it has been well documented that hexachlorocyclotriphosphazene (cyclic trimer) gives rise to a single peak at a chemical shift of approximately +20 ppm, where as poly[(dichloro)phosphazene] (linear high polymer) appears as a singlet at approximately -17 ppm.[67] As can be seen from **Figure 4.1** the expected shifts in ^{31}P NMR spectroscopic analysis of both the trimer starting material and PDCP linear precursor coincided with those previously presented in the literature.
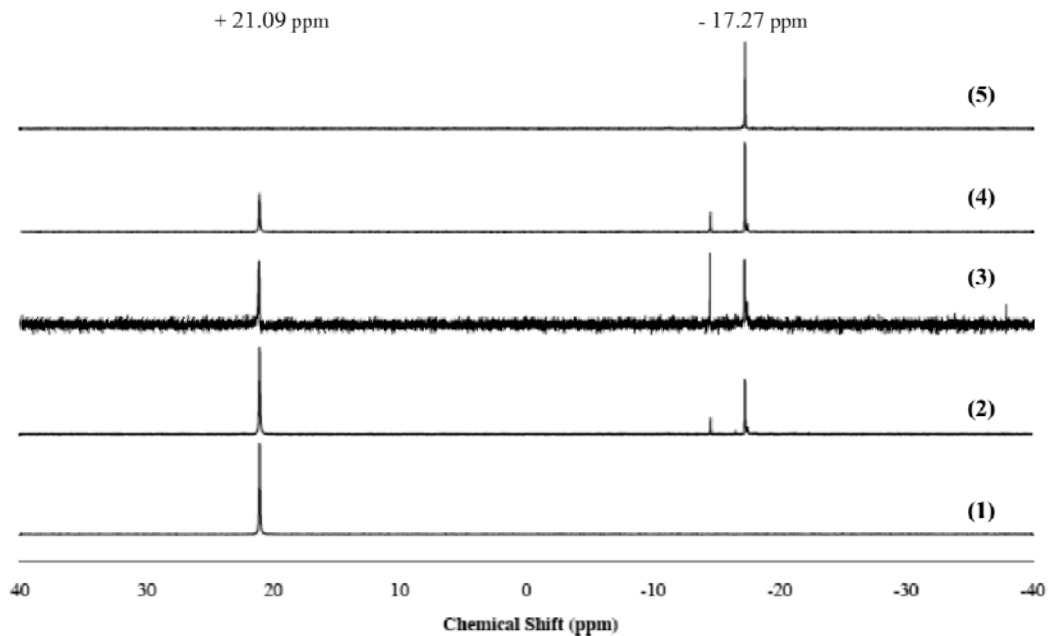
Figure 4.1: ^{31}P NMR of the time-varied facile polymerization of hexachlorocyclotriphosphazene (1) to purified poly[(dichloro)phosphazene] (5) at 230°C. Spectra (2), (3), and (4) are for 21, 23, and 25 hour polymerizations, respectively, without purification.

Polymerizations for longer than 25 hours led to cross-linked materials that were insoluble and could not be reacted further to produce poly[(amino acid ester)phosphazene]s. From comparison of relative peak heights and integration values in the time-varied polymerizations shown in **Figure 4.1** and **Table 4.1**, respectively, the best conversion of hexachlorocyclotriphosphazene to poly[(dichloro)phosphazene] without cross-linking was achieved at 25 hours reaction time at 230°C. These reaction conditions were used for all subsequent polymerizations.

Table 4.1: Summary of the time-varied polymerizations of hexachlorocyclotriphosphazene (trimer) to poly[(dichloro)phosphazene] (linear precursor) with their respective yields and extent of conversion.

Reaction Time (h)	Mass Trimer (g)	Mass Product (g)	Mass Purified Product (g)	% Crude Yield	% Purified Yield	Integration of +20 ppm Peak	Integration of -17 ppm Peak	% Conversion
20	1.083	0.799	0.032	73.8	3.0	-	-	-
21	1.086	0.868	0.095	79.9	8.7	2.48	1.00	28.7
22	1.074	0.843	0.224	78.5	20.9	-	-	-
23	1.075	0.794	0.322	73.9	30.0	1.14	1.00	46.7
24	1.079	0.789	0.397	73.1	36.8	-	-	-
25	1.081	0.703	0.503	65.0	46.5	0.84	1.00	54.3
26	1.075	0.746	N/A	69.4	N/A	-	-	-

4.2 Comparison of the Three Macromolecular Substitution Methods Using Non-Functional Amino Acid Esters

There are two reported methods of amino acid substitution onto poly[(dichloro)phosphazene] that have been successfully used to make poly[(amino acid ester)phosphazene]s.[77, 78, 83, 84, 95] Both methods involve forming the free base of the amino acid ester by reacting the hydrochloride salt of the amino acid ester with triethylamine under refluxing conditions for 3 hours to 24 hours. The first and most common method, referred to as the RT 2S reaction in the methods section, performs the actual substitution reaction at room temperature, whereas the other method, referred to as the LT 2S reaction, performs the substitution at 0°C in an ice bath. In an effort to overcome the need to liberate the free base and simplify the overall reaction, a method that involves adding the hydrochloride salt of the amino acid ester, triethylamine and the poly[(dichloro)phosphazene] linear precursor all together at one time, named the 1P RT reaction, was investigated. This method was proposed since TEA, the base used to form the free base from the hydrochloride salt, is non-nucleophilic and should theoretically not react in a substitution with the poly[(dichloro)phosphazene] linear precursor. An adaptation to the low temperature method described in the literature was also compared, where refluxing the hydrochloride salt of the amino acid ester with TEA was instead

performed at room temperature rather than at reflux, followed by substitution onto poly[(dichloro)phosphazene] at 0°C. The one-pot method was proven successful and the resulting polymers based on non-functional amino acid ethyl esters were characterized and analyzed in comparison to both of the previously described methods found in the literature. The amino acid esters used for this comparison included, alanine ethyl ester (H-Ala-OEt), phenylalanine ethyl ester (H-Phe-OEt), and methionine ethyl ester (H-Met-OEt), since these materials have all been previously reported in the literature with associated characterization and thermal data.[64, 83, 84, 94, 95, 97, 105, 114-118] Also, ethyl esters of amino acids were chosen since ethanol is one of the anticipated degradation products and can be easily processed by cells. The amino acids were chosen on the basis of having side chains that are a short alkyl chain (alanine), a rigid and bulky aromatic chain (phenylalanine), a long and flexible chain (methionine) and a side chain that contains a heteroatom (methionine). Incorporating amino acids with very different side chains gives tunability to the polymers and allows for adjustment of both the degradation and mechanical properties of the materials to suit the intended biomedical application.[83]

4.2.1   FTIR, ^{1}H NMR, and ^{31}P NMR Characterization

Structural characterization techniques used to compare the three methods were nuclear magnetic resonance (NMR) spectroscopy and Fourier Transform Infrared (FTIR) spectroscopy, which are summarized in **Table 4.2**.

Table 4.2: Summary table of the yields, ^{1}H NMR, ^{31}P NMR, and FTIR analyses of PP-A$_{100}$, PP-F$_{100}$, and PP-M$_{100}$ synthesized by the three methods (LT 2S = low temperature two-step reaction, 1P RT = one-pot room temperature reaction, and RT 2S = room temperature two-step reaction). Note: As described in the methods section, the mass of poly[(dichloro)phosphazene] (PDCP) is approximate since it cannot be dried fully and therefore the percentage yields shown are underestimated since yield calculations are based on PDCP as the limiting reagent.

Polymer	Method	% Yield	^{1}H NMR (δ, ppm)	^{31}P NMR (δ, ppm)	FTIR (cm^{-1})
PP-A$_{100}$	LT 2S	26.8	8.72 (br. s) 4.25 (m, 3H) 1.72 (d, 3H) 1.30 (t, 3H)	1.13	3100 – 2700 (C-H stretch) 1740 (C=O, ester) 1210 – 1145 (broad, P=N) 850 – 775 (broad, P-NH)
	1P RT	49.9	8.69 (br. s) 4.25 (m, 3H) 1.72 (d, 3H) 1.30 (t, 3H)	1.34	3100 – 2700 1740 1210 – 1145 850 – 775
	RT 2S	34.5	8.65 (br. s) 4.26 (m, 3H) 1.71 (d, 3H) 1.30 (t, 3H)	-1.42	3100 – 2700 1740 1210 – 1145 850 – 775
PP-F$_{100}$	LT 2S	10.8	8.66 (br. s) 7.29 (m, 5H) 4.21 (br. s, 1H) 4.09 (qd, 2H) 3.21 (dd, 1H) 3.06 (dd, 1H) 1.08 (t, 3H)	-1.55	3100 – 2700 (C-H stretch) 1740 (C=O, ester) 1210 – 1145 (broad, P=N) 865 – 855 (broad, P-NH) 705 (C-H aromatic)
	1P RT	33.9	8.71 (br. s) 7.30 (m, 5H) 4.24 (m, 1H) 4.09 (qd, 2H) 3.22 (dd, 1H) 3.06 (dd, 1H) 1.08 (t, 3H)	-0.97	3100 – 2700 1740 1210 – 1145 865 – 855 750 – 700
	RT 2S	31.5	8.69 (br. s) 7.30 (m, 5H) 4.22 (m, 1H) 4.09 (qd, 2H) 3.22 (dd, 1H) 3.06 (dd, 1H) 1.08 (t, 3H)	-1.81 -9.12	3100 – 2700 1740 1210 – 1145 865 – 855 750 – 700
PP-M$_{100}$	LT 2S	8.9	4.29 (m, 3H) 2.75 (m, 2H) 2.38 (m, 2H) 2.15 (s, 3H) 1.32 (t, 3H)	-0.43	3100 – 2700 (C-H stretch) 1740 (C=O, ester) 1200 – 1100 (broad, P=N) 855 – 840 (broad, P-NH)
	1P RT	33.4	8.87 (br. s) 4.28 (m, 3H) 2.79 (m, 2H) 2.38 (m, 2H) 2.13 (s, 3H) 1.32 (t, 3H)	3.51	3100 – 2700 1740 1200 – 1100 855 – 840
	RT 2S	59.5	8.84 (br. s) 4.29 (m, 3H) 2.78 (m, 2H) 2.38 (m, 2H) 2.13 (s, 3H) 1.32 (t, 3H)	1.14	3100 – 2700 1740 1200 – 1100 855 – 840

The FTIR spectroscopic analyses for the alanine, phenylalanine, and methionine ethyl ester polyphosphazenes synthesized using the three different methods are shown in

Figures 4.2 – 4.4. Enlarged spectra of specific regions to show peak broadening have been included in the Appendix (**Appendix 2 - 4**).
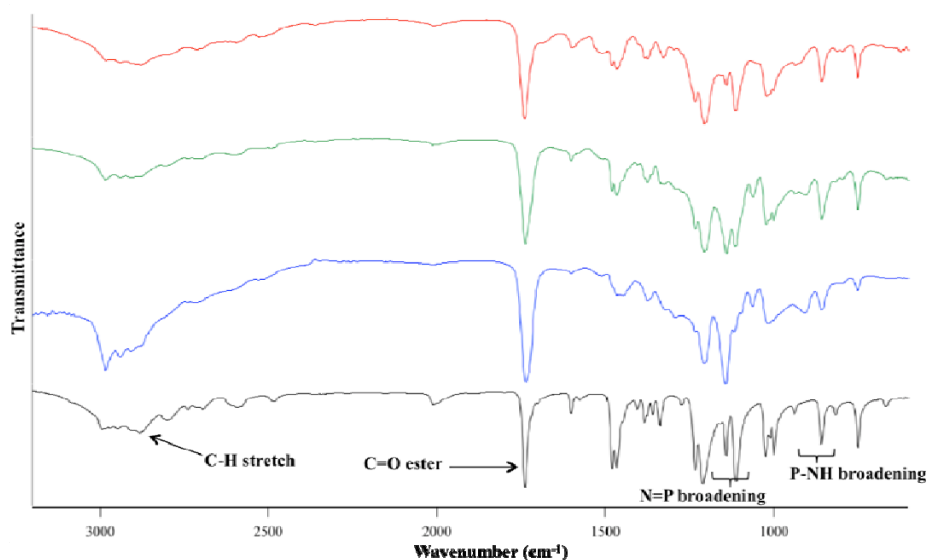
Figure 4.2: FTIR comparison of PP-A$_{100}$'s prepared from three different synthetic methods. The spectra correspond to L-alanine ethyl ester hydrochloride salt (black), and PP-A$_{100}$'s from LT 2S method (blue), 1P RT method (green), and RT 2S method (red).
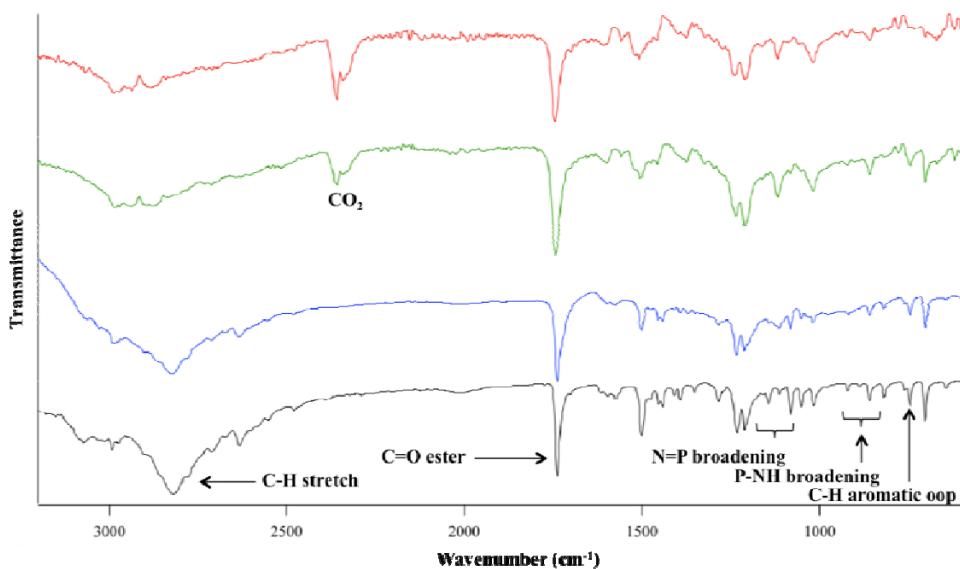
Figure 4.3: FTIR comparison of PP-F$_{100}$'s prepared from three different synthetic methods. The spectra correspond to L-phenylalanine ethyl ester hydrochloride salt (black), and PP-F$_{100}$'s from LT 2S method (blue), 1P RT method (green), and RT 2S method (red).
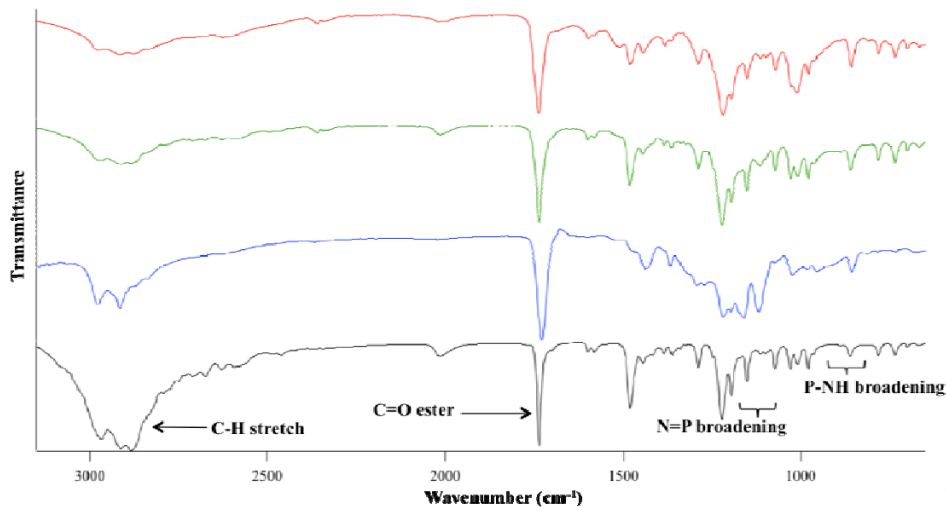
Figure 4.4: FTIR comparison of PP-M$_{100}$'s s prepared from three different synthetic methods. The spectra correspond to L-methionine ethyl ester hydrochloride salt (black), and PP-M$_{100}$'s from LT 2S method (blue), 1P RT method (green), and RT 2S method (red).

The ^{1}H NMR spectroscopic analyses for the alanine, phenylalanine, and methionine ethyl ester polyphosphazenes synthesized using the three different methods are shown in **Figures 4.5 – 4.7**.
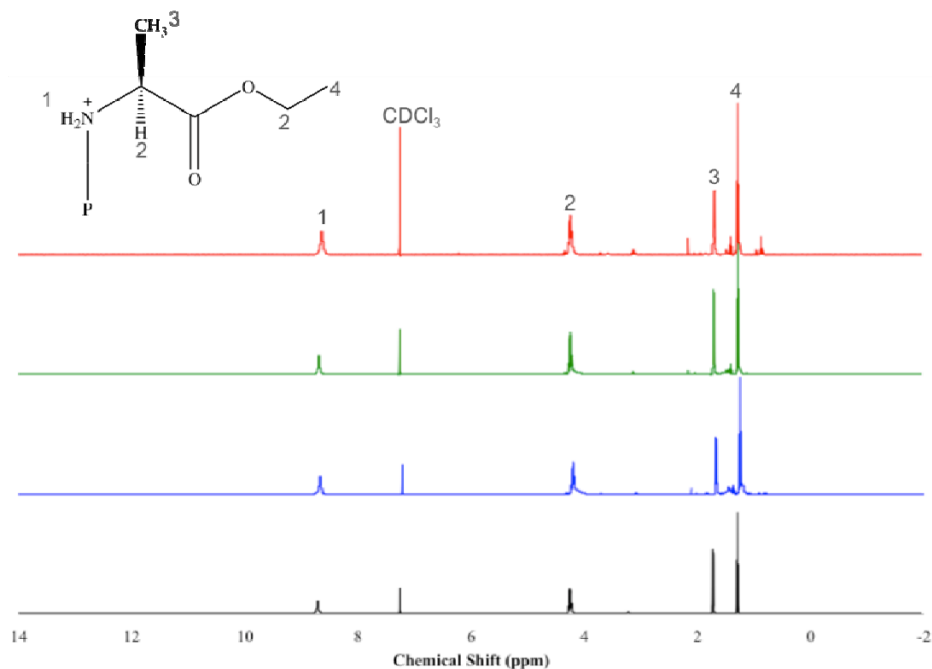
Figure 4.5: ^{1}H NMR comparison of PP-A$_{100}$'s prepared from three different synthetic methods. The spectra correspond to L-alanine ethyl ester hydrochloride salt (black), and PP-A$_{100}$'s from LT 2S method (**blue**), 1P RT method (**green**), and RT 2S method (**red**). All small, unlabeled peaks are impurities that cannot be removed from dissolution/reprecipitation techniques.
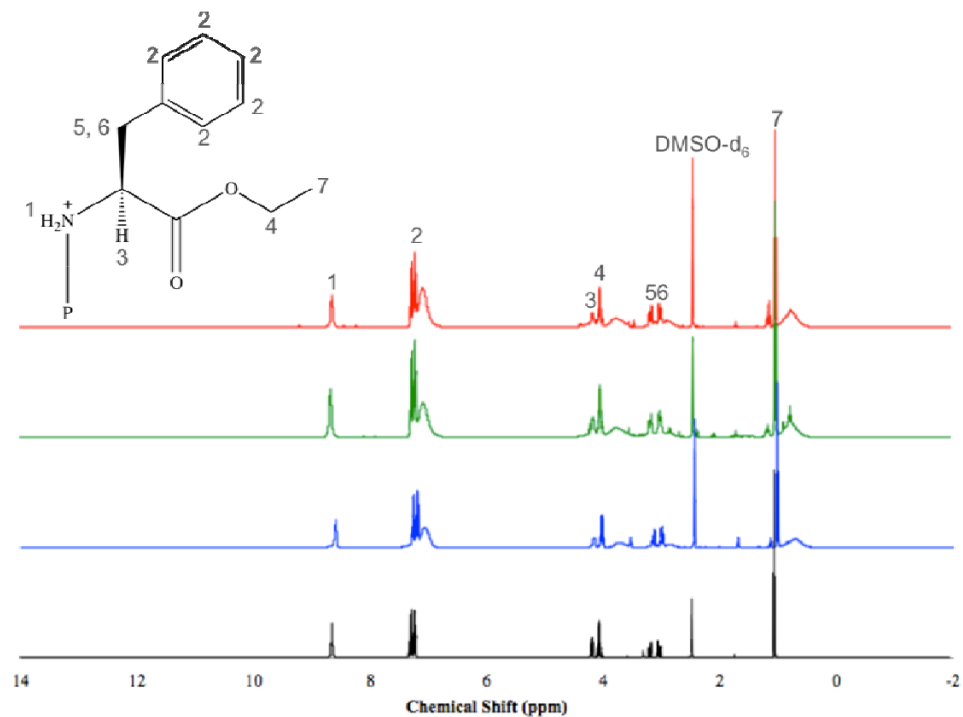
Figure 4.6: ^{1}H NMR comparison of PP-F$_{100}$'s prepared from three different synthetic methods. The spectra correspond to L-phenylalanine ethyl ester hydrochloride salt (black), and PP-F$_{100}$'s from LT 2S method (blue), 1P RT method (green), and RT 2S method (red). All small, unlabeled peaks are impurities that cannot be removed from dissolution/reprecipitation techniques.
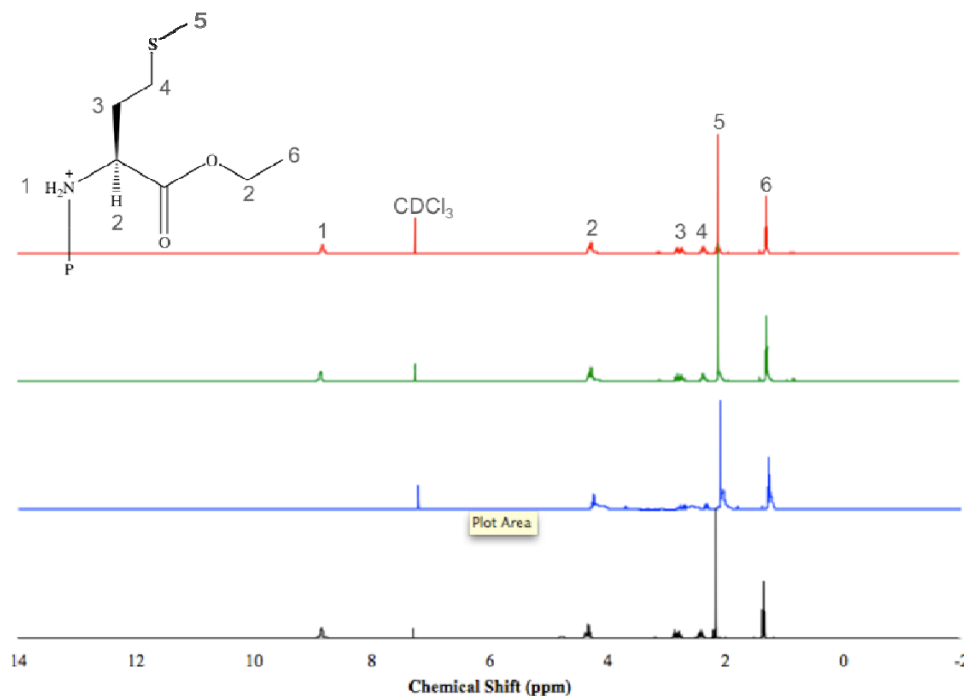
Figure 4.7: ^{1}H NMR comparison of PP-M$_{100}$'s prepared from three different synthetic methods. The spectra correspond to L-methionine ethyl ester hydrochloride salt (black), and PP-M$_{100}$'s from LT 2S method (blue), 1P RT method (green), and RT 2S method (red). All small, unlabeled peaks are impurities that cannot be removed from dissolution/reprecipitation techniques.

Since the ^{31}P NMR spectra consist of a broad single or bimodal peak for all of the poly[(amino acid ester)phosphazene]s, they have been included as tabulated data (**Table 4.2**) rather than spectra for simplicity. As an example of the changes in ^{31}P NMR from hexachlorocyclotriphosphazene (trimer) to poly[(dichloro)phosphazene] (PDCP, linear precursor) to an amino acid ester substituted polyphosphazene, the transition from trimer to PP-M$_{90}$E$^*_{10}$ has been included (**Figure 4.8**).
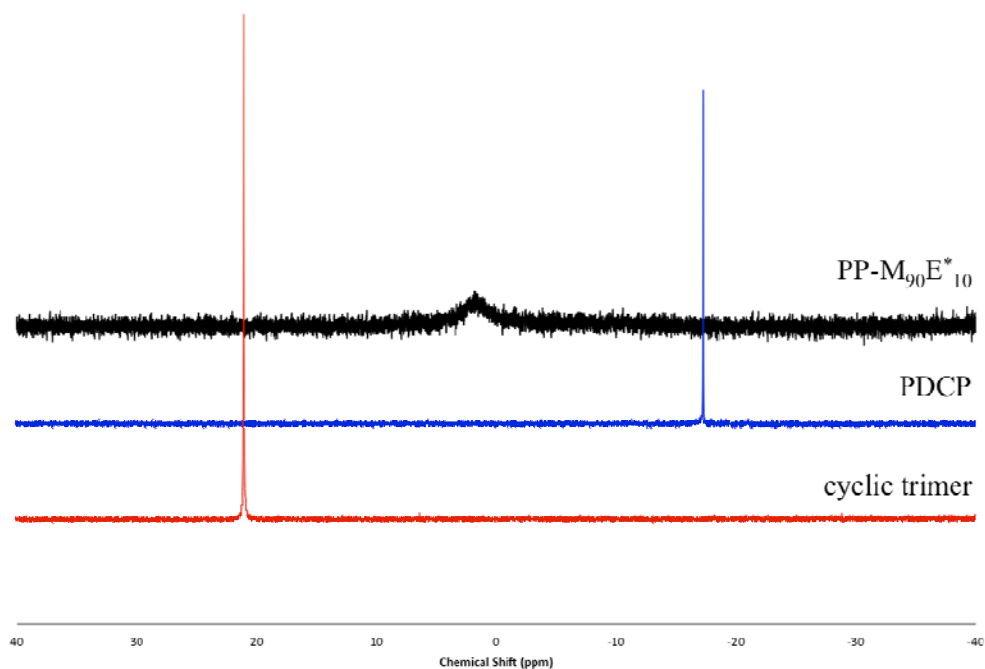
Figure 4.8: 31P NMR of the transition from hexachlorocyclotriphosphazene (cyclic trimer) to poly[(dichloro)phosphazene] (PDCP) and finally to the methionine ethyl ester and benzyl protected glutamic acid ethyl ester co-substituted polyphosphazene (PP-M$_{90}$E$^*_{10}$).

From the FTIR, ^{1}H NMR, and ^{31}P NMR data it is evident that all of the substitution methods with all of the non-functional amino acid esters were successful, with the exception of the low temperature two-step reaction with methionine ethyl ester giving mixed results.

In the FTIR spectra of the PP-A$_{100}$'s peaks corresponding to the C-H stretch (alkanes) and N-H stretch were observed between 3100 - 2700 cm^{-1}, correlating to the side chain methyl group, α-carbon, and ethyl C-H bonds and the N-H bonds of the amine terminus of the amino acid, respectively. The sharp peak at 1740 cm^{-1} corresponds to the C=O stretch of the ester carbonyl of the amino acid. The P=N of the backbone P-NH bonds that connect the amino acid esters to the phosphorus atoms in the backbone are observed as a broadening of peaks between 1210 – 1145 cm^{-1} in comparison to the already present peaks from L-alanine ethyl ester itself. A similar phenomenon is observed with the P-NH, where peaks between 850 – 775 cm^{-1} are broadened relative to alanine ethyl ester

alone. The incidence of these peak broadenings, which could realistically be two separate bands appearing as one, fall within the areas previously attributed to P=N and P-NH bonds in the literature.[64, 103, 105, 114, 119-124] Peak-broadened spectra are included in the Appendix (**Appendix 2**) for reference, although these broadened peaks alone are not sufficient to definitively conclude that the PP-A$_{100}$ has been formed. As such, ^{1}H and ^{31}P NMR spectra were collected and analyzed to verify the success of the PP-A$_{100}$ syntheses.

From the ^{1}H NMR spectra, it is apparent that the appropriate chemical shifts and splitting that correspond to the types of protons on L-alanine ethyl ester are present, with minimal impurities. The ^{1}H NMR spectra of the PP-A$_{100}$ synthesized via the 1P RT method will be discussed in detail although the PP-A$_{100}$'s from the other two methods gave similar spectra with only minor differences in chemical shifts (see **Table 4.2**). The broad singlet at a chemical shift of 8.69 ppm with non-integer integration between 1 – 2 protons represents the protons bound to the amine terminus of the amino acid since it is somewhat similar to an amide (HRN-P=N vs. HRN-C=O). The amine peak has either not been observed or is omitted from the literature; thus it was of interest to see this peak in this work[83, 84, 94, 97] Since amine protons do not always appear in ^{1}H NMR spectra based on whether or not the NMR solvent can undergo hydrogen-deuterium exchange reactions, the polymer was also analyzed in deuterated methanol (MeOH-d$_4$), a solvent that readily undergoes exchange, to confirm that this peak corresponded to an amine and not some other impurity. Upon running ^{1}H NMR of the PP-A$_{100}$ in MeOH-d$_4$ the peak at 8.69 ppm disappeared, further confirming the identity of the peak as that of the amine protons. The non-integer integration for this peak leads us to believe that not all of the nitrogen atoms have been deprotonated (i.e. 2 protons to 1 proton) after the substitution reaction, leaving the polymer cationic at some or all of the nitrogen atoms, unlike what has been shown in the chemical structures reported in the literature that show the nitrogen atoms bearing only 1 proton and a neutral charge. Next, the multiplet at 4.25 ppm (integration for 3H) corresponds to the proton on the α-carbon and the two protons of the CH$_2$ of the ethyl ester. This is slightly different than some literature sources[83, 84, 94, 97, 116], which identify two separate peaks at 4.4 and 4.1 ppm corresponding to the proton on the α-carbon and ethyl group, respectively, rather than the multiplet for both that is found in this work. Lastly, the doublet at 1.72 ppm (integration for 3H) and triplet at 1.30 ppm (integration

for 3H) agree well with the literature with only minor differences in chemical shift. They correspond to the methyl side chain of the amino acid, which is split into a doublet by the proton on the α-carbon, and the CH_3 group of the ethyl ester, which is split into a triplet by the two methylene protons of the ethyl group, respectively.

In ^{31}P NMR analysis of the PP-A_{100}'s, broad humps with chemical shifts between 1.13 and -1.42 ppm were observed, which is comparable to the literature as shifts between -1.10 and -3.50 ppm have been reported and broadened peaks are to be expected with polyphosphazenes.[67] Overall, despite these subtle differences, the PP-A_{100}'s were successfully synthesized via all three reaction methods.

In the FTIR spectra of the PP-F_{100}'s peaks corresponding to the C-H stretch (alkanes) and N-H stretch were observed between 3100 – 2700 cm^{-1}. The sharp peak at 1740 cm^{-1} corresponds to the C=O stretch of the ester carbonyl of the amino acid. The P=N of the backbone and the P-NH bonds broadening of peaks between 1210 – 1145 cm^{-1} and 865 – 855 cm^{-1}, respectively, in comparison to the already present peaks from L-phenylalanine ethyl ester alone. Another peak, which was not observed with the PP-A_{100}'s, but is observed in the PP-F_{100}'s is the aromatic C-H out of plane vibration from the benzene ring in the amino acid side chain. Peak broadening spectra are included in the Appendix (**Appendix 3**) for reference, although, like with the PP-A_{100}'s, these broadened peaks alone are not conclusive enough. Therefore, ^{1}H and ^{31}P NMR spectra were also analyzed to confirm the success of the PP-F_{100} syntheses.

In the ^{1}H NMR spectra of the PP-F_{100}'s the chemical shifts that correspond to the types of protons on L-phenylalanine ethyl ester are present, along with a few trace impurities. The ^{1}H NMR spectra of the PP-F_{100} synthesized via the 1P RT method will be discussed in detail although the PP-F_{100}'s from the other two methods gave similar spectra with only slight differences in chemical shifts (see **Table 4.2**). The broad singlet at a chemical shift of 8.71 ppm with non-integer integration between 1 – 2 protons represents the protons bound to the amino terminus of the amino acid. Like with the PP-A_{100}'s, this integration indicates that some or all of the nitrogen atoms are likely to have 2 protons, implying a positive charge. The multiplet at 7.30 ppm (integration for 5H) corresponds to the

aromatic protons of the benzene ring in the phenylalanine side chain, which is not far off of the 7.6 ppm peak reported in the literature[84, 95] and still falls in the typical range for aromatic protons (8.5 – 6.0 ppm). The proton attached to the α-carbon of the amino acid was observed as a multiplet with a chemical shift of 4.24 ppm. The quartet of doublets at 4.09 ppm (integration for 2H) signifies the methylene of the ethyl group since the two protons are each split by the terminal CH_3 of the ethyl group, yet they each have their own unique magnetic environments and appear at slightly different chemical shifts giving rise to the overlap of two quartets slightly offset from one another. Two doublets of doublets at 3.21 ppm (integration for 1H) and 3.06 ppm (integration for 1H), represent the two protons on the methylene group of the phenylalanine side chain. Both of these protons see the α-carbon splitting them into a doublet and, like the protons described above, they also have their own unique environments and thus split each other leading to the doublet of doublet that is observed. Lastly, the triplet at 1.08 ppm (integration for 3H) corresponds to the CH_3 of the ethyl group, which is split by the two methylene protons on the adjacent carbon.

In ^{31}P NMR analysis of the PP-F_{100}'s, broad singlets or bimodal humps with chemical shifts between -0.97 and -9.12 ppm were observed although no data has been reported in the literature for mono-substituted PP-F_{100} polymers. There was only one spectrum that gave rise to a bimodal hump, that being the PP-F_{100} made via the room temperature two-step method, which may suggest that incomplete substitution occurred. This is postulated since the chemical shift of PDCP where chlorine atoms are the only substitute gives rise to a chemical shift of -17.27 ppm and -9.12 ppm, which is somewhat in between the single peak PP-F_{100} chemical shifts observed at -1.55 and -0.97 ppm and that of PDCP. Therefore, it is proposed that the hump at -9.12 ppm corresponds to phosphorus atoms with 1 L-phenylalanine ethyl ester and 1 chlorine substituent, which could be due to the increased steric hindrance of the bulky phenylalanine groups in comparison to both alanine and chlorine substituents. Overall, despite these minor differences the PP-F_{100}'s were successfully synthesized via all three reaction methods according to FTIR, ^1H NMR and ^{31}P NMR characterization, although substitution may be incomplete in the room temperature two-step reaction.

Peaks from the C-H stretch (alkanes), N-H stretch, and C=O stretch of the ester carbonyl gave rise to peaks at wavenumbers similar to those of PP-A_{100}'s and PP-F_{100}'s. Also, the P=N of the backbone and the P-NH bonds showed broadening of peaks between 1210 – 1145 cm^{-1} and 855 – 840 cm^{-1}, respectively, in comparison to the already present peaks from L-methionine ethyl ester alone. Peak broadening spectra are included in the Appendix (**Appendix 4**) for reference. ^{1}H and ^{31}P NMR spectra were also analyzed to prove the success of the PP-M_{100} syntheses.

The chemical shifts in the ^{1}H NMR spectra of the PP-M_{100}'s relate to the types of protons present in L-methionine ethyl ester. The ^{1}H NMR spectra of the PP-M_{100} synthesized via the 1P RT method will be discussed in detail although the PP-M_{100}'s from the other two methods gave similar spectra with only slight differences in chemical shifts (see **Table 4.2**). The broad singlet peak at a chemical shift of 8.84 ppm represents the protons on the amino terminus of the amino acid ester and integrates for a non-integer value between 1 – 2 protons indicating full or partial cationic charge at the nitrogen atom. In the PP-M_{100} synthesized via the low temperature two-step method this peak is not present, which could indicate that the nitrogen atoms were fully deprotonated after substitution and are more capable than their protonated cationic counterpart at interacting in a hydrogen-deuterium exchange reaction with the solvent. It could also indicate that the amine protons are some how lost and that the reaction did not proceed as expected, although the first scenario is probably more likely since ^{1}H NMR spectra of poly[(amino acid ester)phosphazene]s lacking the amine protons are common in the literature.[95, 118] The multiplet at 4.28 ppm (integration for 3H) corresponds to the proton on the α-carbon and the methylene protons of the ethyl group. The methylene protons of the methionine side chain appear at 2.79 and 2.38 ppm as multiplets with integration for 2 protons each. The singlet at 2.13 ppm (integration for 3H) represents the methyl group next to the sulfur atom in the methionine side chain, which is isolated from other protons by distance and therefore is unsplit. Finally, the triplet at 1.32 ppm (integration for 3H) symbolizes the methyl of the ethyl group, which is split into a triplet by the two protons of the adjacent methylene group.

In ^{31}P NMR analysis of the PP-M$_{100}$'s, broad humps with chemical shifts between 3.51 and -0.43 ppm were observed which is comparable to the literature as a shift of -0.226 ppm has been reported.[118] Taken together, PP-M$_{100}$'s were successfully synthesized via all three reaction methods except for slight differences in characterization spectra with the LT 2S method, although low yields and more demanding procedures have prevented further exploration of materials synthesized via the LT 2S method.

Upon analysis of the PP-A$_{100}$, PP-F$_{100}$, and PP-M$_{100}$ polymers synthesized via the three substitution methods using FTIR, ^{1}H NMR, and ^{31}P NMR spectroscopy, it was determined that there was very little difference between the LT 2S and 1P RT methods, in terms of successful substitution and purity, and further characterization and comparison would only be performed on polymers made from the well-established RT 2S and the new 1P RT methods. This decision was also influenced by the improved yields of the one-pot synthesis over the LT 2S procedure (see **Table 4.2**).

4.2.2   TGA, DSC, and GPC Characterization

TGA and DSC were used to analyze the thermal properties of the materials, including their decomposition temperature (T$_d$), glass transition temperature (T$_g$), and melting temperature (T$_m$), if applicable. Tabulated data from both TGA and DSC analyses has been included in **Table 4.3**. The TGA analyses of the 1P RT and RT 2S synthesized materials are included in **Figure 4.9**.

Table 4.3: Summary of thermal data from TGA and DSC analysis for PP-A$_{100}$, PP-F$_{100}$, and PP-M$_{100}$ materials synthesized via either the 1P RT or RT 2S method. The decomposition temperatures are presented as the peak decomposition temperatures rather than onset, meaning they are the values of maximal rate of change in weight % for all phases of the decomposition (i.e. maxima of the derivative of weight % plot).

Polymer	Method	T$_d$ (°C)	T$_g$ (°C)	T$_m$ (°C)
PP-A$_{100}$	1P RT	217	-41.8	-
	RT 2S	219	-20.8	-
PP-F$_{100}$	1P RT	234, 324	42.8	-
	RT 2S	222, 334	46.3	-
PP-M$_{100}$	1P RT	232, 309	-23.3	43.5
	RT 2S	220, 308	-19.4	62.2
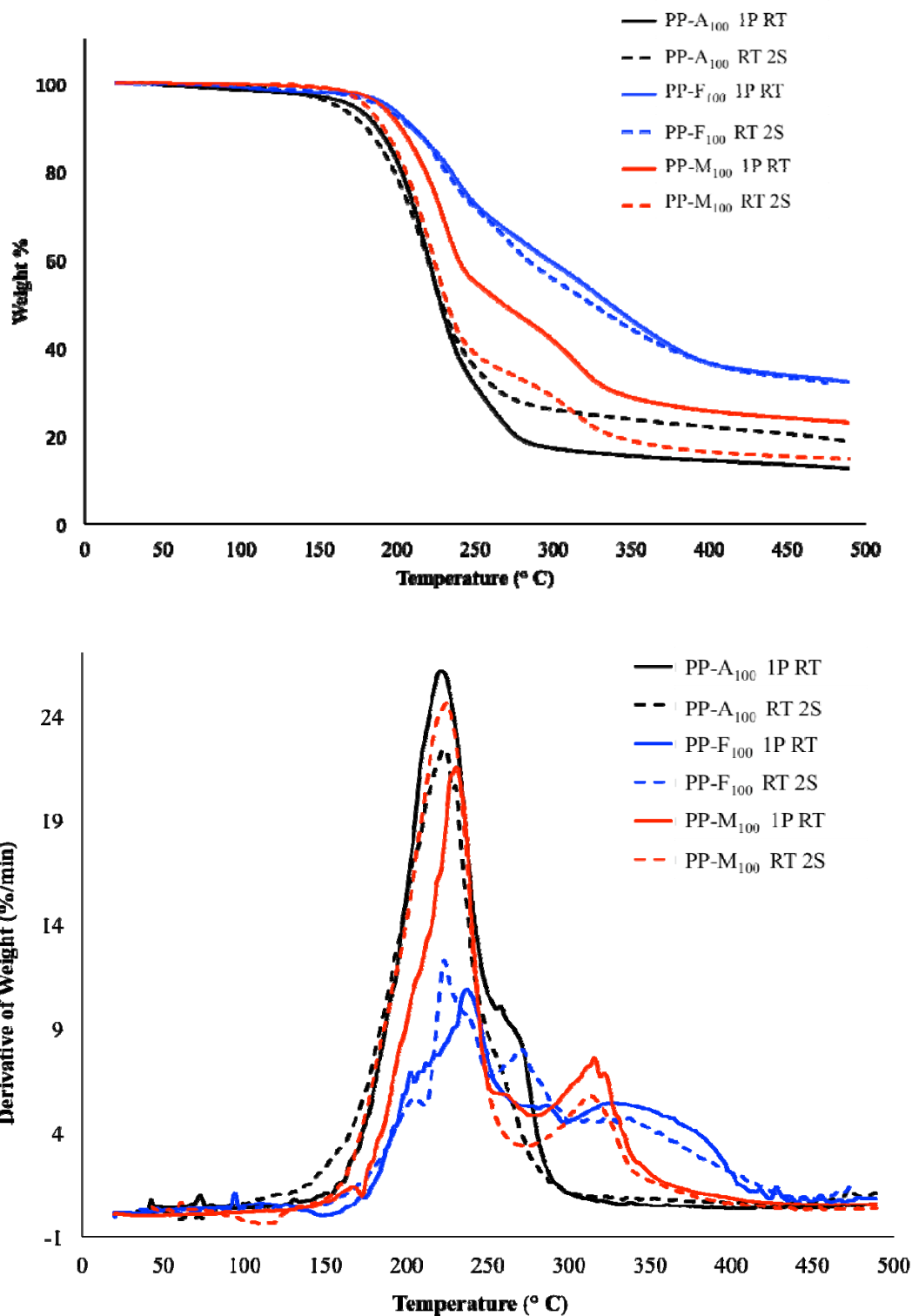
Figure 4.9: TGA analysis for the PP-A$_{100}$, PP-F$_{100}$, and PP-M$_{100}$ materials prepared using the 1P RT and RT 2S methods. The top graph represents the weight percent vs. temperature, where as the bottom graph shows the derivative of weight percent vs. temperature.

From the TGA analyses, it is clear that the phenylalanine-based polyphosphazenes (PP-F_{100}'s) were the most thermally stable materials as can be seen by their higher temperature of decomposition onset in comparison to the PP-A_{100} and PP-M_{100} materials. This is due to the increased rigidity of the bulky aromatic side chain with very stable C=C bonds. The PP-A_{100} and PP-M_{100} materials on the other hand do not contain any C=C bonds in their side chains and thus decomposed at lower temperatures. The bimodal decomposition profile of the PP-F_{100}'s (which is more obvious from the derivative of weight % plot) can be accounted by the initial decomposition of the amino acid backbone in the first peak and followed by the actual decomposition of the aromatic ring of the side chain in the second peak. For the PP-M_{100}'s, which had the second highest onset decomposition temperature, there was also a two-phase decomposition that occurred, with the first peak likely corresponding to the decomposition of the amino acid backbone, like in the PP-F_{100}'s, followed by decomposition of the methionine side chains. It is likely that the PP-M_{100}'s had the intermediate decomposition temperature due to their long aliphatic chains in comparison to the short methyl and bulky aromatic side chains of alanine and phenylalanine, respectively. Lastly, the PP-A_{100} materials had the lowest decomposition onset temperature due to their small aliphatic side chain containing only C-C and C-H bonds. The decomposition of these materials were primarily single stage with a slight hump on the edge of the curves indicating that both the backbone and the side chain of the amino acids degraded at approximately the same temperature. Overall, decomposition onset temperatures for all of the materials were in excess of 140°C although the individual peak T_d values have been included in **Table 4.3**. The decomposition temperatures of poly[(amino acid ester)phosphazene]s are not well recorded in the literature besides one paper that cites the T_ds of PNEA and PNEF as 136 and 185°C, respectively.[84] The reason that the decomposition profiles do not completely reach a weight % of zero is that the inorganic backbone components (P=N and P-N bonds) decomposes at temperatures in excess of 500°C and these temperatures are not reached in these experiments.

The DSC thermograms of the one-pot room temperature and room temperature two-step synthesized materials are included in **Figure 4.10**.
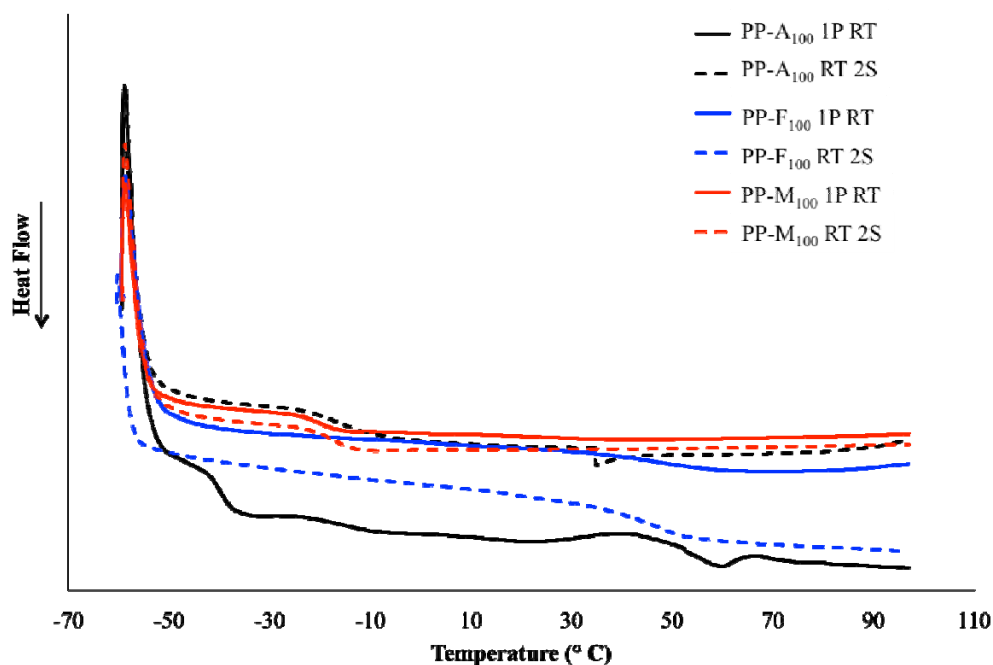
Figure 4.10: DSC thermograms of PP-A$_{100}$, PP-F$_{100}$, and PP-M$_{100}$ materials prepared using the 1P RT and RT 2S methods. The glass transition temperatures (T$_g$s), which were collected from the second heating cycle, range from -41.8 to +46.3°C.

From the DSC, it is evident that the polymers based on the three different amino acids give rise to materials with substantially different T$_g$ values, which is important with respect to scaffold fabrication. Ideal scaffold materials should have T$_g$s near body temperature (37°C) so that they exhibit properties of both the rubbery and glassy material, which better mimics the natural ECM. The rubbery characteristics are ideal for cell-material interactions that enhance cell proliferation on the materials, whereas the hard and brittle characteristics impart mechanical strength to the scaffold as it acts as a support material for neo-tissue growth.[125-128] The bulky and rigid aromatic ring in the side chain of phenylalanine increases the T$_g$s of PP-F$_{100}$'s (42.8 to 46.3°C) in comparison to both PP-A$_{100}$'s and PP-M$_{100}$'s, which is in agreement with the literature where alanine, phenylalanine, and methionine based polyphosphazenes have T$_g$s in the order of PNEA $\approx$ PNEM < PNEF.[83, 84, 94, 95, 97, 115, 116, 118] The steric hindrance of the bulky aromatic side chains of phenylalanine decreases movement in the polymer backbone thus increasing their T$_g$s. This trend is maintained as the PP-M$_{100}$'s (-23.3 to -19.4°C) have T$_g$s that are

similar to the PP-A$_{100}$'s and lower than PP-F$_{100}$'s. The increased flexibility of the aliphatic side chain in methionine in comparison to the rigid ring structure in phenylalanine lowers the T$_g$s of the PP-M$_{100}$ materials. The substantial difference in T$_g$ values for the PP-A$_{100}$'s prepared using the two different methods may be due to large differences in molecular weights, which is known to have an effect on glass transitions in low molecular weight materials.[129] Another possibility is that residual solvent could have had a plasticizing effect on the RT 2S synthesized material, thus giving the appearance of a decreased T$_g$ value. Overall, the T$_g$s for the PP-A$_{100}$'s synthesized in this work fall outside of the range of T$_g$s presented in the literature (-10 to 19°C),[83, 84, 94, 97, 116] but again this could potentially be accounted for by significant differences in the molecular weights of the materials, as they are prepared using different methods. When comparing the literature cited PNEFs (40 to 68°C)[84, 95] to the T$_g$s of the PP-F$_{100}$'s prepared in this work they are very similar with T$_g$s ranging from 42.8 to 46.3°C, which is promising. To the best of our knowledge only one T$_g$ for PNEM has been reported in the literature (9°C),[118] so comparison of this work to that single study should be taken with caution, although the T$_g$s of the PP-M$_{100}$'s synthesized in this work are far lower than the cited T$_g$, they are on par with the PP-A$_{100}$'s, which is in agreement with the literature.

The molecular weights of the polymers synthesized were determined by means of GPC using triple-detection (light scattering, refractive index, and viscometry). Light scattering detection relies on monitoring the changes in refractive index of the polymer solutions with varying concentrations, also known as the differential index of refraction or the refractive index increment (*dn*/*dc*), to determine absolute molecular weights.[130] This method gives the most accurate results if changes in *dn*/*dc* values are large enough, which is not always the case. In the event that *dn*/*dc* values are too low, other detection methods such as refractive index can be employed and molecular weights can be determined by comparing the materials to standards such as polystyrene. For this work, light scattering determination of absolute molecular weights was attempted for all materials, although in some cases *dn*/*dc* were too low and relative molecular weights (relative to polystyrene) were determined instead. **Table 4.4** summarizes the GPC data for the polyphosphazenes based on non-functional amino acids.

Table 4.4: GPC analysis of PP-A$_{100}$, PP-F$_{100}$, and PP-M$_{100}$ materials using triple detection and refractive index detection. A (-) indicates that analysis using that detection method was not possible and the relative molecular weights are calculated based on polystyrene standards.

Polymer	Method	Triple Detection: Absolute Molecular Weights			Refractive Index Detection: Relative Molecular Weights		
		M_w (Da)	M_n (Da)	PDI	M_w (Da)	M_n (Da)	PDI
PP-A$_{100}$	1P RT	-	-	-	14, 780	4, 440	3.329
	RT 2S	-	-	-	9, 946	3, 727	2.668
PP-F$_{100}$	1P RT	203, 471	176, 518	1.153	19, 426	8, 886	2.186
	RT 2S	279, 111	249, 103	1.121	211, 910	19, 497	10.869
PP-M$_{100}$	1P RT	350, 721	316, 127	1.109	10, 238	6, 025	1.699
	RT 2S	93, 136	62, 478	1.493	6, 018	1, 902	3.164

As an example of the overlap of the traces collected from GPC for the triple detection method, the traces from all four detectors (refractive index, right angle light scattering, low angle light scattering, and viscometery) for the PP-M$_{100}$ material synthesized via the one-pot room temperature method has been included in **Figure 4.11**. Only the refractive index traces are included for the remaining polymers, which can be seen in **Figure 4.12**.
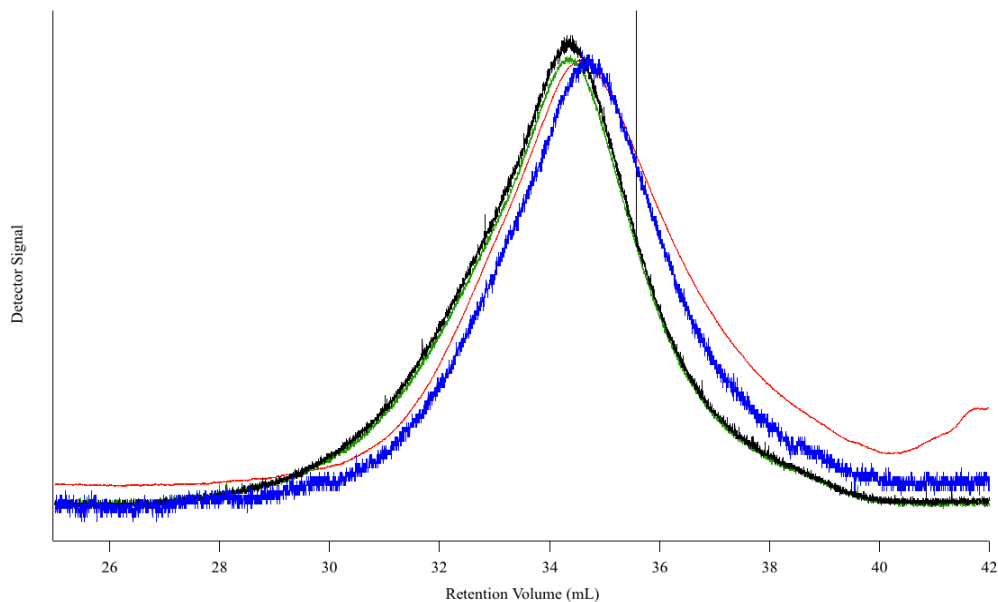
Figure 4.11: Detector signal versus retention volume (mL) traces from GPC analysis of PP-M$_{100}$ synthesized via the 1P RT method. Detector traces correspond to refractive index (red), right angle light scattering (green), low angle light scattering (black) and viscometer (blue).
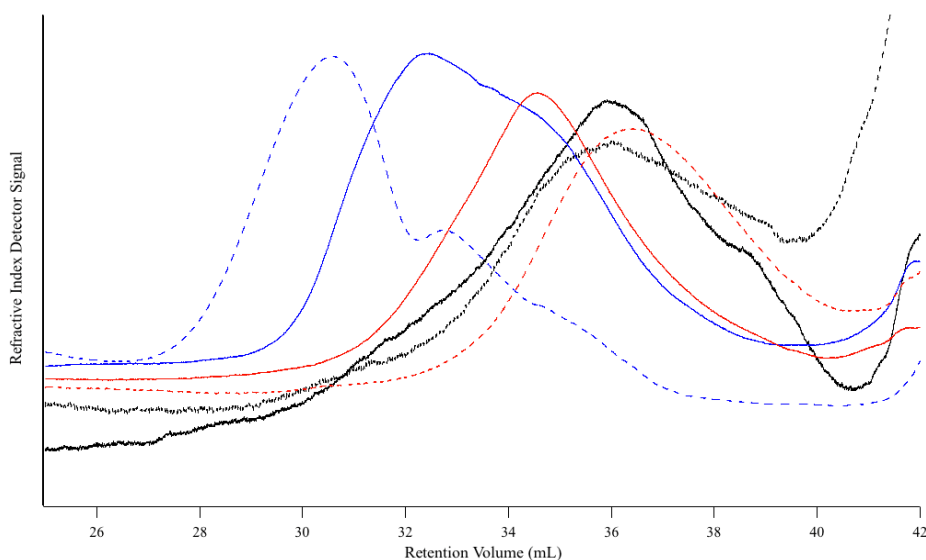
Figure 4.12: GPC traces from the refractive index detector for PP-A$_{100}$ (----1P RT, - - - RT 2S), PP-F$_{100}$ (---- 1P RT, - - - RT 2S), and PP-M$_{100}$ (---- 1P RT, - - - RT 2S).

The traces from the four detectors (**Figure 4.11**) overlap well indicating that readings from all of the detectors corroborate with each other. As such, the light scattering detection traces and measured *dn*/*dc* values can be used to determine the absolute

molecular weights of the polymers with the assumption that the materials are homopolymers and therefore, there are no unsubstituted P-Cl bonds remaining in the materials.[130] This is a reasonable assumption for all of the materials except the PP-F$_{100}$ synthesized via the room temperature two-step method as it gave 2 signals rather than 1 in ^{31}P NMR, indicating the possibility of a partially substituted polymer (likely some phosphorus atoms with only one phenylalanine ethyl ester attached and a remaining P-Cl bond rather than two phenylalanine ethyl esters attached). Therefore, the absolute molecular weights for PP-F$_{100}$ 1P RT, PP-M$_{100}$M 1P RT, and PP-M$_{100}$ RT 2S can be considered valid. Another note to consider with light scattering detection for absolute molecular weight analysis is that PDI values are underestimated using this technique and should be taken with caution.[130] Unfortunately, similar polyphosphazenes have not been analyzed using a triple detection method for GPC in published literature and therefore the values determined in this work cannot be compared to cited values.

For the polymers that could not be analyzed via light scattering detection due to low *dn*/*dc* values, refractive index detection was used instead and molecular weights were calculated relative to polystyrene standards (see **Table 4.4**). From the refractive index traces (**Figure 4.12**), it is evident that PP-F$_{100}$ materials tend to give rise to bimodal chromatograph indicating that there is likely a mixture of high and low molecular weight polymers, which is also evident from the large PDIs. Overall, the relative molecular weights of the non-functional amino acid ester based polyphosphazene materials of this work appeared to be lower than those of the literature.[83, 84, 94, 97, 115, 117, 118] This is likely due to the presence of moisture during the polymerization and substitution steps of the synthesis in the new techniques. Moisture has been shown to initiate premature hydrolysis of the materials leading to decreased molecular weights.[81] It is interesting to note that the molecular weights of the materials from the one-pot method are higher than those from the traditional two-step reaction, indicating that this method may even increase molecular weights further if applied to inert atmosphere reactions. This was surprising as lower pH solutions have been shown to increase the rate of degradation of poly[(amino acid ester)phosphazene]s and forming the free base in solution during the substitution has the potential to release hydrochloric acid.[81] The exception to this is with the PP-F$_{100}$ materials but the relative molecular weights of the RT 2S are vastly different

than the remainder of the materials and should be considered with caution. The two peaks in the ^{31}P NMR spectra are also an indication that this material may not actually be the expected material proposed and therefore comparison to this material should be used sparingly or not at all. The substantial difference in absolute molecular weights versus relative molecular weights could be accounted for by differences in behavior of the polymers in the GPC eluent (10 mM n-butylammonium nitrate in THF). For example, the conformation of the polystyrene standards may take on a compact shape in an attempt to exclude the eluent thus giving rise to a smaller hydrodynamic radius, whereas the polyphosphazenes may take on an extended conformation in which the eluent is free to interact with the polymer leading to a larger hydrodynamic radius for a polyphosphazene than polystyrene of the same molecular weight.[131] These differences in conformation can lead to problems in calculating the molecular weights of the polyphosphazenes based on polystyrene standards. Despite this, poly[(amino acid ester)phosphazene]s based on alanine ethyl ester, phenylalanine ethyl ester, and methionine ethyl ester, have been successfully synthesized and characterized (FTIR, ^{1}H NMR, ^{31}P NMR, TGA, DSC, and GPC) in a non-inert atmosphere with a simplified substitution method that eliminated the requirement of liberating the free base of the amino acid ester hydrochloride salt prior to substitution. These two new methods (polymerization and one-pot substitution) will be applied further for the development of novel materials with functional handles for biomolecule conjugation.

4.3   Esterification of Fmoc- and Boc-Glu(OBzl)-OH

Although amino acid esters with no functionality in their side chains, like alanine, phenylalanine, and methionine, are readily available as their hydrochloride salts, amino acid esters with added functional groups in their side chains, like glutamic acid, aspartic acid, and lysine, are not and must therefore be synthesized before incorporation into poly[(amino acid ester)phosphazene]s. Glutamic acid was selected as the functional amino acid to be co-substituted with the non-functional amino acids of the base polymers due to its carboxylic acid group that can be used to attach small molecules and proteins and potentially enhance cell-material interaction. Glutamic acid was chosen over aspartic acid, which also contains a carboxylic acid group, because of its extra methylene in the

side chain that extends the functional group out further from the polymer backbone decreasing the likelihood of unsuccessful biomolecule conjugation due to steric hindrance alone. Lysine is another viable option as a functional amino acid co-substituent with its amine group in the side chain, although it was not considered in this work.

Since glutamic acid could not be purchased as the ethyl ester at the C terminus, variations with the N terminus and side chain carboxylic acid orthogonally protected were acquired instead and the C terminus was esterified with ethanol in-house. Fmoc and Boc protected N termini with a benzyl ester protected side chain were selected based on their availability, as Fmoc and Boc protected amino acids are common in peptide synthesis[132, 133], relatively inexpensive, and mild deprotection conditions are required (mild base and acid, respectively).[134] The benzyl ester protecting group of the side chain was selected on the basis of its base stability and deprotection using hydrogenation rather than acid, which could cause cleavage of the amino acid esters or hydrolysis of the polyphosphazene backbone.[134] It is important that the glutamic acid side chain be protected since it can also act as a nucleophile in the substitution with poly[(dichloro)phosphazene], which would lead to a mixture of amino acid esters bound through both the nitrogen of the N terminus and the oxygen of the carboxylic acid side chain. This could also be problematic as the two reactive sites could react with each other forming amide bonds and causing crosslinking of the polymers, which is not ideal. Esterification of the C terminus was attempted using a carbodiimide coupling chemistry method that was previously reported[135]. In this cited paper, esterifications on Boc protected amino acids were attempted, although it was predicted that it may also work for Fmoc protected amino acids since only catalytic amounts of base were required. In fact successful esterification of Boc-Glu(OBzl)-OH with methanol (MeOH), *t*-butanol (t-BuOH), and benzyl alcohol (PhCH$_2$OH) nucleophiles was shown[135] although ethanol (EtOH) had not been investigated. In this work, ethyl esterification of both Fmoc-Glu(OBzl)-OH and Boc-Glu(OBzl)-OH were attempted, although initial experiments with Fmoc-Glu(OBzl)-OH led to a mixture of products as determined by ^{13}C and ^{1}H NMR. It is believed that the base-labile Fmoc group was cleaved during the esterification giving way to potential self-condensation reactions and a plethora of side products, which could not be removed using standard liquid-liquid extraction purification. Further

experiments with Fmoc-Glu(OBzl)-OH were not attempted and esterification of Boc-Glu(OBzl)-OH was pursued. Boc- Glu(OBzl)-OH was successful esterified with ethanol via the DMAP and EDC coupling chemistry [135] as determined by ^{1}H NMR analysis of the starting material in comparison to the esterification product (**Figure 4.13**). The appearance of the quartet at 4.16 ppm and the triplet at 1.24 ppm corresponding to the methylene and methyl protons of the ethyl ester, as well as the disappearance of the broad singlet at 10.61 ppm from the COOH indicate complete esterification of the C terminus. The purification of the product was modified from that of the paper by performing the DI water washes with 60°C DI water rather room temperature since ureas, which are the byproduct of carbodiimide coupling chemistry, are known to be more water-soluble at higher temperatures and remain dissolved in the aqueous layer upon cooling.[136] Initial esterifications gave ^{1}H NMR spectra that indicated incomplete removal of urea byproduct impurities in the Boc-Glu(OBzl)-OEt product but upon implementation of the higher temperature washes, these impurities were successfully removed leaving only pure Boc-Glu(OBzl)-OEt. Before the esterified glutamic acid could be used in substitution reactions with poly[(dichloro)phosphazene], its amine terminus needed to be deprotected so that the amine could act as a nucleophile in the substitution reaction.
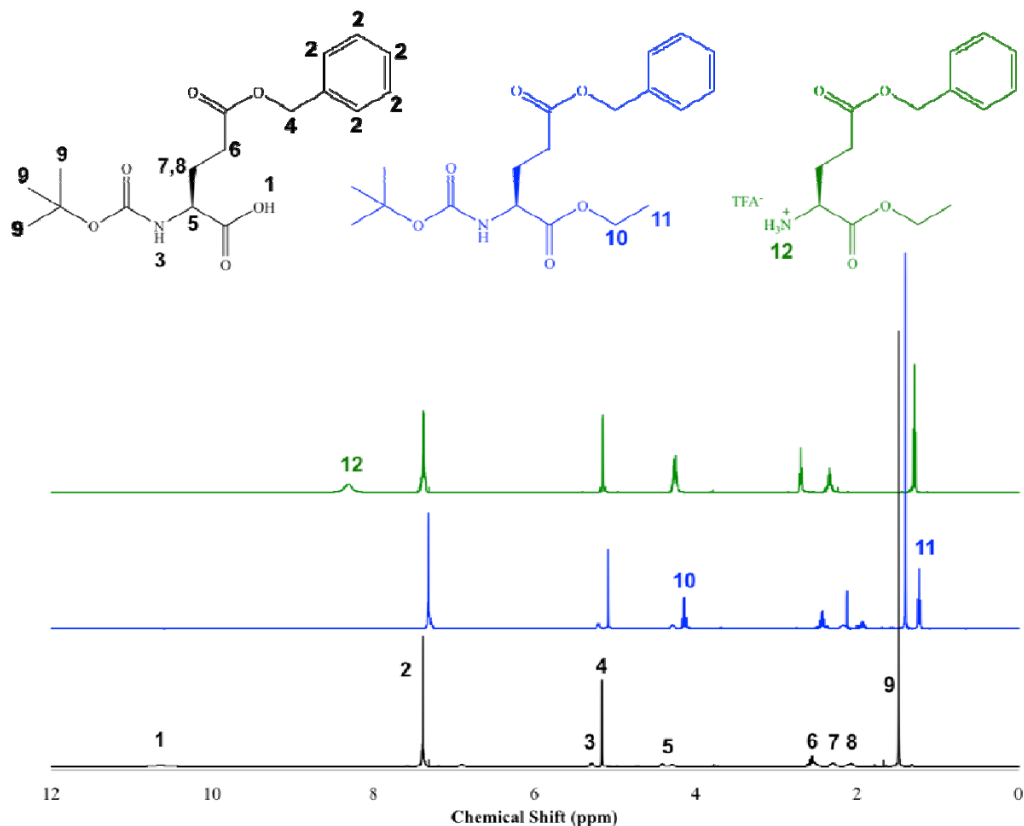
Figure 4.13: ^{1}**H NMR spectra of the esterification with ethanol and deprotection with 25% TFA in DCM of Boc-Glu(OBzl)-OH (black). The ethyl esterified product, Boc-Glu(OBzl)-OEt, is shown blue and the Boc deprotected product, TFA$^-$/H$_3$N$^+$-Glu(OBzl)-OEt, is shown in green. Unlabeled peaks in the Boc-Glu(OBzl)-OEt and TFA$^-$/H$_3$N$^+$-Glu(OBzl)-OEt spectra are equivalent to the labeled peaks with the same chemical shift in the Boc-Glu(OBzl)-OH spectrum.**

4.4 TFA Deprotection of Boc-Glu(OBzl)-OEt

The Boc protecting group on amines has been shown to be removed by 50% trifluoroacetic acid (TFA) in dichloromethane (DCM), so this deprotection step was employed to the Boc-Glu(OBzl)-OEt molecule synthesized in Section 3.3.[134] From ^{1}H NMR analysis, it was observed that this concentration of TFA also lead to partial deprotection of the benzyl ester of the side chain (appearance of a broad singlet at 11.98 and singlet at 2.19 ppm, presumably indicating COOH and toluene, respectively). In an effort to deprotect the Boc group and minimize concurrent benzyl deprotection, 25% TFA in DCM was attempted. This method was successful in deprotecting the Boc group while maintaining the integrity of the benzyl ester as is shown in **Figure 4.13,** which is

observed as a disappearance of the singlet at 1.24 ppm corresponding to the Boc protecting group and the appearance of a broad singlet at 8.29 ppm which represents the amine protons.

4.5   Macromolecular Co-Substitution of Functional and Non-Functional Amino Acid Esters

In order to improve cell-material interactions, more often than not biomolecules are attached to the materials, either through adsorption or by covalent linkage to the scaffold itself. With adsorption, the biomolecules can quickly diffuse away from the material once submerged in culture media or body fluid if the non-covalent interactions are weak leading to decreased efficiency and minimal improvement in cell-material interactions.[53] Conjugation of the biomolecules through covalent bonds, on the other hand, prevents this diffusion problem and maintains the biomolecule at the material surface, ideally leading to a sustained and enhanced effect on the cell-material interactions. As such, the development of materials containing functional handles for biomolecule attachment is being actively pursued.[53] In this work, glutamic acid, with its carboxylic acid functional group in the side chain, was explored as a co-substituent in poly[(amino acid ester)phosphazene]s, giving the mixed polymers a reactive site for biomolecule conjugation.

Initial substitution reactions investigated the sequential addition of the amino acid esters, where the bulkier substituent (glutamic acid ethyl ester in this case) was reacted first, followed by the less bulky amino acid ester (alanine ethyl ester, phenylalanine ethyl ester, or methionine ethyl ester) in excess, as is described in the literature. In these reactions, the polymer precipitated out of solution before complete substitution was achieved, making co-substitution via this method unfeasible. This problem is likely due to the glutamic acid ester substituents being already bound either directing the subsequent substitution in a tactic fashion that leads to an insoluble polymer or that the glutamic acid substituents cause crosslinking in the polymer also leading to insolubility issues. Therefore, a new step-wise synthesis was employed that reacted half of the total less bulky and non-functional amino acid ester first, followed by all of the required amount of glutamic acid ester, and completion of substitution with an excess of the non-functional

amino acid ester. The reasoning behind this method was to eliminate the proposed glutamic acid interactions described above that lead to precipitation by partially substituting the poly[(dichloro)phosphazene] with the non-functional amino acid esters, which prevent the glutamic acid ester substituents from grouping together. This method was used to make polymers with approximately 90% substitution of the non-functional amino acid ester and 10% benzyl protected glutamic acid ethyl ester. These functional polymers (PP-A$_{90}$E$^*_{10}$, PP-F$_{90}$E$^*_{10}$, and PP-M$_{90}$E$^*_{10}$) were then characterized by FTIR, ^{1}H NMR, ^{31}P NMR, TGA, DSC, and GPC and compared to their non-functional base polymers made from the one-pot room temperature synthesis method. It was not possible to compare the characterization data to literature values, as these are novel compounds that have not been previously published.

4.5.1   FTIR, ^{1}H NMR, and ^{31}P NMR Characterization

Table 4.5 summarizes the spectroscopic characterization using FTIR, ^{1}H NMR, and ^{31}P NMR along with percent yields for the three poly[(amino acid ester)phosphazene]s co-substituted with a non-functional amino acid ester (alanine, phenylalanine, or methionine) and the functional glutamic acid ethyl ester.

Table 4.5: Summary of percent yields, ^{1}H NMR, ^{31}P NMR and FTIR characterization of the co-substituted poly[(amino acid ester)phosphazene]s.

Polymer	% Yield	^{1}H NMR (δ, ppm)	^{31}P NMR (δ, ppm)	FTIR (cm^{-1})
PP-A$_{90}$E$^*_{10}$	37.7	8. 55 (br. s) 7.23 (m) 5.00 (d) 4.17 (m) 3.64 (m) 3.14 (qd) 2.33 (q) 1.59 (d) 1.30 (t) 1.18 (t)	1.84	3100 – 2700 (C-H stretch) 1740 (C=O, ester from Ala) 1660 (C=O, ester from Glu)
PP-F$_{90}$E$^*_{10}$	23.9	8.62 (br. s) 8.33 (s) 7.30 (m) 5.11 (m) 4.22 (m) 4.10 (m) 3.12 (m) 2.50 (m) 1.14 (t) 1.08 (t)	0.06 -10.50	3100 – 2700 (C-H stretch) 1740 (C=O, ester from Phe) 700 (C-H aromatic from Phe & Glu)
PP-M$_{90}$E$^*_{10}$	22.0	8.72 (br. s) 7.32 (m) 5.11 (d) 4.26 (m) 3.14 (qd) 2.75 (m) 2.35 (m) 2.11 (s) 1.38 (t) 1.32 (t)	1.87	3100 – 2700 (C-H stretch) 1740 (C=O, ester from Met) 1660 (C=O, ester from Glu)

The FTIR spectra of the co-substituted poly[(amino acid ester)phosphazene]s in comparison to their parent base polymers and TFA$^-$/H$_3$N$^+$-Glu(OBzl)-OEt are shown in **Figures 4.14 – 4.16**.
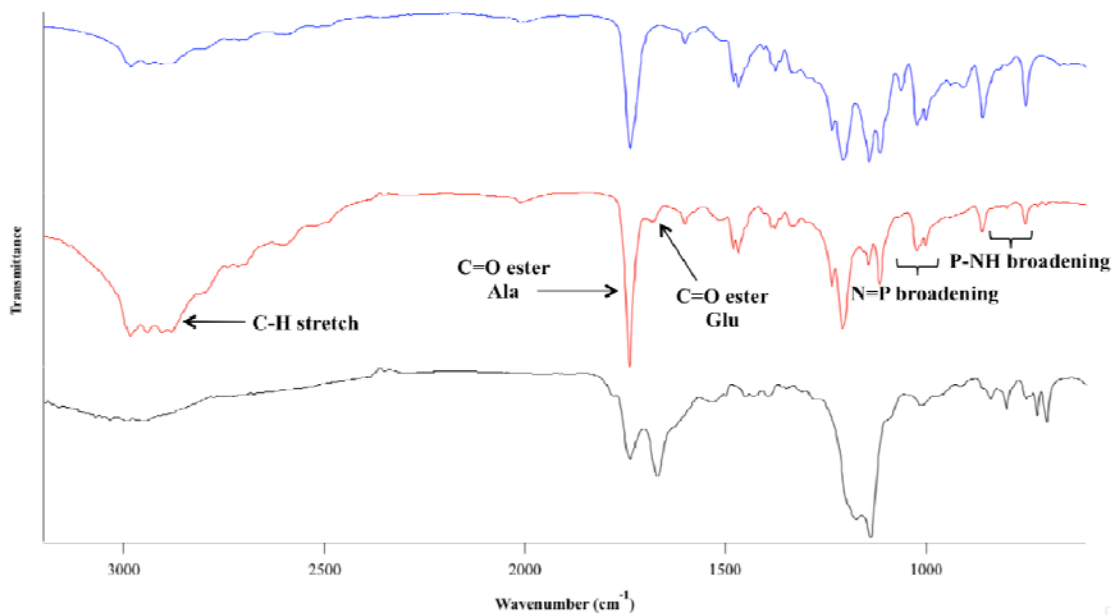
Figure 4.14: FTIR spectra of TFA$^-$/H$_3$N$^+$-Glu(OBzl)-OEt (black), PP-A$_{90}$E$^*_{10}$ (red) , and PP-A$_{100}$ synthesized via the 1P RT method (blue).
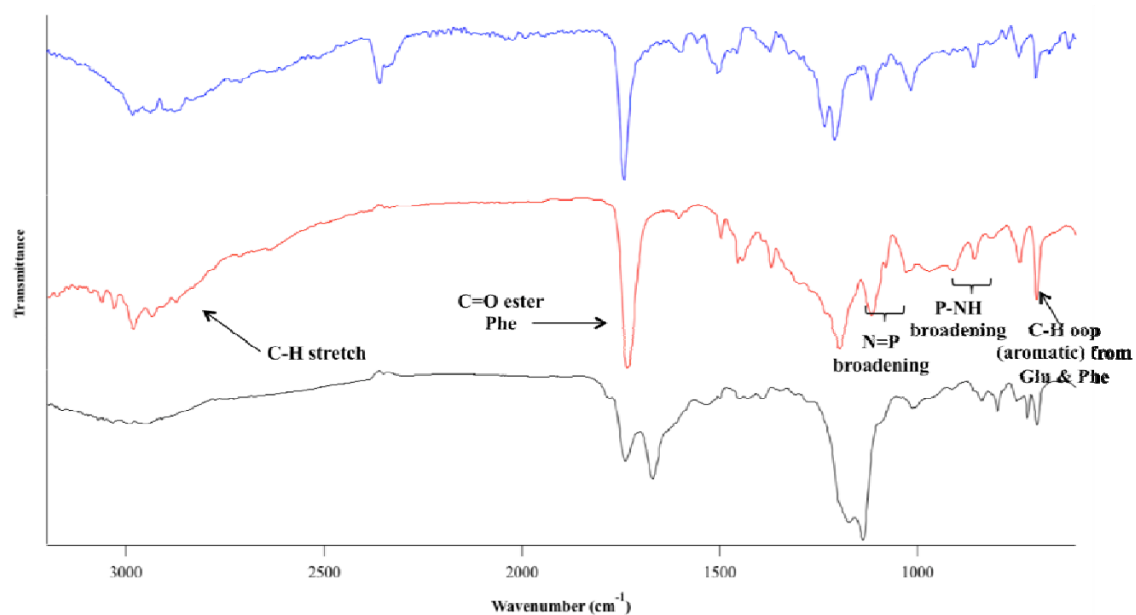
Figure 4.15: FTIR spectra of TFA$^-$/H$_3$N$^+$-Glu(OBzl)-OEt (black), PP-F$_{90}$E$^*_{10}$ (red) , and PP-F$_{100}$ synthesized via the 1P RT method (blue).
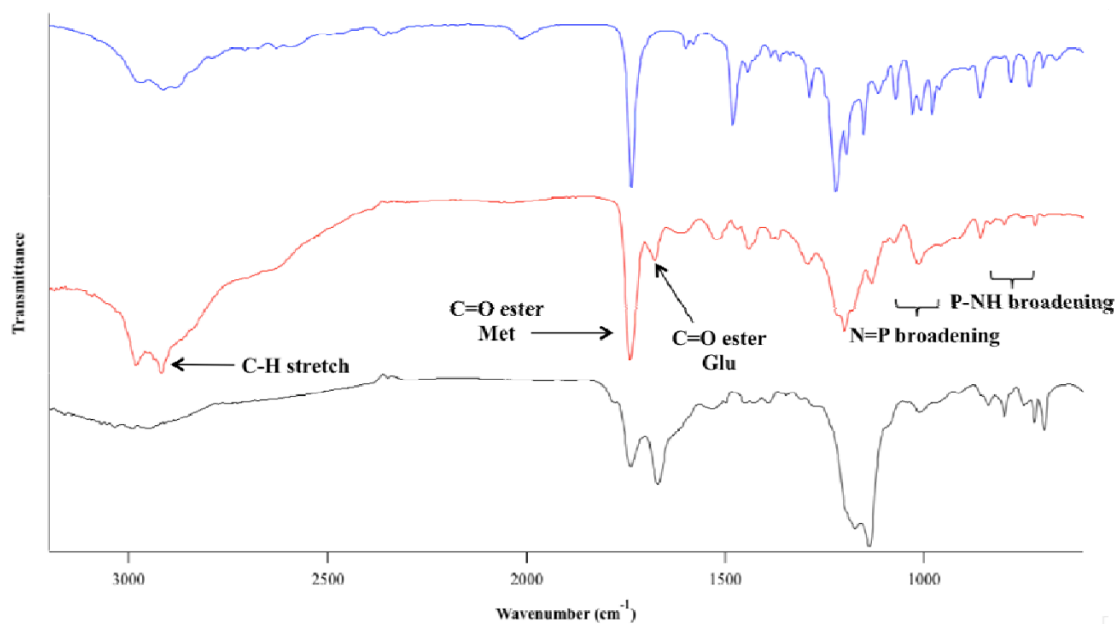
Figure 4.16: FTIR spectra of TFA$^-$/H$_3$N$^+$-Glu(OBzl)-OEt (black), PP-M$_{90}$E$^*_{10}$ (red) , and PP-M$_{100}$ synthesized via the 1P RT method (blue).

The overlapped ^{1}H NMR spectra of TFA$^-$/H$_3$N$^+$-Glu(OBzl)-OEt, the co-substituted poly[(amino acid ester)phosphazene]s, and their base non-functional polyphosphazenes for all three of the functional polymers are presented in **Figures 4.17 – 4.19**.
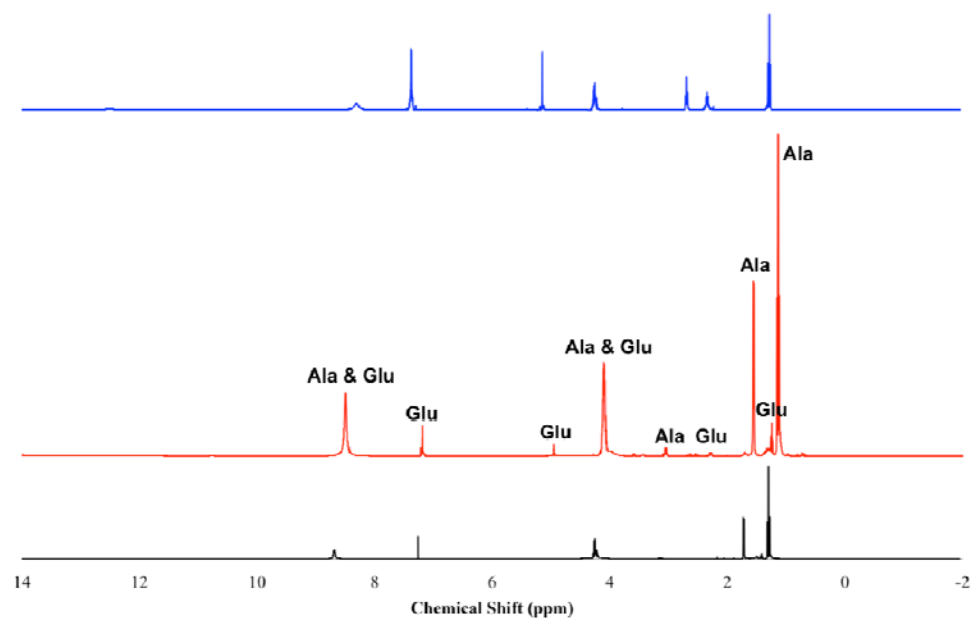
Figure 4.17: ^{1}H NMR spectra of TFA$^-$/H$_3$N$^+$-Glu(OBzl)-OEt (black), PP-A$_{90}$E$^*_{10}$, (red), and PP-A$_{100}$ from the 1P RT method (blue).
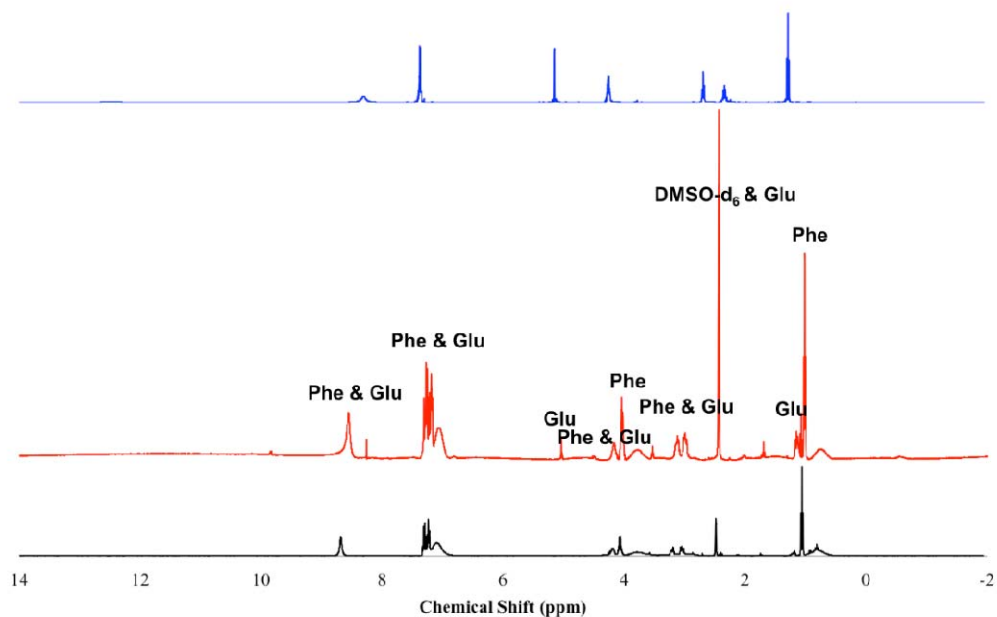
Figure 4.18: ^{1}H NMR spectra of TFA$^-$/H$_3$N$^+$-Glu(OBzl)-OEt (black), PP-F$_{90}$E$^*_{10}$ (red), and PP-F$_{100}$ from the 1P RT method (blue).
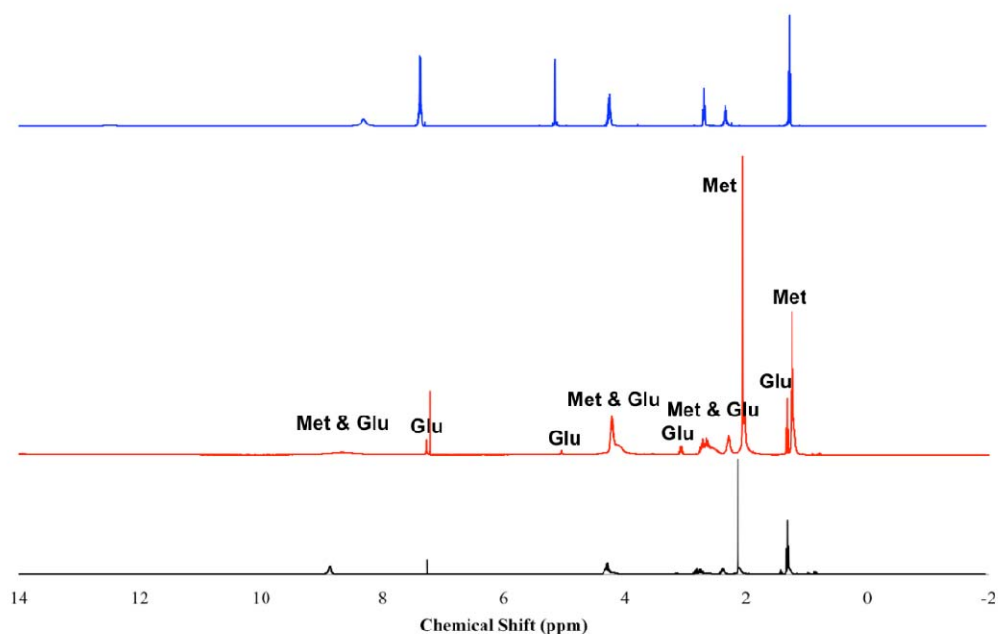
Figure 4.19: ^{1}H NMR spectra of TFA$^-$/H$_3$N$^+$-Glu(OBzl)-OEt (black), PP-M$_{90}$E$^*_{10}$ (red), and PP-M$_{100}$ from the 1P RT method (blue).

From the FTIR and ^{1}H NMR of all of the co-substituted poly[(amino acid ester)phosphazene]s, it is clear that the benzyl protected glutamic acid ethyl ester substituent has been successfully incorporated as a co-substituent in all of the materials. This was demonstrated by the presence of FTIR peaks from both the base polyphosphazene material (PP-A$_{100}$, PP-F$_{100}$, and PP-M$_{100}$) and from the TFA$^-$/H$_3$N$^+$-Glu(OBzl)-OEt amino acid ester substituent. For example, in the PP-A$_{90}$E$^*_{10}$ FTIR spectrum we see a peak at approximately 1740 cm^{-1} that corresponds to the C=O of the ester group of the amino acid backbones and another peak at approximately 1660 cm^{-1} that identifies the C=O of the ester group in glutamic acid side chain. In ^{1}H NMR spectra of the co-substituted poly[(amino acid ester)phosphazene]s, the peaks with correct chemical shift and multiplicity that are equivalent to the parent non-functional polymer and glutamic acid ethyl ester substituent are all present. For example, in PP-A$_{90}$E$^*_{10}$ the multiplet at 7.23 ppm corresponds to the aromatic protons of the benzyl protecting group in glutamic acid ethyl ester, whereas the triplet at 1.18 ppm represents the terminal CH$_3$ group of the ethyl ester on alanine. From ^{31}P NMR, it is again clear that the polymers were formed with the appearance of a singlet, for all except PP-F$_{90}$E$^*_{10}$, around 0 ppm

and the disappearance of the singlet at approximately -17 ppm for the poly[(dichloro)phosphazene] linear precursor (see **Table 4.5** for exact chemical shifts). In the case of PP-F$_{90}$E$^{*}_{10}$ a two-hump peak was again observed like with the PP-F$_{100}$ synthesized via the RT 2S method. In this case, the peak could again correspond to phosphorus atoms that have residual chlorine atoms bound but could also indicate tacticity in the polymer where initial phenylalanine substitution directs the incorporation of the glutamic acid ester co-substituent. Two peaks in the ^{31}P NMR could potentially indicate that the phenylalanine ethyl ester substituents selectively attached on either side of the same phosphorus atom, giving rise to one of the peaks, leaving the glutamic acid ester substituents to also attach to the same phosphorus atom as themselves, giving rise to the second peak (i.e. phosphorus atoms with two phenylalanine groups and others with two glutamic acid groups).

Considering that in ^{1}H NMR peak areas correlate to relative numbers of protons, integration of the peaks solely from the non-functional amino acid ester and solely from the functional glutamic acid ester were compared to determine the amounts of each of the co-substituents on the polymer. The reaction schemes were designed to theoretically incorporate 10% of benzyl protected glutamic acid ethyl ester with the remaining 90% being substituted by the non-functional amino acid esters although steric hindrance and other factors may have limited the actual amount of the glutamic acid ester that was actually incorporated. The experimentally determined percentages of benzyl protected glutamic acid ethyl ester substituents were 6.8, 7.7, and 9.3% for the PP-A$_{90}$E$^{*}_{10}$, PP-F$_{90}$E$^{*}_{10}$, and PP-M$_{90}$E$^{*}_{10}$, respectively.

4.5.2   TGA, DSC, and GPC Characterization

This next section describes the thermal properties and molecular weights of the functional polyphosphazenes. As with the non-functional base polymers, thermal data was collected to determine the decomposition, glass transition, and melting temperatures, where applicable, for all of the functional polymers co-substituted with benzyl protected glutamic acid ethyl ester and results are summarized in **Table 4.6**.

Table 4.6: Summary of thermal data from TGA and DSC analysis for PP-A$_{90}$E$^*_{10}$, PP-F$_{90}$E$^*_{10}$, and PP-M$_{90}$E$^*_{10}$ polymers. The decomposition temperatures are presented as the peak decomposition temperatures rather than onset, meaning they are the values of maximal rate of change in weight % for all phases of the decomposition (i.e. maxima of the derivative of weight % plot).

Polymer	T_d (°C)	T_g (°C)	T_m (°C)
PP-A$_{90}$E$^*_{10}$	225, 285	-49.4	-
PP-F$_{90}$E$^*_{10}$	210, 295	44.5	-
PP-M$_{90}$E$^*_{10}$	225, 315	-42.5	-

Thermogravimetric (TGA) analysis data showing thermal decomposition properties are shown in **Figure 4.20**.
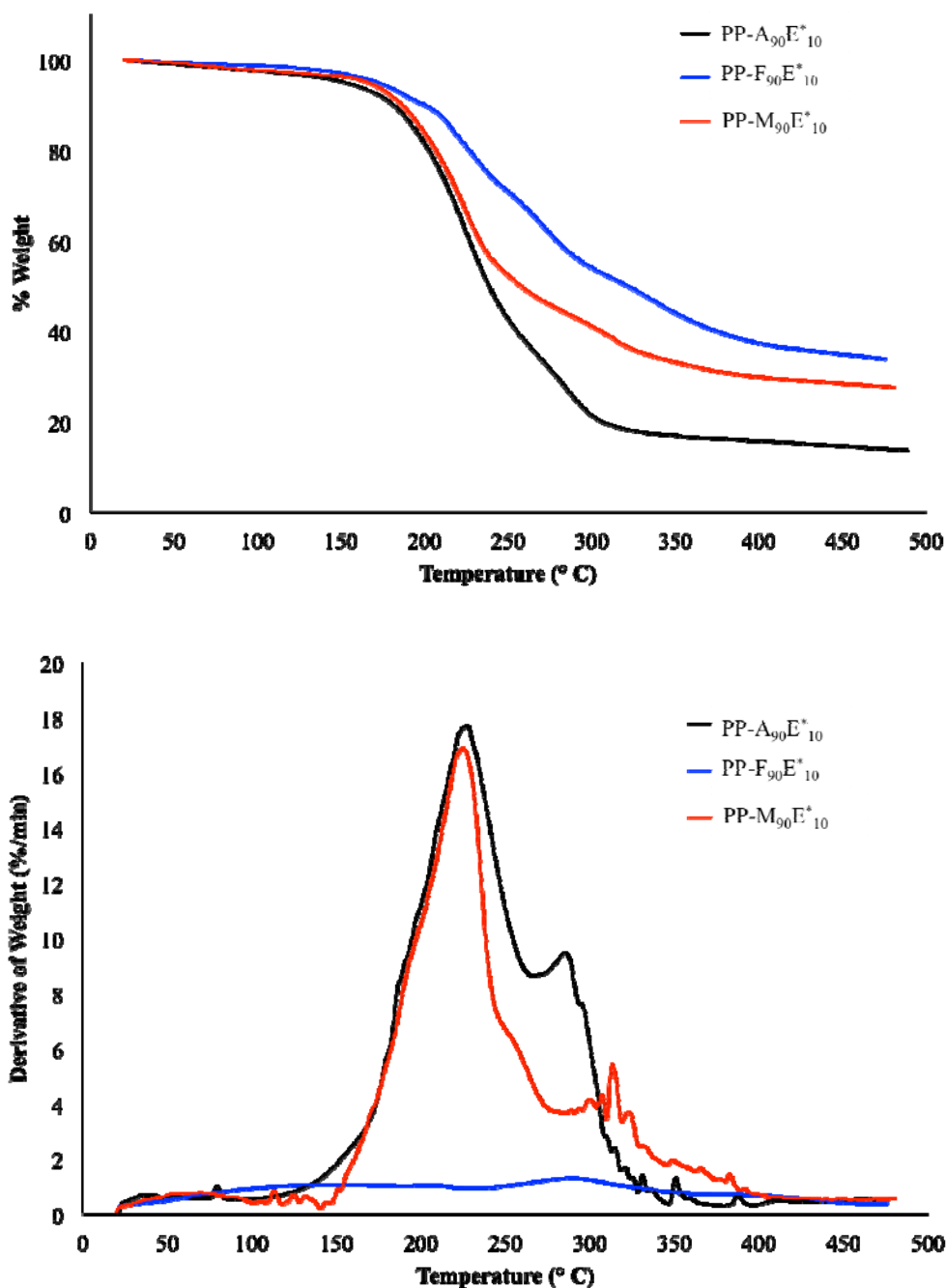
Figure 4.20: TGA analysis for the PP-A$_{90}$E$^*_{10}$, PP-F$_{90}$E$^*_{10}$, and PP-M$_{90}$E$^*_{10}$ polymers. The first graph represents the weight percent vs. temperature, where as the second graph shows the derivative of weight percent vs. temperature.

From TGA analyses, all three of the polymers exhibited similar thermal stability with onset of decomposition in excess of approximately 150°C for all. Unlike the single phase

decomposition observed with the PP-A$_{100}$ base polymer, all of the functional polyphosphazenes showed two-step decomposition processes, similar to PP-F$_{100}$ and PP-M$_{100}$. The reason behind the two-step decompositions with the functional polymers is the presence of the C=C bonds aromatic bonds of the benzyl protecting group, and phenylalanine side chain in PP-F$_{90}$E$^*_{10}$, which give rise to the second peak of the process as these bonds are more stable than the C-C and C-H bonds of the amino acid backbone. All of the TGA traces were relatively similar to one another, which is to be expected when the all contain not only C-C and C-H bonds but also the more stable C=C bonds. Like with the non-functional base polymers, the decomposition profiles do not completely reach a weight % of zero since the inorganic backbone of the polyphosphazenes does not decompose in the temperature range of the experiments.

The differential scanning calorimetry (DSC) analyses of the functional polyphosphazenes are presented in **Figure 4.21**.
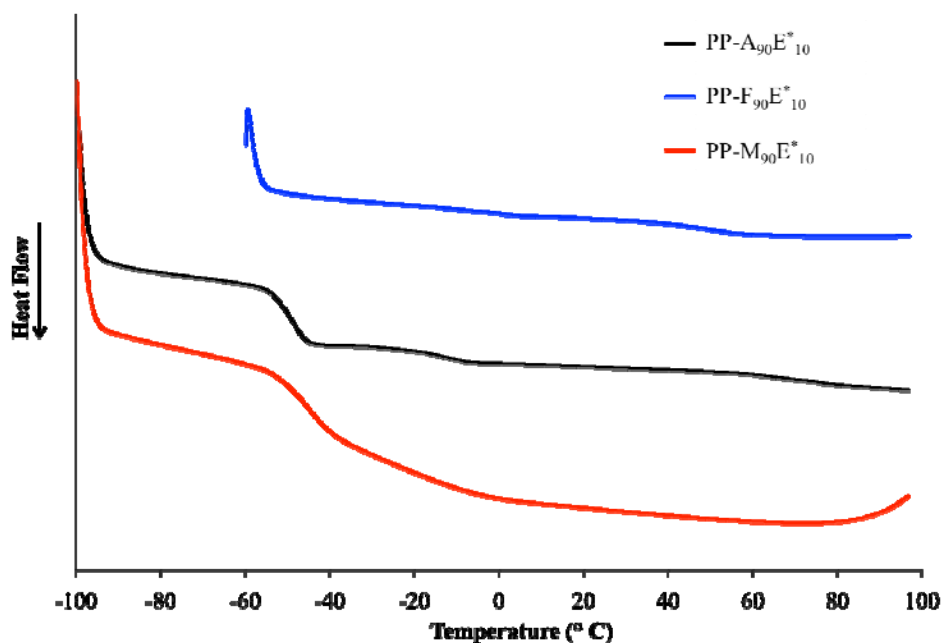
Figure 4.21: DSC thermograms of PP-A$_{90}$E$^*_{10}$, PP-F$_{90}$E$^*_{10}$, and PP-M$_{90}$E$^*_{10}$ polymers. The glass transition temperatures (T$_g$s), which were collected from the second heating cycle, range from -49.4 to +44.5°C.

Overall the T_gs of the functional polymers follow the same trend as those of the non-functional base polymers, where the T_gs are in the order PP-A$_{100}$ ≈ PP-M$_{100}$ < PP-F$_{100}$. Due to the small percent substitution of the glutamic acid substituent, approximately 10%, the functional polymers are expected to have T_gs on par with their non-functional counterparts. The T_gs are also in approximately the same range as for the base polymers except with the methionine based functional polymer, which is much lower than the base polymers. This is likely due to the role that molecular weight plays in the glass transition temperature of polymers.

Like with the non-functional polymers, GPC analysis was performed using triple detection and refractive index detection alone to determine the absolute and relative molecular weights, respectively. In this case, since the polymers are no longer homopolymers their *dn/dc* must be approximated using their parent non-functional polymers, leading to uncertainty in the absolute molecular weights calculated from light scattering-based triple detection methods. Therefore, it is more appropriate to consider the relative molecular weights that have been calculated based on polystyrene standards rather than the absolute molecular weights, although the absolute molecular weights have been included in this work for completeness. The results of GPC analysis of the functional polyphosphazenes are summarized in **Table 4.7**.

Table 4.7: GPC analysis of PP-A$_{90}$E$^*_{10}$, PP-F$_{90}$E$^*_{10}$, and PP-M$_{90}$E$^*_{10}$ materials using triple detection and refractive index detection. A (-) indicates that analysis using that detection method was not possible and the relative molecular weights are calculated based on polystyrene standards.

Polymer	Triple Detection: Absolute Molecular Weights			Refractive Index Detection: Relative Molecular Weights		
	M_w (Da)	M_n (Da)	PDI	M_w (Da)	M_n (Da)	PDI
PP-A$_{90}$E$^*_{10}$	297,101	218,519	1.359	3,645	2,767	1.317
PP-F$_{90}$E$^*_{10}$	165,512	131,614	1.258	10,705	6,740	1.588
PP-M$_{90}$E$^*_{10}$	-	-	-	1,525	864	1.766
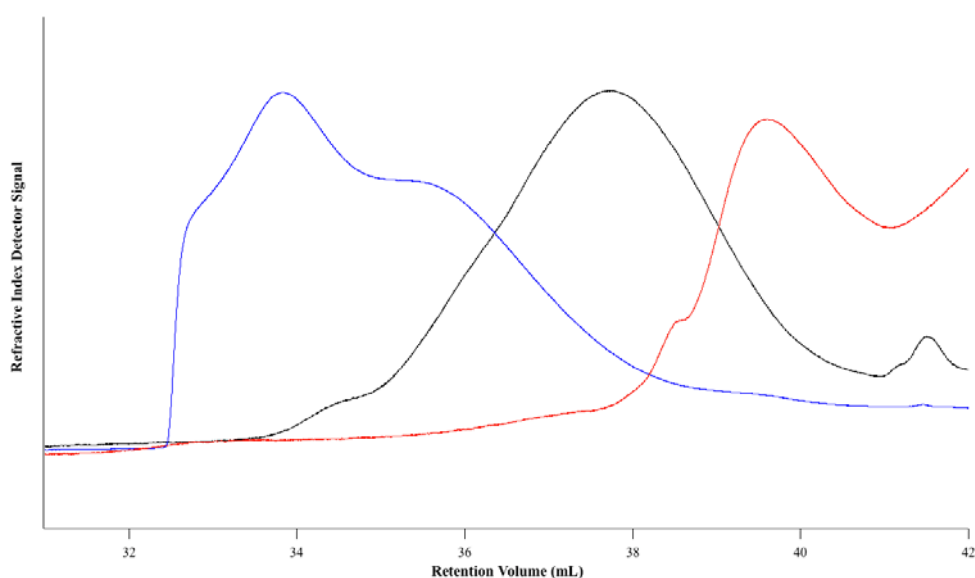
Figure 4.22: GPC traces from the refractive index detector for PP-A$_{90}$E$^*_{10}$ (black), PP-F$_{90}$E$^*_{10}$ (blue), and PP-M$_{90}$E$^*_{10}$ (red).

From the refractive index traces (**Figure 4.22**) it is evident that PP-F$_{90}$E$^*_{10}$ material produced a bimodal spectra indicating that there is likely a mixture of higher and lower molecular weight polymers. Overall, the relative molecular weights of the co-substituted amino acid ester based polyphosphazene materials are lower than those of the non-functional parent polymers. This could be the case if the higher molecular weight polymers have a tendency to precipitate out of solution prior to complete substitution, leading to their filtration and loss during the purification steps. This is postulated due to the fact that initial experiments where benzyl protected glutamic acid ethyl ester was

added before the non-functional amino acid ester led to problems with precipitation of the polymers before complete substitution was achieved, indicating that if large amounts glutamic acid substituents were present on the polymer that solubility issues could arise. Despite the lower molecular weights of the polymers, overall characterization by FTIR, ^{1}H NMR, ^{31}P NMR, TGA, DSC and GPC have proven that co-substituted polyphosphazenes of alanine ethyl ester, phenylalanine ethyl ester, methionine ethyl ester, and benzyl protected glutamic acid ethyl ester polymers are feasible for the development of poly[(amino acid ester)phosphazene]s with functional handles for biomolecule conjugation.

4.6 Hydrogenation of Glutamic Acid Co-Substituted Polyphosphazenes for Model Compound Conjugation

After the benzyl protected glutamic acid substituent is successfully incorporated into polyphosphazenes, it is necessary to remove the benzyl ester protecting group to free the carboxylic acid functionality, as it is this group that allows covalent attachment of biomolecules. Benzyl esters are commonly removed by either highly acidic conditions, which would be detrimental to the polymer backbone and lead to ester hydrolysis in this case, or by hydrogenation using a palladium catalyst. In this work, a Pd/C catalyst system was attempted for the hydrogenation of the benzyl protecting groups. The effect of hydrogenation reactions on P=N bonds is not well-documented in the literature, although their dissimilarity from C=C bonds lead us to believe that they may withstand hydrogenation conditions. The PP-A$_{90}$E$^*_{10}$ material was dissolved in anhydrous ethanol and mixed with a suspension of Pd/C catalyst under an H$_2$ atmosphere for 3.5 hours. The reaction successfully removed the benzyl esters as indicated by the disappearance of the multiplet at 7.23 ppm in ^{1}H NMR corresponding to the aromatic protons of the benzyl group (see red spectrum of **Figure 4.12**). Unfortunately, the reaction also reduced the P=N bonds of the polymer backbone and led to backbone cleavage. This was identified by the disappearance of the peak at around 1.84 ppm in ^{31}P NMR, which is indicative of the presence of the polymer backbone. Another indication that the hydrogenation reaction attacked the polymer backbone was that the materials were water-soluble after hydrogenation, which is not the case for the intact materials. To overcome this problem

it is suggested that allyl protected glutamic acid groups should be used in place of benzyl protected ones. For allyl protecting groups, which are both acid and base stable, a $Pd(PPh_3)_4$ transition metal catalyst be used for deprotection in place of hydrogenation to prevent disruption of the P=N bonds. Morozowich *et al.*[90] have shown successful removal of allyl protecting groups on antioxidant substituted polyphosphazenes without any detriment to the backbone using this catalyst system.

4.7 Cytotoxicity and Cell Proliferation on Non-Functional and Functional Two-Dimensional Polyphosphazene Films

Upon successful synthesis of the base and functional polymers using the new one-pot room temperature synthesis method, it was necessary to evaluate the interaction of the materials with cells to ensure their cytocompatibility. For this, two-dimensional films of the polymers were coated onto the bottom of the wells of a 96-well tissue culture plate, then cytoxicity and cell proliferation were analyzed using MTT assays. A mouse fibroblast cell line (NIH-3T3) was used to evaluate the effect of the polymers on cell viability and metabolic activity over a time period of five days. **Figure 4.23** shows the metabolic activity of the cells normalized to TCPS at day 1. As can be observed from the overall comparison of the two graphs in **Figure 4.23**, preconditioning the materials overnight in HBSS leads to an increase in initial cell viability (higher absorbances at day 1 with preconditioning), although it does not change the fact that with and without preconditioning cells are capable of proliferating on the materials over the entire 5-day span (metabolic activity persists until day 5 on the materials with and without preconditioning). It is also clear from the confocal microscopy images of **Figure 4.25** that the cells on the unconditioned materials (Panels A, C, E, G, I, K, and M) are still viable based on their elongated morphology with long filamentous F-actin protrusions (green). Preconditioning is common practice in cell studies with biomaterials as it acts as a buffering period in which the materials are washed of small molecules on their surface that can disrupt proper interaction of the cells with the materials themselves.[50, 51, 53, 94, 114] Moreover, the preconditioning period "wets" the surface of the materials allowing them to interact properly with the aqueous cell suspensions, rather than seeding the cells on the dry films, which may suppress cell-material interaction and lead to diminished cell

attachment, and thus reduced viability, on the materials. Therefore, all statistical analysis of comparisons between materials in terms of cell viability and proliferation were conducted for the preconditioned films. At Day 1, both of the phenylalanine-based polyphosphazenes (PP-F_{100} and PP-$F_{90}E^*_{10}$) showed significantly higher ($p<0.001$) metabolic activity of fibroblasts in comparison to the TCPS positive control. At Day 3, the PP-$F_{90}E^*_{10}$ material continues to exhibit significantly higher ($p<0.01$) metabolic activity of the cells in comparison with the TCPS control. By Day 5, it seems that cell proliferation begins to plateau, which may be due to crowding of the fibroblasts, and the PP-$F_{90}E^*_{10}$ material performs on par with the TCPS control in terms of metabolic activity. For the PP-F_{100} material, the metabolic activity of the fibroblasts in comparison to TCPS was not significant by Day 3. Taken together, these indicate that the phenylalanine-based polyphosphazenes synthesized via the new 1P RT method are suitable as biomaterials and should be explored further. For the remainder of the materials, it should be noted that despite having initial metabolic activity lower than the TCPS controls, these materials are also non-cytotoxic. This is shown in **Figure 4.24,** where it is clear that the metabolic activity is increasing from Day 1 to Day 5 for all of the functional and non-functional polymers, despite lower initial activity at Day 1, indicating that the cells are thriving on these materials. The decreased Day 1 activity levels may be due to decreased affinity of the cells to attach to the materials initially, although once they have successfully attached they are capable of surviving. The confocal images of the preconditioned materials in **Figure 4.25** (Panels, B, D, F, H, J, L, and N) also shows that the cells are morphologically healthy and spreading well on the materials.
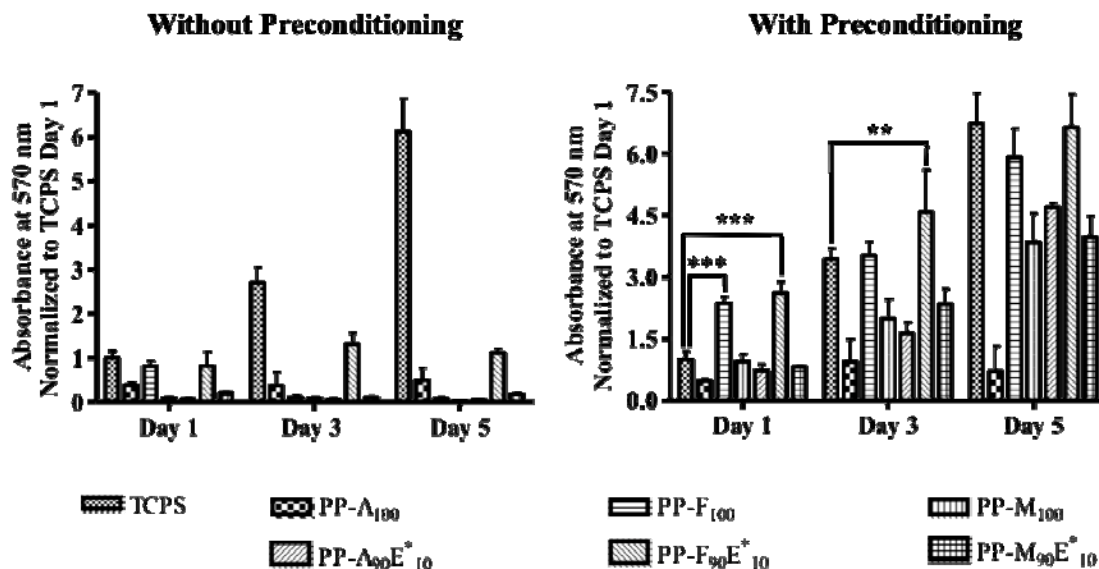
Figure 4.23: Fibroblast metabolic activity as determined by MTT assay grouped by day to compare metabolic activity levels between materials and TCPS. Cells were seeded at 8,000 cells/well on 2-D polyphosphazene films (PP-A_{100}, PP-F_{100}, PP-M_{100}, PP-$A_{90}E^*_{10}$, PP-$F_{90}E^*_{10}$, and PP-$M_{90}E^*_{10}$) that were either unconditioned or preconditioned in HBSS at room temperature overnight. The cells were cultured for 1, 3, and 5 days with 5 replicates for each. The data are presented as the mean ± standard deviation and are normalized to TCPS at Day 1. (** = $p<0.01$, *** = $p<0.001$)
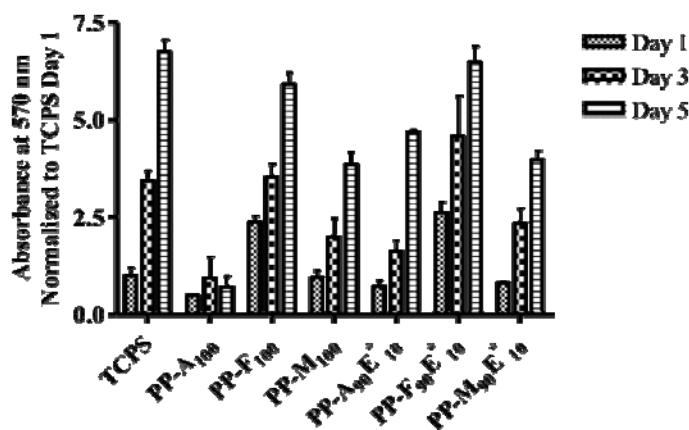
Figure 4.24: Fibroblast metabolic activity as determined by MTT assay grouped by material to show non-cytotoxicity from day 1 to day 5. Cells were seeded at 8,000 cells/well on 2-D polyphosphazene films (PP-A_{100}, PP-F_{100}, PP-M_{100}, PP-$A_{90}E^*_{10}$, PP-$F_{90}E^*_{10}$, and PP-$M_{90}E^*_{10}$) that were preconditioned in HBSS at room temperature overnight. The cells were cultured for 1, 3, and 5 days with 5 replicates for each.

The data are presented as the mean ± standard deviation and are normalized to TCPS at Day 1.
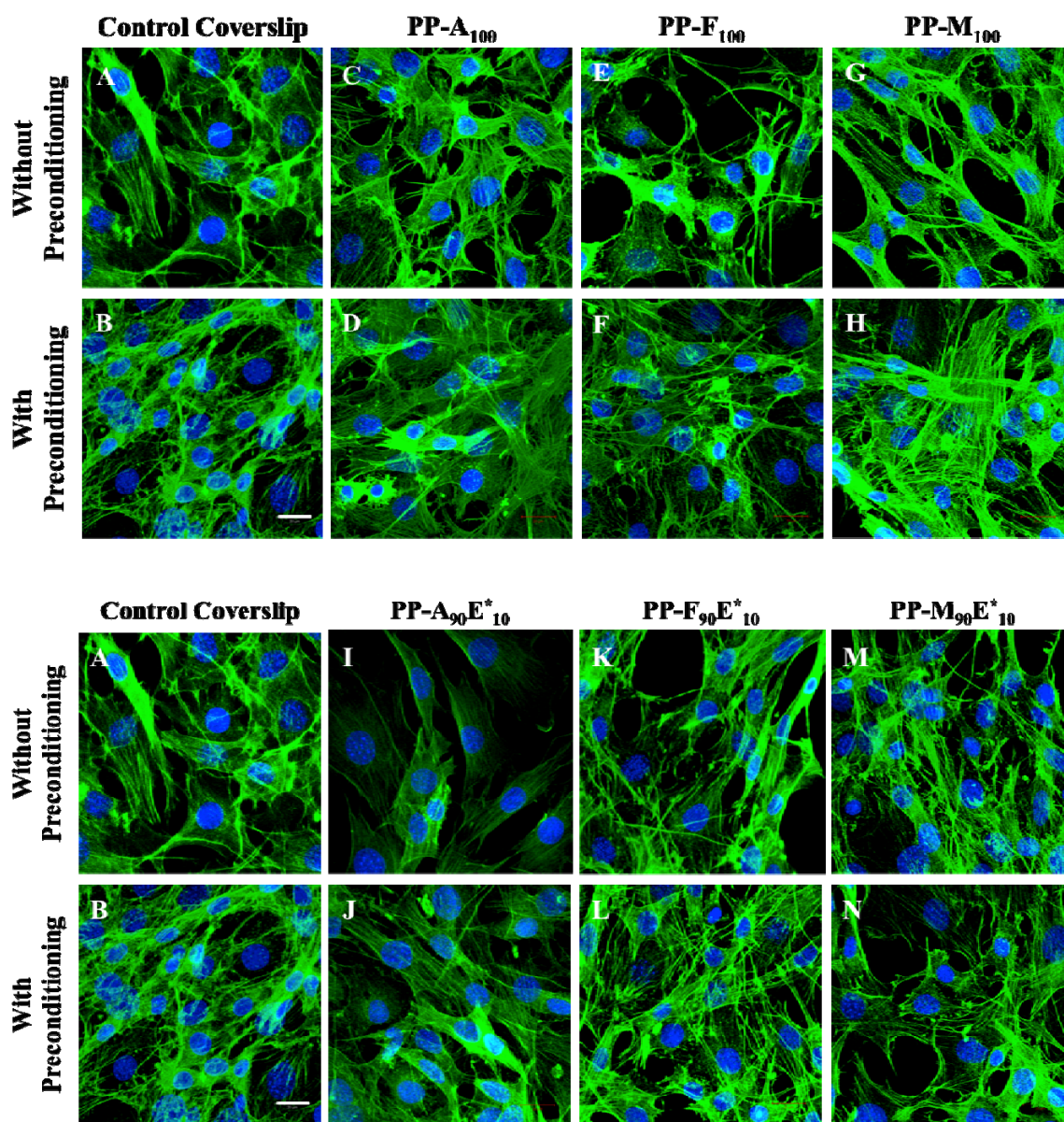
Figure 4.25: Confocal microscopy images showing the morphology and spreading of fibroblasts on the unconditioned and preconditioned polyphosphazene materials after 3 days of culture. The cells were seeded at a density of 30,000 cells/well on the polymer coated glass coverslips in a 24-well tissue culture plate. Untreated glass cover slips were used as a positive control in these experiments. The fibroblasts were stained for F-actin (green) and nuclei (blue). Scale bar = 20 μm (panel B).

4.8 Electrospinning of Poly[(amino acid ester)phosphazene]s and PCL Blend Materials

In order for the new materials to be useful in scaffolds for tissue engineering, they must be processable into 3-D constructs using one of the scaffold fabrication techniques alluded to in the introduction. As such, preliminary proof of concept, electrospinning was attempted using PP-A$_{100}$ materials synthesized via the 1P RT reaction. Since similar polyphosphazene materials had been successfully electrospun into fibrous mats in the literature, the electrospinning parameters from these experiments were used as a starting point. Some difficulties in attempting to implement these conditions with the new PP-A$_{100}$ materials were that the molecular weights of the polymers were vastly different, therefore requiring changes to the concentrations to maintain sufficient viscosity of the polymer solution, and also that the solvents used in the literature were relatively toxic (ex. hexafluoroisopropanol and trifluoroethanol) in comparison to standard solvents (ex. chloroform, ethanol, and tetrahydrofuran) and thus, suitable replacements were required.[64, 105, 137, 138] It was also suspected that the charged nature of the polymers synthesized in this work, in comparison to the uncharged polymers of the literature, may pose a problem with electrospinning since the technique is based on the exploitation of electrical charges.

Initial trials investigated PP-A$_{100}$ concentrations between 3 and 37 weight by volume percent (w/v %) in solvents and co-solvent systems based on CHCl$_3$, DCM, EtOH, THF, and DMF. Sufficient viscosities were achieved to form the polymer jet in electrospinning, although it was noticed that upon hitting the collector the fibers remained standing up out from the aluminum foil, rather than laying flat on the surface. This was presumably due to a build up of charges from the positively charged nitrogen atoms of the polyphosphazene backbone repelling one another and pushing the newly deposited fibers of the collector towards the needle tip. It is believed that a rotating mandrel setup, rather than a stationary collector, may help with this problem by forcing the extended polymer chains to collapse back on one another as the mandrel rotates, allowing a fibrous mat to be collected.

Unfortunately, a rotating mandrel setup was unavailable to test this theory and instead polymer blends of PP-A$_{100}$ and polycaprolactone (PCL), a well-known biocompatible and degradable polymer, were attempted to be electrospun as proof that fabricating fibrous mats of these polymers was feasible. Various w/v % concentrations and ratios of PP-A$_{100}$ to PCL were attempted, although a mixture of 50% PP-A$_{100}$ and 50% PCL gave the best results and was capable of forming non-woven fibers as determined by scanning electron microscopy (SEM) imaging. The spinning solution was a 5 w/v % solution of 50% PP-A$_{100}$ and 50% PCL by weight in DCM. The electrospinning parameters were an 18kV accelerating voltage, 18-gauge needle tip, 9 cm working distance between the tip of the needle and the collector, and flow rate of 0.1 mL/h. Although the electrospinning parameters were not optimized to give ideal fiber diameters and morphologies, it can be seen from the SEM images (**Figure 4.26**) that the polymer blend gave relatively uniform fiber diameters with a bead-free morphology and good porosity, which are key aspects to a successful scaffold. Optimization of the electrospinning parameters could enable the fabrication of fibrous mats based on polyphosphazene/PCL blend materials with appropriate fiber diameters, morphology, and porosity for vascular tissue engineering applications.
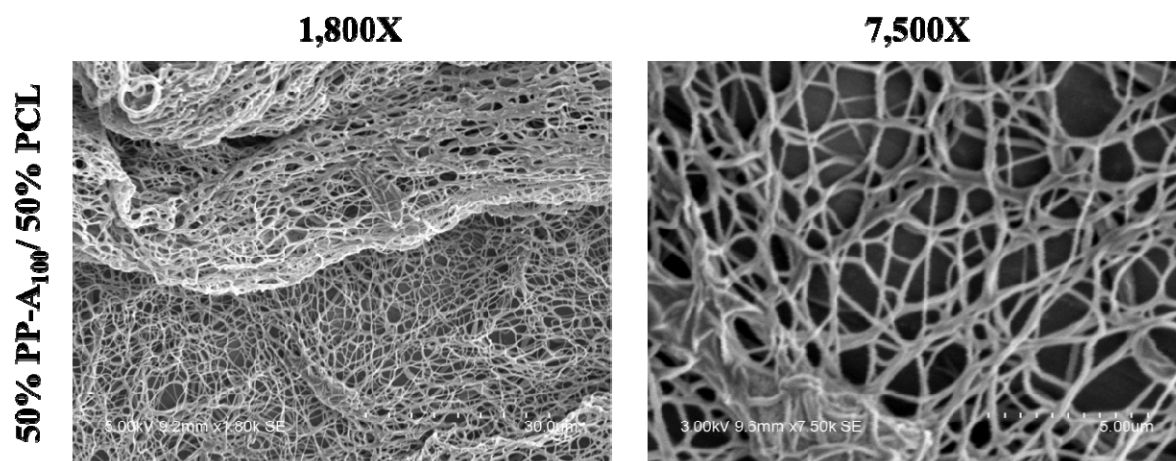
Figure 4.26: Scanning electron micrographs of electrospun fibers of a 5 w/v % polymer solution in DCM containing 50% PP-A$_{100}$/50% PCL by weight.

4.9   Novelty of This Work

Overall, the research conducted in this thesis has led to the successful synthesis of polyphosphazene materials based on both non-functional and functional amino acid esters using a simplified method. The facile synthesis is an improvement over the demanding techniques previously presented in the literature, overcoming the necessity of specialized equipment to maintain an inert atmosphere and the use of toxic solvents. The materials were characterized extensively and exhibited partial cationic charge at the nitrogen atom of the amino acid, which had not been reported in the literature before with similar materials. Lastly, novel polyphosphazenes containing mixed substituents of non-functional amino acids and functional glutamic acid were synthesized which are materials that had not been reported prior to this work.

5   Conclusions and Future Directions

5.1   Conclusions

In this work, the objectives outlined in Chapter 1 were all successfully realized, except for the biomolecule conjugation due to problems with deprotection. A thermal ring opening polymerization method that did not require controlled moisture-free atmospheres was developed and optimized for best conversion of the hexachlorocyclotriphosphazene trimer to linear poly[(dichloro)phosphazene] (PDCP). From there, the PDCP was successfully used in the synthesis of a family of non-functional poly[(amino acid ester)phosphazene]s, based on L-alanine ethyl ester, L-phenylalanine ethyl ester, and L-methionine ethyl ester, using three different substitution methods. Upon characterization by FTIR, ^{1}H NMR, and ^{31}P NMR spectroscopic studies, it was determined that all three methods produced materials which were similar to those described in the literature, indicating that the new facile one-pot room temperature (1P RT) method, which also eliminated the necessity of an inert atmosphere, was suitable for future polyphosphazenes syntheses. The new 1P RT method was selected over the low temperature two-step method (LT 2S), based on yields and characterization data, for further comparison to the materials synthesized via the room temperature two-step (RT 2S) method in terms of thermal and molecular weight analysis. It was also observed that the 1P RT gave improved purity and higher molecular weights over the well-established room temperature two-step (RT 2S) method that is routinely used in the literature. Despite the fact that the molecular weights of the polyphosphazenes synthesized using these two methods were lower in comparison with the literature, they were a step towards polyphosphazene synthesis that did not require advanced synthetic chemistry and expensive laboratory equipment. These two new methods (polymerization and one-pot substitution) were then employed to fabricate novel functional co-substituted poly[(amino acid ester)phosphazene]s with functional handles for biomolecule immobilization. Prior to the co-substitution, Boc protected glutamic acid ethyl ester was successfully synthesized via the esterification of Boc-Glu(OBzl)-OH with ethanol, a feat that had yet to be accomplished. The newly synthesized Boc-Glu(OBzl)-OEt was then deprotected and used in a substitution reaction with poly[(dichloro)phosphazene] to give a family of

novel functional co-substituted polyphosphazenes based on L-glutamic acid, L-alanine, L-phenylalanine, and L-methionine. A step-wise substitution method was developed for the formation of these novel polymers, where the non-functional amino acid ester was partially substituted, followed by complete addition of stoichiometric amounts of the functional glutamic acid substitution, and finally fully substituted by addition of excess non-functional amino acid ester. These new materials were fully characterized using FTIR, NMR, TGA, DSC, and GPC. Unfortunately, the polymer backbone was affected when hydrogenation of the benzyl protecting group was attempted and further work in this area is required before biomolecule conjugation can be successfully achieved although similar materials with allyl protecting groups are expected to overcome this. As it is important that these materials be biocompatible for use in vascular tissue engineering applications, their cytotoxicity and cell proliferation characteristics were evaluated using MTT assays and confocal imaging of immunofluorescently tagged cells. MTT assays of the non-functional and functional polymers showed non-cytotoxicity of the preconditioned two-dimensional films towards NIH-3T3 mouse fibroblasts over a study period of five days. The MTT assays also showed enhanced cell attachment at Day 1 versus TCPS positive controls for the PP-F$_{100}$ and PP-F$_{90}$E$^*_{10}$ phenylalanine-based polyphosphazenes and significant metabolic activity of cells seeded on these materials, which is promising for their use in biomedical applications. Lastly, electrospinning was used to develop fibers from the new polyphosphazene materials. While preliminary trials with PP-A$_{100}$ alone were unsuccessful in fabricating fibers, a 50% PP-A$_{100}$ and 50% PCL blend was effectively used to develop fibers at a polymer concentration of 5 w/v % in DCM. These fibers were then imaged using scanning electron microscopy (SEM) to show the bead-free morphology and nanometer-scale diameter of the fibers. It is important that biomaterials can be processed into desired configurations for use in biomedical applications and in this study not only 2-D films but also 3-D fibers were successfully fabricated based on the poly[(amino acid ester)phosphazene]s and blends thereof. Overall, this work suggested that poly[(amino acid ester)phosphazene]s can be synthesized in non-inert atmosphere and that non-functional and functional co-substituted polyphosphazenes based on L-phenylalanine ethyl ester may be suitable for biomedical applications such as tissue engineering.

5.2   Future Directions

In light of the work presented here, future work on this project should include:

- Substituting the benzyl group with a different protecting group like allyl and deprotection with $Pd(PPh_3)_4$ catalyst, followed by conjugation of a biomolecule known to enhance cell-material interactions

- Performing electrospinning trials with a rotating mandrel for 100% polyphosphazenes polymer solutions or optimization of the electrospinning process for polyphosphazenes/PCL blend materials

- Performing *in vitro* degradation studies on two-dimensional polymer and three-dimensional non-woven fibrous mats from electrospinning

- Performing long-term *in vitro* cell studies using not only fibroblasts but also other native blood vessel cells, like endothelial cells and vascular smooth muscle cells, on 2-D films and 3-D mats of the non-functional and functional poly[(amino acid ester)phosphazene]s

- Perform mechanical testing (cyclic loading tensile testing) on 2-D films and 3-D fibers of the poly(amino acid ester)phosphazene materials to ensure appropriateness for vascular tissue engineering applications

References

1.   Naderi, H.; Matin, M. M.; Bahrami, A. R., Review paper: critical issues in tissue engineering: biomaterials, cell sources, angiogenesis, and drug delivery systems. *J Biomater Appl* **2011,** 26, (4), 383-417.

2.   Freed, L. E.; Vunjak-Novakovic, G.; Biron, R. J.; Eagles, D. B.; Lesnoy, D. C.; Barlow, S. K.; Langer, R., Biodegradable polymer scaffolds for tissue engineering. *Nat Biotechnol* **1994,** 12, (7), 689-93.

3.   Sell, S.; Barnes, C.; Smith, M.; McClure, M.; Madurantakam, P.; Grant, J.; McManus, M.; Bowlin, G., Extracellular Matrix Regenerated: Tissue Engineering via Electrospun Biomimetic Nanofibers. *Polym Int* **2007,** 56, (11), 1349-1360.

4.   Sell, S. A.; Wolfe, P. S.; Garg, K.; McCool, J. M.; Rodriguez, I. A.; Bowlin, G. L., The Use of Natural Polymers in Tissue Engineering: A Focus on Electrospun Extracellular Matrix Analogues. *Polymers* **2010,** 2, (4), 522-553.

5.   Nair, L. S.; Laurencin, C. T., Biodegradable polymers as biomaterials. *Prog Polym Sci* **2007,** 32, (8-9), 762-798.

6.   Puppi, D.; Chiellini, F.; Piras, A. M.; Chiellini, E., Polymeric materials for bone and cartilage repair. *Prog Polym Sci* **2010,** 35, (4), 403-440.

7.   Athanasiou, K. A.; Niederauer, G. G.; Agrawal, C. M., Sterilization, toxicity, biocompatibility and clinical applications of polylactic acid polyglycolic acid copolymers. *Biomaterials* **1996,** 17, (2), 93-102.

8.   de Jong, S. J.; Arias, E. R.; Rijkers, D. T. S.; van Nostrum, C. F.; Kettenes-van den Bosch, J. J.; Hennink, W. E., New insights into the hydrolytic degradation of poly(lactic acid): participation of the alcohol terminus. *Polymer* **2001,** 42, (7), 2795-2802.

9.   Taylor, M. S.; Daniels, A. U.; Andriano, K. P.; Heller, J., 6 Bioabsorbable Polymers - in-Vitro Acute Toxicity of Accumulated Degradation Products. *J Appl Biomater* **1994,** 5, (2), 151-157.

10.   Ma, P. X., Biomimetic materials for tissue engineering. *Adv Drug Deliv Rev* **2008,** 60, (2), 184-198.

11.   Shin, H.; Jo, S.; Mikos, A. G., Biomimetic materials for tissue engineering. *Biomaterials* **2003,** 24, (24), 4353-4364.

12.   Allcock, H. R.; Morozowich, N. L., Bioerodible polyphosphazenes and their medical potential. *Polym Chem* **2012,** 3, (3), 578-590.

13.   Schacht, E.; Vandorpe, J.; Dejardin, S.; Lemmouchi, Y.; Seymour, L., Biomedical applications of degradable polyphosphazenes. *Biotechnol Bioeng* **1996,** 52, (1), 102-108.

14.   Allcock, H. R., A perspective of polyphosphazene research. *J Inorg Organomet P* **2006,** 16, (4), 277-294.

15.   Deng, M.; Kumbar, S. G.; Wan, Y. Q.; Toti, U. S.; Allcock, H. R.; Laurencin, C. T., Polyphosphazene polymers for tissue engineering: an analysis of material synthesis, characterization and applications. *Soft Matter* **2010,** 6, (14), 3119-3132.

16.   Chen, H. C.; Hu, Y. C., Bioreactors for tissue engineering. *Biotechnol Lett* **2006,** 28, (18), 1415-1423.

17.   Ertl, G.; Thum, T., New insight into healing mechanisms of the infarcted heart. *J Am Coll Cardiol* **2010,** 55, (2), 144-146.

18.   Orlic, D.; Hill, J. M.; Arai, A. E., Stem cells for myocardial regeneration. *Circ Res* **2002,** 91, (12), 1092-1102.

19.   Karamichos, D.; Funderburgh, M. L.; Hutcheon, A. E.; Zieske, J. D.; Du, Y.; Wu, J.; Funderburgh, J. L., A role for topographic cues in the organization of collagenous matrix by corneal fibroblasts and stem cells. *PLoS One* **2014,** 9, (1), e86260.

20.   Kim, M. S.; Ahn, H. H.; Shin, Y. N.; Cho, M. H.; Khang, G.; Lee, H. B., An in vivo study of the host tissue response to subcutaneous implantation of PLGA- and/or porcine small intestinal submucosa-based scaffolds. *Biomaterials* **2007,** 28, (34), 5137-5143.

21.   Wang, C.; Cen, L.; Yin, S.; Liu, Q.; Liu, W.; Cao, Y.; Cui, L., A small diameter elastic blood vessel wall prepared under pulsatile conditions from polyglycolic acid mesh and smooth muscle cells differentiated from adipose-derived stem cells. *Biomaterials* **2010,** 31, (4), 621-630.

22.   Rabkin, E.; Schoen, F. J., Cardiovascular tissue engineering. *Cardiovasc Pathol* **2002,** 11, (6), 305-317.

23.   Lutolf, M. P.; Hubbell, J. A., Synthetic biomaterials as instructive extracellular microenvironments for morphogenesis in tissue engineering. *Nat Biotechnol* **2005,** 23, (1), 47-55.

24.   Martin, Y.; Vermette, P., Bioreactors for tissue mass culture: design, characterization, and recent advances. *Biomaterials* **2005,** 26, (35), 7481-7503.

25.   Chen, X.; Yin, Z.; Chen, J. L.; Liu, H. H.; Shen, W. L.; Fang, Z.; Zhu, T.; Ji, J.; Ouyang, H. W.; Zou, X. H., Scleraxis-overexpressed human embryonic stem cell-derived mesenchymal stem cells for tendon tissue engineering with knitted silk-collagen scaffold. *Tissue Eng Part A* **2014,** 20, (11-12), 1583-1592.

26.   Bramfeldt, H.; Sarazin, P.; Vermette, P., Smooth muscle cell adhesion in surface-modified three-dimensional copolymer scaffolds prepared from co-continuous blends. *J Biomed Mater Res A* **2009,** 91, (1), 305-315.

27.   Baguneid, M. S.; Seifalian, A. M.; Salacinski, H. J.; Murray, D.; Hamilton, G.; Walker, M. G., Tissue engineering of blood vessels. *Br J Surg* **2006,** 93, (3), 282-290.

28.   Karageorgiou, V.; Kaplan, D., Porosity of 3D biomaterial scaffolds and osteogenesis. *Biomaterials* **2005,** 26, (27), 5474-5491.

29.   Barnes, C. P.; Sell, S. A.; Boland, E. D.; Simpson, D. G.; Bowlin, G. L., Nanofiber technology: designing the next generation of tissue engineering scaffolds. *Adv Drug Deliv Rev* **2007,** 59, (14), 1413-1433.

30.   Beachley, V.; Wen, X., Polymer nanofibrous structures: Fabrication, biofunctionalization, and cell interactions. *Prog Polym Sci* **2010,** 35, (7), 868-892.

31.   Lee, J.; Cuddihy, M. J.; Kotov, N. A., Three-dimensional cell culture matrices: state of the art. *Tissue Eng Part B Rev* **2008,** 14, (1), 61-86.

32.   Feugier, P.; Black, R. A.; Hunt, J. A.; How, T. V., Attachment, morphology and adherence of human endothelial cells to vascular prosthesis materials under the action of shear stress. *Biomaterials* **2005,** 26, (13), 1457-1466.

33.   Lee, S. J.; Liu, J.; Oh, S. H.; Soker, S.; Atala, A.; Yoo, J. J., Development of a composite vascular scaffolding system that withstands physiological vascular conditions. *Biomaterials* **2008,** 29, (19), 2891-2898.

34.   Moroni, L.; de Wijn, J. R.; van Blitterswijk, C. A., Integrating novel technologies to fabricate smart scaffolds. *J Biomater Sci Polym Ed* **2008,** 19, (5), 543-572.

35.   Ma, P. X., Tissue Engineering. *Encyclopedia of Polymer Science and Technology* **2004**.

36.   Ma, H.; Hu, J.; Ma, P. X., Polymer scaffolds for small-diameter vascular tissue engineering. *Adv Funct Mater* **2010,** 20, (17), 2833-2841.

37.   Huh, D.; Matthews, B. D.; Mammoto, A.; Montoya-Zavala, M.; Hsin, H. Y.; Ingber, D. E., Reconstituting organ-level lung functions on a chip. *Science* **2010,** 328, (5986), 1662-1668.

38.   Kumbar, S. G.; James, R.; Nukavarapu, S. P.; Laurencin, C. T., Electrospun nanofiber scaffolds: engineering soft tissues. *Biomed Mater* **2008,** 3, (3), 034002.

39.   Sell, S. A.; McClure, M. J.; Garg, K.; Wolfe, P. S.; Bowlin, G. L., Electrospinning of collagen/biopolymers for regenerative medicine and cardiovascular tissue engineering. *Adv Drug Deliv Rev* **2009,** 61, (12), 1007-1019.

40.   Carlisle, C. R.; Coulais, C.; Namboothiry, M.; Carroll, D. L.; Hantgan, R. R.; Guthold, M., The mechanical properties of individual, electrospun fibrinogen fibers. *Biomaterials* **2009,** 30, (6), 1205-1213.

41.   McManus, M.; Boland, E.; Sell, S.; Bowen, W.; Koo, H.; Simpson, D.; Bowlin, G., Electrospun nanofibre fibrinogen for urinary tract tissue reconstruction. *Biomed Mater* **2007,** 2, (4), 257-262.

42.   McManus, M. C.; Boland, E. D.; Simpson, D. G.; Barnes, C. P.; Bowlin, G. L., Electrospun fibrinogen: feasibility as a tissue engineering scaffold in a rat cell culture model. *J Biomed Mater Res A* **2007,** 81, (2), 299-309.

43.   Kim, I. L.; Mauck, R. L.; Burdick, J. A., Hydrogel design for cartilage tissue engineering: a case study with hyaluronic acid. *Biomaterials* **2011,** 32, (34), 8771-8782.

44.   Lee, F.; Kurisawa, M., Formation and stability of interpenetrating polymer network hydrogels consisting of fibrin and hyaluronic acid for tissue engineering. *Acta Biomater* **2013,** 9, (2), 5143-5152.

45.   Nimmo, C. M.; Owen, S. C.; Shoichet, M. S., Diels-Alder Click cross-linked hyaluronic acid hydrogels for tissue engineering. *Biomacromolecules* **2011,** 12, (3), 824-830.

46.   Choi, J. S.; Lee, S. W.; Jeong, L.; Bae, S. H.; Min, B. C.; Youk, J. H.; Park, W. H., Effect of organosoluble salts on the nanofibrous structure of electrospun poly(3-hydroxybutyrate-co-3-hydroxyvalerate). *Int J Biol Macromol* **2004,** 34, (4), 249-256.

47.   Zhong, S.; Teo, W. E.; Zhu, X.; Beuerman, R.; Ramakrishna, S.; Yung, L. Y., Formation of collagen-glycosaminoglycan blended nanofibrous scaffolds and their biological properties. *Biomacromolecules* **2005,** 6, (6), 2998-3004.

48.   Lee, K. Y.; Jeong, L.; Kang, Y. O.; Lee, S. J.; Park, W. H., Electrospinning of polysaccharides for regenerative medicine. *Adv Drug Deliv Rev* **2009,** 61, (12), 1020-1032.

49.   He, X.; Xiao, Q.; Lu, C.; Wang, Y.; Zhang, X.; Zhao, J.; Zhang, W.; Zhang, X.; Deng, Y., Uniaxially aligned electrospun all-cellulose nanocomposite nanofibers reinforced with cellulose nanocrystals: scaffold for tissue engineering. *Biomacromolecules* **2014,** 15, (2), 618-627.

50.   Grenier, S.; Sandig, M.; Holdsworth, D. W.; Mequanint, K., Interactions of coronary artery smooth muscle cells with 3D porous polyurethane scaffolds. *J Biomed Mater Res A* **2009,** 89, (2), 293-303.

51.   Grenier, S.; Sandig, M.; Mequanint, K., Polyurethane biomaterials for fabricating 3D porous scaffolds and supporting vascular cells. *J Biomed Mater Res A* **2007,** 82, (4), 802-809.

52.   Gunatillake, P.; Mayadunne, R.; Adhikari, R., Recent developments in biodegradable synthetic polymers. *Biotechnol Annu Rev* **2006,** 12, 301-347.

53.   Knight, D. K.; Gillies, E. R.; Mequanint, K., Biomimetic l-aspartic acid-derived functional poly(ester amide)s for vascular tissue engineering. *Acta Biomater* **2014**, 10, (8), 3484-3496.

54.   Liu, K. L.; Choo, E. S.; Wong, S. Y.; Li, X.; He, C. B.; Wang, J.; Li, J., Designing poly[(R)-3-hydroxybutyrate]-based polyurethane block copolymers for electrospun nanofiber scaffolds with improved mechanical properties and enhanced mineralization capability. *J Phys Chem B* **2010,** 114, (22), 7489-7498.

55.   Srinath, D.; Lin, S.; Knight, D. K.; Rizkalla, A. S.; Mequanint, K., Fibrous biodegradable l-alanine-based scaffolds for vascular tissue engineering. *J Tissue Eng Regen Med* **2012**, 8, (7), 578-588.

56.   Kim, P.; Yuan, A.; Nam, K. H.; Jiao, A.; Kim, D. H., Fabrication of poly(ethylene glycol): gelatin methacrylate composite nanostructures with tunable stiffness and degradation for vascular tissue engineering. *Biofabrication* **2014,** 6, (2), 024112.

57.   Bettinger, C. J., Synthetic biodegradable elastomers for drug delivery and tissue engineering. *Pure Appl Chem* **2011,** 83, (1), 9-24.

58.   Greenwald, S. E.; Berry, C. L., Improving vascular grafts: the importance of mechanical and haemodynamic properties. *J Pathol* **2000,** 190, (3), 292-299.

59.   Agarwal, S.; Wendorff, J. H.; Greiner, A., Progress in the field of electrospinning for tissue engineering applications. *Adv Mater* **2009,** 21, (32-33), 3343-3351.

60.   Sill, T. J.; von Recum, H. A., Electrospinning: applications in drug delivery and tissue engineering. *Biomaterials* **2008,** 29, (13), 1989-2006.

61.   Xie, J.; Li, X.; Xia, Y., Putting Electrospun Nanofibers to Work for Biomedical Research. *Macromol Rapid Commun* **2008,** 29, (22), 1775-1792.

62.   Courtney, T.; Sacks, M. S.; Stankus, J.; Guan, J.; Wagner, W. R., Design and analysis of tissue engineering scaffolds that mimic soft tissue mechanical anisotropy. *Biomaterials* **2006,** 27, (19), 3631-3638.

63.   Pham, Q. P.; Sharma, U.; Mikos, A. G., Electrospinning of polymeric nanofibers for tissue engineering applications: a review. *Tissue Eng* **2006,** 12, (5), 1197-1211.

64.   Lin, Y. J.; Deng, Q. H.; Jin, R. G., Effects of Processing Variables on the Morphology and Diameter of Electrospun Poly(amino acid ester)phosphazene Nanofibers. *J Wuhan Univ Technol* **2012,** 27, (2), 207-211.

65.   Pillay, V.; Dott, C.; Choonara, Y. E.; Tyagi, C.; Tomar, L.; Kumar, P.; Toit, L. C. d.; Ndesendo, V. M. K., A Review of the Effect of Processing Variables on the

Fabrication of Electrospun Nanofibers for Drug Delivery Applications. *J Nanomater* **2013,** vol. 2013, Article ID 789289, 22 pages.

66.   Allcock, H. R., The synthesis of functional polyphosphazenes and their surfaces. *Appl Organomet Chem* **1998,** 12, (10-11), 659-666.

67.   Allcock, H. R., *Chemistry and Applications of Polyphosphazenes*. Wiley Interscience: Hoboken, New Jersey, 2003; pgs 725.

68.   Andrianov, A. K., *Polyphosphazenes for Biomedical Applications*. John Wiley & Sons, Inc.: Hoboken, New Jersey, 2009.

69.   Stokes, H. N., On The Chloronitrides of Phosphorus (II). *American Chemical Journal* **1897,** 19, 782-796.

70.   Allcock, H. R.; Kugel, R. L., Synthesis of High Polymeric Alkoxy- and Aryloxphosphonitriles. *J Am Chem Soc* **1965,** 87, (18), 4216-4217.

71.   Mujumdar, A. N.; Young, S. G.; Merker, R. L.; Magill, J. H., A Study of Solution Polymerization of Polyphosphazenes. *Macromolecules* **1990,** 23, (1), 14-21.

72.   Allcock, H. R.; Crane, C. A.; Morrissey, C. T.; Nelson, J. M.; Reeves, S. D.; Honeyman, C. H.; Manners, I., "Living" cationic polymerization of phosphoranimines as an ambient temperature route to polyphosphazenes with controlled molecular weights. *Macromolecules* **1996,** 29, (24), 7740-7747.

73.   Allcock, H. R.; Nelson, J. M.; Reeves, S. D.; Honeyman, C. H.; Manners, I., Ambient-temperature direct synthesis of poly(organophosphazenes) via the "living" cationic polymerization of organo-substituted phosphoranimines. *Macromolecules* **1997,** 30, (1), 50-56.

74.   Allcock, H. R.; Reeves, S. D.; de Denus, C. R.; Crane, C. K., Influence of reaction parameters on the living cationic polymerization of phosphoranimines to polyphosphazenes. *Macromolecules* **2001,** 34, (4), 748-754.

75.   Honeyman, C. H.; Manners, I.; Morrissey, C. T.; Allcock, H. R., Ambient-Temperature Synthesis of Poly(Dichlorophosphazene) with Molecular-Weight Control. *J Am Chem Soc* **1995,** 117, (26), 7035-7036.

76.   Peterson, E. S.; Luther, T. A.; Harrup, M. K.; Klaehn, J. R.; Stone, M. L.; Orme, C. J.; Stewart, F. F., On the contributions to the materials science aspects of phosphazene chemistry by Professor Christopher W. Allen: The one-pot synthesis of linear polyphosphazenes. *J Inorg Organomet P* **2007,** 17, (2), 361-366.

77.   Conconi, M. T.; Lora, S.; Baiguera, S.; Boscolo, E.; Folin, M.; Scienza, R.; Rebuffat, P.; Parnigotto, P. P.; Nussdorfer, G. G., In vitro culture of rat neuromicrovascular endothelial cells on polymeric scaffolds. *J Biomed Mater Res A* **2004,** 71, (4), 669-674.

78.   Conconi, M. T.; Lora, S.; Menti, A. M.; Carampin, P.; Parnigotto, P. P., In vitro evaluation of poly[bis(ethyl alanato)phosphazene] as a scaffold for bone tissue engineering. *Tissue Eng* **2006,** 12, (4), 811-819.

79.   Dhalluin, G.; Dejaeger, R.; Chambrette, J. P.; Potin, P., Synthesis of Poly(Dichlorophosphazenes) from Cl3p=Np(O)Cl2 .1. Kinetics and Reaction-Mechanism. *Macromolecules* **1992,** 25, (4), 1254-1258.

80.   Gleria, M.; De Jaeger, R., Aspects of phosphazene research. *J Inorg Organomet P* **2001,** 11, (1), 1-45.

81.   Allcock, H. R.; Gardner, J. E.; Smeltz, K. M., .21. Series on Phosphorus-Nitrogen Compounds - Polymerization of Hexachlorocyclotriphosphazene - Role of Phosphorus-Pentachloride, Water, and Hydrogen-Chloride. *Macromolecules* **1975,** 8, (1), 36-42.

82.   Burg, K. J. L.; Porter, S.; Kellam, J. F., Biomaterial developments for bone tissue engineering. *Biomaterials* **2000,** 21, (23), 2347-2359.

83.   Singh, A.; Krogman, N. R.; Sethuraman, S.; Nair, L. S.; Sturgeon, J. L.; Brown, P. W.; Laurencin, C. T.; Allcock, H. R., Effect of side group chemistry on the properties of biodegradable L-alanine cosubstituted polyphosphazenes. *Biomacromolecules* **2006,** 7, (3), 914-918.

84.   Allcock, H. R.; Pucher, S. R.; Scopelianos, A. G., Poly[(Amino-Acid-Ester)Phosphazenes] - Synthesis, Crystallinity, and Hydrolytic Sensitivity in Solution and the Solid-State. *Macromolecules* **1994,** 27, (5), 1071-1075.

85.   Crommen, J.; Vandorpe, J.; Schacht, E., Degradable Polyphosphazenes for Biomedical Applications. *J Control Release* **1993,** 24, (1-3), 167-180.

86.   Deng, M.; Kumbar, S. G.; Nair, L. S.; Weikel, A. L.; Allcock, H. R.; Laurencin, C. T., Biomimetic Structures: Biological Implications of Dipeptide-Substituted Polyphosphazene–Polyester Blend Nanofiber Matrices for Load-Bearing Bone Regeneration. *Adv Funct Mater* **2011,** 21, 2641-2651.

87.   Laurencin, C. T.; ElAmin, S. F.; Ibim, S. E.; Willoughby, D. A.; Attawia, M.; Allcock, H. R.; Ambrosio, A. A., A highly porous 3-dimensional polyphosphazene polymer matrix for skeletal tissue regeneration. *J Biomed Mater Res* **1996,** 30, (2), 133-138.

88.   Laurencin, C. T.; Morris, C. D.; Pierres-Jacques, H.; Schwartz, E. R.; Keaton, A. R.; Zou, L., The development of bone bioerodible polymer composites for skeletal tissue regeneration: studies of initial cell attachment and spread. *Polym Adv Technol* **1992**, (3), 369-364.

89.   Laurencin, C. T.; Norman, M. E.; Elgendy, H. M.; Elamin, S. F.; Allcock, H. R.; Pucher, S. R.; Ambrosio, A. A., Use of Polyphosphazenes for Skeletal Tissue Regeneration. *J Biomed Mater Res* **1993,** 27, (7), 963-973.

90.   Morozowich, N. L.; Nichol, J. L.; Mondschein, R. J.; Allcock, H. R., Design and examination of an antioxidant-containing polyphosphazene scaffold for tissue engineering. *Polym Chem* **2012,** 3, (3), 778-786.

91.   Nair, L. S.; Lee, D. A.; Bender, J. D.; Barrett, E. W.; Greish, Y. E.; Brown, P. W.; Allcock, H. R.; Laurencin, C. T., Synthesis, characterization, and osteocompatibility evaluation of novel alanine-based polyphosphazenes. *J Biomed Mater Res A* **2006,** 76A, (1), 206-213.

92.   Nichol, J. L.; Morozowich, N. L.; Allcock, H. R., Biodegradable alanine and phenylalanine alkyl ester polyphosphazenes as potential ligament and tendon tissue scaffolds. *Polym Chem* **2013,** 4, (3), 600-606.

93.   Sethuraman, S.; Nair, L. S.; El-Amin, S.; Farrar, R.; Nguyen, M. T. N.; Singh, A.; Allcock, H. R.; Greish, Y. E.; Brown, P. W.; Laurencin, C. T., In vivo biodegradability and biocompatibility evaluation of novel alanine ester based polyphosphazenes in a rat model. *J Biomed Mater Res A* **2006,** 77A, (4), 679-687.

94.   Sethuraman, S.; Nair, L. S.; El-Amin, S.; Nguyen, M. T.; Singh, A.; Krogman, N.; Greish, Y. E.; Allcock, H. R.; Brown, P. W.; Laurencin, C. T., Mechanical properties and osteocompatibility of novel biodegradable alanine based polyphosphazenes: Side group effects. *Acta Biomater* **2010,** 6, (6), 1931-1937.

95.   Allcock, H. R.; Fuller, T. J.; Mack, D. P.; Matsumura, K.; Smeltz, K. M., Synthesis of Poly[(Amino Acid Alkyl Ester)Phosphazenes]. *Macromolecules* **1977,** 10, (4), 824-830.

96.   Yang, S. F.; Leong, K. F.; Du, Z. H.; Chua, C. K., The design of scaffolds for use in tissue engineering. Part 1. Traditional factors. *Tissue Eng* **2001,** 7, (6), 679-689.

97.   Allcock, H. R.; Pucher, S. R.; Scopelianos, A. G., Poly[(Amino Acid Ester)Phosphazenes] as Substrates for the Controlled-Release of Small Molecules. *Biomaterials* **1994,** 15, (8), 563-569.

98.   Andrianov, A. K.; Marin, A.; Peterson, P., Water-soluble biodegradable polyphosphazenes containing N-ethylpyrrolidone groups. *Macromolecules* **2005,** 38, (19), 7972-7976.

99.   Crommen, J. H. L.; Schacht, E. H., Synthesis and Evaluation of the Hydrolytical Stability of Ethyl 2-(Alpha-Amino Acid)Glycolates and Ethyl 2-(Alpha-Amino Acid)Lactates. *B Soc Chim Belg* **1991,** 100, (10), 747-758.

100.   Lakshmi, S.; Katti, D. S.; Laurencin, C. T., Biodegradable polyphosphazenes for drug delivery applications. *Adv Drug Deliv Rev* **2003,** 55, (4), 467-482.

101.   Qiu, L. Y.; Zhu, K. J., Novel biodegradable polyphosphazenes containing glycine ethyl ester and benzyl ester of amino acethydroxamic acid as cosubstituents: Syntheses, characterization, and degradation properties. *J Appl Polym Sci* **2000,** 77, (13), 2987-2995.

102.   Chlupac, J.; Filova, E.; Bacakova, L., Blood Vessel Replacement: 50 years of Development and Tissue Engineering Paradigms in Vascular Surgery. *Physiol Res* **2009,** 58, S119-S139.

103.   Gumusderelioglu, M.; Gur, A., Synthesis, characterization, in vitro degradation and cytotoxicity of poly[bis(ethyl 4-aminobutyro)phosphazene]. *React Funct Polym* **2002,** 52, (2), 71-80.

104.   Armstrong, C.; Staples, J. F., The role of succinate dehydrogenase and oxaloacetate in metabolic suppression during hibernation and arousal. *J CompPhysiol B* **2010,** 180, (5), 775-783.

105.   Carampin, P.; Conconi, M. T.; Lora, S.; Menti, A. M.; Baiguera, S.; Bellini, S.; Grandi, C.; Parnigotto, P. P., Electrospun polyphosphazene nanofibers for in vitro rat endothelial cells proliferation. *J Biomed Mater Res A* **2007,** 80A, (3), 661-668.

106.   Langone, F.; Lora, S.; Veronese, F. M.; Caliceti, P.; Parnigotto, P. P.; Valenti, F.; Palma, G., Peripheral-Nerve Repair Using a Poly(Organo)Phosphazene Tubular Prosthesis. *Biomaterials* **1995,** 16, (5), 347-353.

107.   Crommen, J. H. L.; Schacht, E. H.; Mense, E. H. G., Biodegradable Polymers .2. Degradation Characteristics of Hydrolysis-Sensitive Poly[(Organo)Phosphazenes]. *Biomaterials* **1992,** 13, (9), 601-611.

108.   Fan, Y. J.; Kobayashi, M.; Kise, H., Synthesis and biodegradation of poly(ester amide)s containing amino acid residues: The effect of the stereoisomeric composition of L- and D-phenylalanines on the enzymatic degradation of the polymers. *J Polym Sci Pol Chem* **2002,** 40, (3), 385-392.

109.   Altman, G. H.; Horan, R. L.; Lu, H. H.; Moreau, J.; I, M.; Richmond, J. C.; Kaplan, D. L., Silk matrix for tissue engineered anterior cruciate ligaments. *Biomaterials* **2002,** 23, (20), 4131-4141.

110.   Katti, K. S., Biomaterials in total joint replacement. *Colloid Surface B* **2004,** 39, (3), 133-142.

111.   Konig, G.; McAllister, T. N.; Dusserre, N.; Garrido, S. A.; Iyican, C.; Marini, A.; Fiorillo, A.; Avila, H.; Wystrychowski, W.; Zagalski, K.; Maruszewski, M.; Jones, A. L.; Cierpka, L.; de la Fuente, L. M.; L'Heureux, N., Mechanical properties of completely autologous human tissue engineered blood vessels compared to human saphenous vein and mammary artery. *Biomaterials* **2009,** 30, (8), 1542-1550.

112.   Sarkar, S.; Salacinski, H. J.; Hamilton, G.; Seifalian, A. M., The mechanical properties of infrainguinal vascular bypass grafts: Their role in influencing patency. *Euro J Vasc Endovasc* **2006,** 31, (6), 627-636.

113.   Laurencin, C. T.; Ambrosio, A. M.; Borden, M. D.; Cooper, J. A., Jr., Tissue engineering: orthopedic applications. *Annu Rev Biomed Eng* **1999,** 1, 19-46.

114.   Duan, S.; Yang, X.; Mao, J.; Qi, B.; Cai, Q.; Shen, H.; Yang, F.; Deng, X.; Wang, S., Osteocompatibility evaluation of poly(glycine ethyl ester-co-alanine ethyl ester)phosphazene with honeycomb-patterned surface topography. *J Biomed Mater Res A* **2012,** 101, (2), 307-317.

115.   Krogman, N. R.; Singh, A.; Nair, L. S.; Laurencin, C. T.; Allcock, H. R., Miscibility of bioerodible polyphosphazene/poly(lactide-co-glycolide) blends. *Biomacromolecules* **2007,** 8, (4), 1306-1312.

116.   Nicoli Aldini, N.; Fini, M.; Rocca, M.; Martini, L.; Giardino, R.; Caliceti, P.; Veronese, F. M.; Lora, S.; Maltarello, M. C., Peripheral Nerve Reconstruction with Bioabsorbable Polyphosphazene Conduits. *J Bioact Compat Pol* **1997,** 12, 3-13.

117.   Oredein-McCoy, O.; Krogman, N. R.; Weikel, A. L.; Hindenlang, M. D.; Allcock, H. R.; Laurencin, C. T., Novel factor-loaded polyphosphazene matrices: potential for driving angiogenesis. *J Microencapsul* **2009,** 26, (6), 544-555.

118.   Weikel, A. L.; Owens, S. G.; Morozowich, N. L.; Deng, M.; Nair, L. S.; Laurencin, C. T.; Allcock, H. R., Miscibility of choline-substituted polyphosphazenes with PLGA and osteoblast activity on resulting blends. *Biomaterials* **2010,** 31, (33), 8507-8515.

119.   Allcock, H. R.; Smeltz, K. M.; Mack, D. P., United States Patent - Poly(amino acid alkyl ester phosphazenes). In *US 1975/3,893,980*, **1975**.

120.   Chittenden, R. A.; Thomas, L. C., Characteristic Infra-Red Absorption Frequencies of Organophosphorus Compounds .4. P-X Bonds. *Spectrochim Acta* **1965,** 21, (5), 861-876.

121.   Chittenden, R. A.; Thomas, L. C., Characteristic Infra-Red Absorption Frequencies of Organophosphorus Compounds .6. Bonds between Phosphorus and Nitrogen. *Spectrochim Acta* **1966,** 22, (8), 1449-1463.

122.   Harvey, R. B.; Mayhood, J. E., Some Correlations of the Molecular Structure of Organic Phosphorus Compounds with Their Infrared Spectra. *Can J Chem* **1955,** 33, (10), 1552-1565.

123.   Ruiz, E. M.; Ramirez, C. A.; Aponte, M. A.; Barbosacanovas, G. V., Degradation of Poly[Bis(Glycine Ethyl Ester)Phosphazene] in Aqueous-Media. *Biomaterials* **1993,** 14, (7), 491-496.

124.   Teasdale, I. P.; Nischanga, I.; Bruggemann, O.; Wilfert, S., United States Patent Application Publication - Biodergradable, Water Soluble and pH Responsive Poly(organo)phosphazenes. In *US 2013/0324490 A1*, **2013**.

125.   Ehrbar, M.; Sala, A.; Lienemann, P.; Ranga, A.; Mosiewicz, K.; Bittermann, A.; Rizzi, S. C.; Weber, F. E.; Lutolf, M. P., Elucidating the role of matrix stiffness in 3D cell migration and remodeling. *Biophys J* **2011,** 100, (2), 284-293.

126.   Even-Ram, S.; Yamada, K. M., Cell migration in 3D matrix. *Curr Opin Cell Biol* **2005,** 17, (5), 524-532.

127.   Fraley, S. I.; Feng, Y.; Krishnamurthy, R.; Kim, D. H.; Celedon, A.; Longmore, G. D.; Wirtz, D., A distinctive role for focal adhesion proteins in three-dimensional cell motility. *Nat Cell Biol* **2010,** 12, (6), 598-604.

128.   Song, Y.; Kamphuis, M. M.; Zhang, Z.; Sterk, L. M.; Vermes, I.; Poot, A. A.; Feijen, J.; Grijpma, D. W., Flexible and elastic porous poly(trimethylene carbonate) structures for use in vascular tissue engineering. *Acta Biomater* **2010,** 6, (4), 1269-1277.

129.   Blanchard, L.-P.; Hesse, J.; Malhotra, S. L., Effect of Molecular-Weight on Glass-Transition by Differential Scanning Calorimetry. *Can J Chem* **1974,** 52, (18), 3170-3175.

130.   Podzimek, S., The Use of Gpc Coupled with a Multiangle Laser-Light Scattering Photometer for the Characterization of Polymers - on the Determination of Molecular-Weight, Size, and Branching. *Journal of Applied Polymer Science* **1994,** 54, (1), 91-103.

131.   Fried, J., *Polymer Science and Technology*. Third ed.; Prentice Hall: 2014; pgs 688.

132.   King, D. S.; Fields, C. G.; Fields, G. B., A Cleavage Method Which Minimizes Side Reactions Following Fmoc Solid-Phase Peptide-Synthesis. *International Journal of Peptide and Protein Research* **1990,** 36, (3), 255-266.

133.   Schnolzer, M.; Alewood, P.; Jones, A.; Alewood, D.; Kent, S. B. H., Insitu Neutralization in Boc-Chemistry Solid-Phase Peptide-Synthesis - Rapid, High-Yield Assembly of Difficult Sequences. *Int J Pept Prot Res* **1992,** 40, (3-4), 180-193.

134.   Wuts, P. G. M.; Greene, T. W., *Greene's Protective Groups in Organic Synthesis*. Fourth ed.; John Wiley & Sons, Inc.: Hoboken, NJ, 2006; pgs 1110.

135.   Dhaon, M. K.; Olsen, R. K.; Ramasamy, K., Esterification of N-Protected Alpha-Amino-Acids with Alcohol/Carbodiimide/4-(Dimethylamino)-Pyridine - Racemization of Aspartic and Glutamic-Acid Derivatives. *J Org Chem* **1982,** 47, (10), 1962-1965.

136.   Finer, E. G.; Franks, F.; Tait, M. J., Nuclear Magnetic-Resonance Studies of Aqueous Urea Solutions. *J Am Chem Soc* **1972,** 94, (13), 4424-4429.

137.   Lin, Y. J.; Cai, Q.; Li, L.; Li, Q. F.; Yang, X. P.; Jin, R. G., Co-electrospun composite nanofibers of blends of poly[(amino acid ester)phosphazene] and gelatin. *Polym Int* **2010,** 59, (5), 610-616.

138.   Nair, L. S.; Bhattacharyya, S.; Bender, J. D.; Greish, Y. E.; Brown, P. W.; Allcock, H. R.; Laurencin, C. T., Fabrication and optimization of methylphenoxy substituted polyphosphazene nanofibers for biomedical applications. *Biomacromolecules* **2004,** 5, (6), 2212-2220.

Appendices

Appendix 1: Summary of literature values for the characterization and thermal properties of poly[(amino acid ester)phosphazene]s. GPC data are relative to polystyrene standards in all cases.

Polymer	NMR (ppm)			FTIR (cm^{-1})	Thermal Properties (°C)			GPC (x 10^5 Da)			Reference
	^{1}H	^{13}C	^{31}P		T_d	T_g	T_m	M_w	M_n	PDI	
PNEG	4.3 (2H) 3.9 (1H) 3.7 (2H) 1.4 (3H)	176 65 60 26	1.5			-40		1.8			97
PNEG	4.2 3.7 1.3		1.5			-15.7		0.526		2.1	115
PNEG$_{33}$EA$_{67}$	4.7 (3H) 4.3 (2H) 2.0 (3H) 1.3 (3H)			1750 (C=O, ester) 1220 (-P=N-) 860 (-P-N-)							114
PNEG$_{33}$EA$_{67}$	4.7 4.3 2.0 1.3			1220 (br. P=N) 1750 (C=O, ester) 860 (P-N)							64
PNEA	4.4 (1H) 4.1 (2H) 1.6 (3H) 1.3 (3H)	177 81 59 28 26	-1.1			19		1.7			97
PNEA	3.80 – 4.30 (br. s OCH$_2$- CH$_3$, -CH$_3$-CH) 1.30 – 1.50 (br. s –CH$_3$-CH) 1.10 – 1.30 (br. s. OCH$_2$- CH$_3$)					12					116
PNEA	4.4 (1H) 4.1 (2H) 1.6 (3H) 1.3 (3H)	177 81 59 28 26	-1.1		136	19		1.7			84
PNEA	4.1 – 4.08 (br, 3.6H) 1.4 – 1.27 (br, 3H) 1.2 – 1.19 (t, 3H)		-3.5			-10		1.96	0.89	2.2	83
PNEA	4.4 (1H) 4.1 (2H) 1.6 (3H) 1.3 (3H)		-1.10			-3.0		4.08			94
PNEF	7.6 (5H) 4.7 (1H) 4.4 (2H) 4.1 (2H) 1.2 (3H)	178 144 140 139 138 136 72 68			185	68	158	2.2			84

		45 23							
PNEF					40 65	2 – 40			95
PNEF$_{75}$EG$_{25}$	7.1 (4H) 7.2 (1H) 4.2 (3H) 3.8 (1H) 3.0 (1H) 2.1 (2H) 1.0 (2H)					5.88	5.05	1.16	117
PNEF$_{70}$EG$_{30}$	7.14 (br. s, Ph) 4.3 – 3.7, 3.1 (br, CH_2, CH, NH) 1.12, 0.95 (CH_3)	175.76 172.91 137.54 130.09 128.69 127.45 61.31 56.17 43.44 41.17 14.63 14.43	0.45	3400 – 3200 (br, C-H) 1730 (s, C=O ester) 1200 – 1130 (s, P=N) 908 (P-NH)					105
PNEM	4.21 (2H) 3.67 (1H) 2.67 (2H) 2.11 (5H) 1.30 (3H)		-0.226		9	1.28		1.79	118
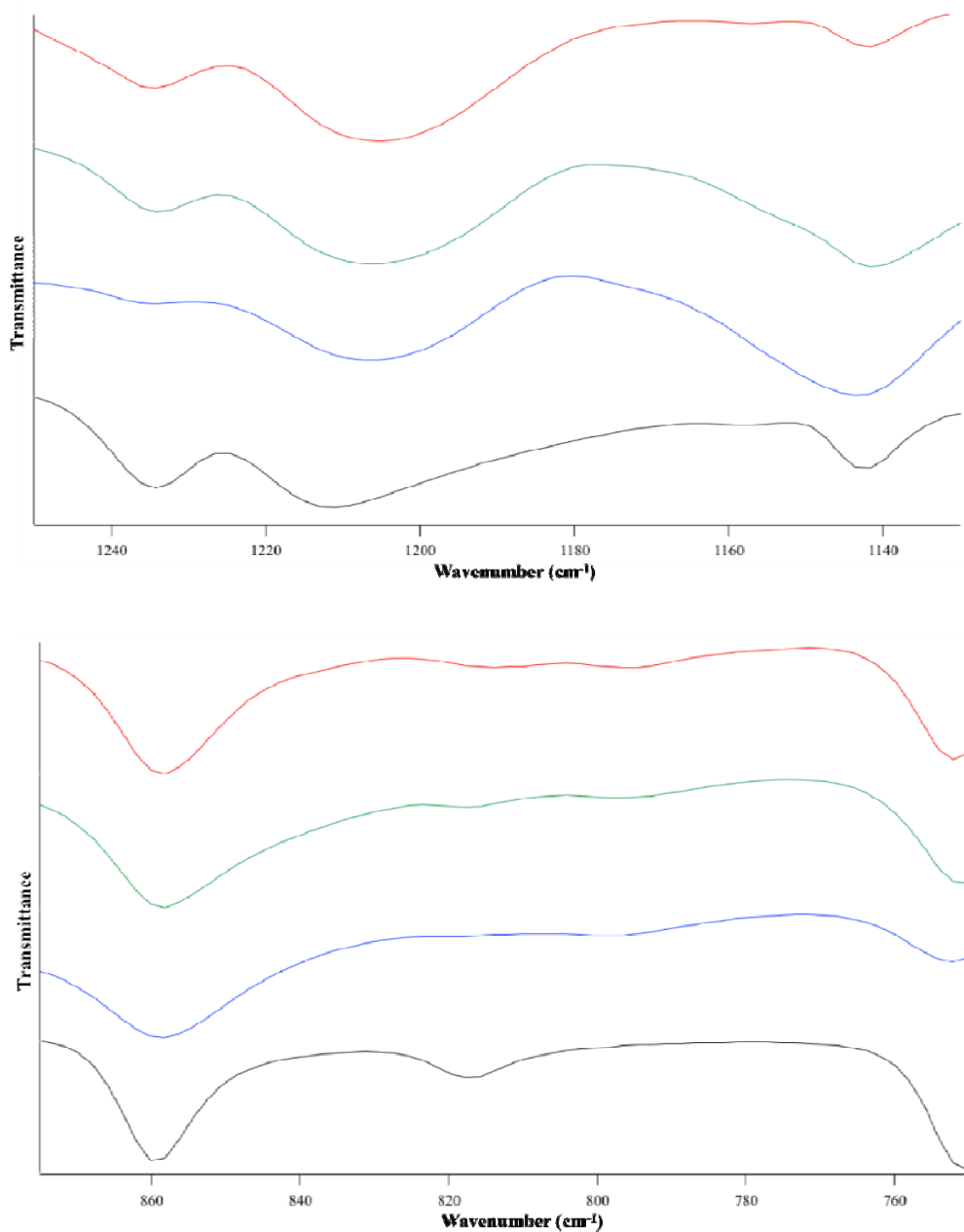
Appendix 2: Enlarged regions of the PP-A$_{100}$ FTIR spectra showing P=N and P-NH peak broadening. The spectra correspond to L-alanine ethyl ester hydrochloride (black), and PP-A$_{100}$'s made by the LT 2S (blue), 1P RT (green), RT 2S (red) reactions.
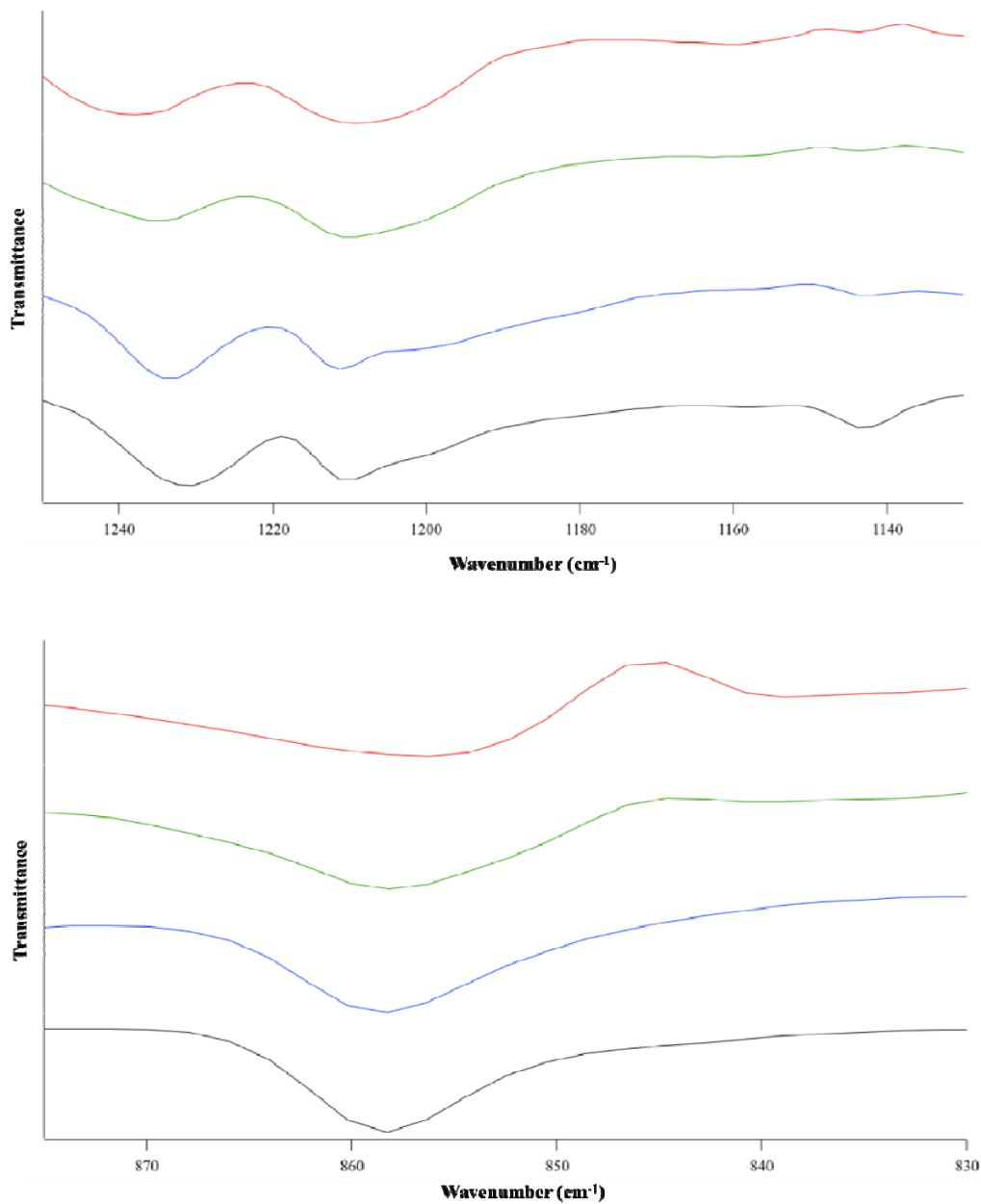
Appendix 3: Enlarged regions of the PP-F$_{100}$ FTIR spectra showing P=N and P-NH peak broadening. The spectra correspond to L-phenylalanine ethyl ester hydrochloride (black), and PP-F$_{100}$'s made by the LT 2S (blue), 1P RT (green), RT 2S (red) reactions.
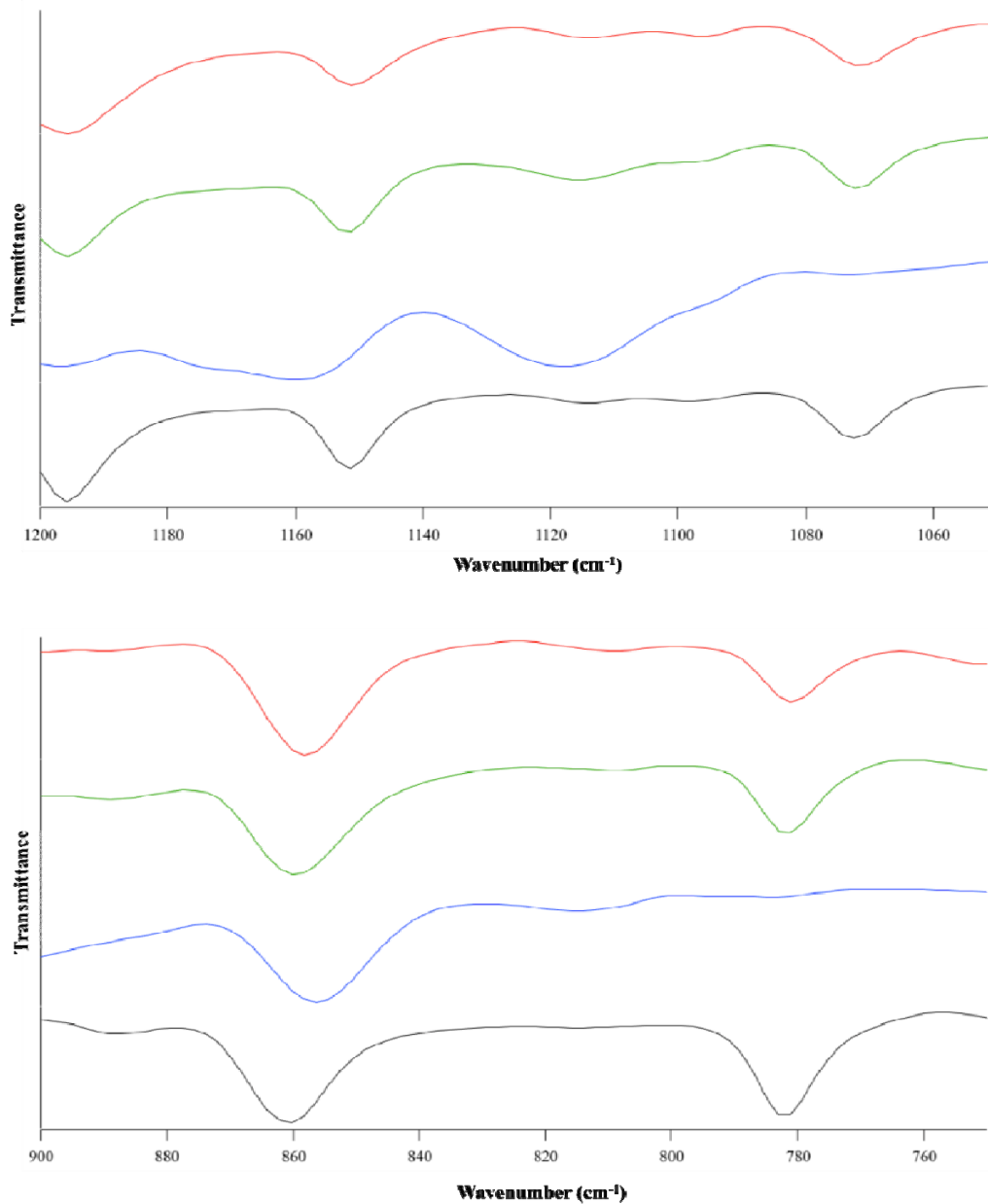
Appendix 4: Enlarged regions of the PP-M$_{100}$ FTIR spectra showing P=N and P-NH peak broadening. The spectra correspond to L-methionine ethyl ester hydrochloride (black), and PP-M$_{100}$'s made by the LT 2S (blue), 1P RT (green), RT 2S (red) reactions.

Curriculum Vitae

Amanda Baillargeon

EDUCATION

Sept. 2012 – June 2014	Master's of Engineering Science Graduate Program in Biomedical Engineering The University of Western Ontario, London, Ontario, Canada *Supervisor:* Dr. Kibret Mequanint
Sept. 2007 – April 2012	Bachelor of Science (With Distinction, Western Scholar) Honors Specialization in Chemistry The University of Western Ontario, London, Ontario, Canada *Honors Thesis Supervisor:* Dr. Ken Yeung

POSITIONS

Sept. 2012 – Dec. 2013	**Graduate Teaching Assistant** Industrial Organic Chemistry Department of Chemical and Biochemical Engineering The University of Western Ontario, London, Ontario, Canada
Sept. 2010 – Aug. 2011	**Research Assistant, Undergraduate Science Internship Program** Butyl Business Unit Global R&D LANXESS Inc., London, Ontario, Canada
May 2009 – Aug. 2009, May 2010 – Aug. 2010	**Research Assistant, Summer Research Assistantship** Departments of Chemistry and Biochemistry The University of Western Ontario, London, Ontario, Canada

ACADEMIC AWARDS, SCHOLARSHIPS, and DISTINCTIONS

May 2013 – April 2014	Natural Sciences and Engineering Research Council of Canada (NSERC) Alexander Graham Bell Canada Graduate Scholarship (CGS-M)
May 2013	Ontario Graduate Scholarship (OGS) – *Declined*
Sept. 2012 – Aug. 2014	Canadian Institutes of Health Research (CIHR) Strategic Training Program in Vascular Research

March 2012	2nd Place in the Bio-analytical/Analytical Division at the 40th Southern Ontario Undergraduate Student Chemistry Conference (SOUSCC) – *Oral Presentation*
Nov. 2010 – Feb. 2011	NSERC Industrial Undergraduate Student Research Award (I-USRA) LANXESS Inc.
Sept. 2007 –	Western Scholar, Dean's Honor List, The Queen Elizabeth II Aiming for the Top Scholarship
Sept. 2007	Christina A. MacKerracher Admission Scholarship (Western Scholarship of Excellence)

PUBLICATIONS and PRESENTATIONS

A   Refereed Journal Manuscripts (1)

1. **Baillargeon, Amanda L**; Mequanint, Kibret, Biodegradable Polyphosphazene Biomaterials for Tissue Engineering and Delivery of Therapeutics. *Biomed. Res. Int.* vol. 2014, Article ID 761373, 16 pages, 2014. doi:10.1155/2014/761373

B   Non-Peer Reviewed Oral Presentations (1) **presenter*

1. **Baillargeon, Amanda L***; Booker, Christina J; Yeung, Ken K-C, Using Capillary Electrophoresis and Magnetic Beads for Miniaturized Protein Sample Preparation. 40th Southern Ontario Undergraduate Student Chemistry Conference (SOUSCC), The University of Guelph, Guelph, Ontario, Canada (24 March 2012).

C   Peer Reviewed Poster Presentations (2) **presenter*

1. **Baillargeon, Amanda L***; Mequanint, Kibret, Vascular Tissue Engineering: Synthesis of Novel Functionalized Scaffold Biomaterials. London Health Research Day (LHRD), London Convention Centre, London, Ontario, Canada (19 March 2013).

2. **Baillargeon, Amanda L***; Mequanint, Kibret, Vascular Tissue Engineering: Synthesis of Novel Functionalized Polyphosphazene Scaffolds. 30th Annual Meeting of the Canadian Biomaterials Society (CBS), University of Ottawa, Ottawa, Ontario, Canada (29 May 2013 – 1 June 2013).